Depositional setting and metabolism of microbial mats in the Archean Moodies Group, Barberton Greenstone Belt, South Africa

Kumulative Dissertation

zur Erlangung des Doktorgrades der Naturwissenschaften

"doctor rerum naturalium“

(Dr. rer. nat.)

von

Dipl.-Geol. Martin Homann

Eingereicht im Fachbereich Geowissenschaften

an der Freien Universität Berlin

Berlin, den 16.Dezember 2015

Diese Arbeit wurde von dem Promotionsausschuss des Fachbereiches Geowissenschaften der Freien Universität Berlin am 11. Februar 2014 genehmigt.

……

Prof. Dr. Christoph Heubeck (Erstgutachter)

Friedrich-Schiller-Universität Jena

Prof. Dr. Alessandro Airo (Zweitgutachter)

Freie Universität Berlin

Die Disputation erfolgte am: 12. Februar 2016

Erklärung

Hiermit erkläre ich, Martin Homann, dass diese Arbeit ausschließlich auf Grundlage der angegebenen Hilfsmittel und Hilfen selbstständig von mir verfasst wurde. Diese Arbeit wurde in keinem früheren Promotionsverfahren eingereicht.

Berlin, den 16. Dezember 2015

Martin Homann

Zusammenfassung

Das Archaikum umfasst etwa ein Drittel der Erdgeschichte. Während dieses Zeitraums von 1.5 Milliarden Jahren entwickelten sich die wichtigsten biochemischen Stoffwechselwege, einschließlich der oxygenen Photosynthese von Cyanobakterien, welche die Biosphäre bis heute dominiert. Die biologische Sauerstoffproduktion war die physiologische Basis für die Evolution von komplexen, multizellularen Lebensformen. Alter und Ursprung von Cyanobakterien sind jedoch nach wie vor ein kontroverses Thema, welches bis heute noch nicht eindeutig geklärt werden konnte. Aus diesem Grund ist es von essentieller Bedeutung die ältesten Gesteine mit gut erhalten Spuren mikrobiellen Lebens zu untersuchen, um Rückschlüsse auf deren früheren Lebensraum und Metabolismus ziehen zu können. Ein idealer Ort um nach Antworten auf diese offenen Fragen zu suchen, ist die paläoarchaische (~3.22 Ga) Moodies Group des Barberton Greenstone Belts (BGB) in Südafrika, welche Sandsteine mit außerordentlich gut erhaltenen Überresten mikrobieller Matten und sedimentärer Strukturen beinhaltet.

Die kerogenhaltigen Laminationen der fossilen Mikrobenmatten sind besonders gut in einer ~1000 m mächtigen Abfolge von fein- bis grobkörnigen Sandsteinen und Konglomeraten in der Saddleback Synclinale des zentralen BGB erhalten, welche sich lateral über 15 km verfolgen lässt. Die Biomatten wuchsen einst in küstennahen Schwemmfächern, und in inter- und supratidalen Paläolebensräumen. In situ $\delta^{13}C_{PDB}$ Messungen des Kerogens liegen im Bereich von -32.3‰ bis -21.3‰ und sind konsistent mit dem biogenen Ursprung der Laminationen. Die Restriktion der Matten auf ehemals flachmarine Habitate und das Vorhandensein von gut ausgebildeten mikrobiellen „tufts“ legen nahe, dass sie photosynthetisch waren und möglicherweise von anzestralen Cyanobakterien gebildet wurden. Es ist jedoch schwer zu belegen, dass die Mikroben damals wirklich schon freien Sauerstoff produzierten. Dies wird daher eine zentrale Frage zukünftiger Studien sein.

Die Identifikation von fossilen mikrobiellen Gemeinschaften, die einst in Hohlräumen unterhalb der Biomatten lebten, hat das geologisches Alter dieser kryptischen Mikroben um ~500 Ma erweitert. Überdies könnten die identifizierten mikrobiellen Matten in fluvial-alluvialen Konglomeraten und Sandsteinen die erste sichtbare Spur für die Kolonialisierung und mikrobielle Stabilisierung archaischer Landmassen darstellen und somit den Ursprung terrestrischen Lebens um ~400 Ma erweitern.

Abstract

The Archean eon encompasses about one-third of Earth's history. During its 1.5 Ga time span, most of the principal biochemical pathways had evolved, including cyanobacterial oxygenic photosynthesis, which keeps dominating the modern biosphere. Biological oxygen production provided the physiological base for the expansion of life, particularly the evolution of complex multicellular organisms. However, the antiquity and origin of oxygenic photosynthesis is vigorously debated. Hence, the study of Earth's oldest well-preserved microbial mats and their paleoenvironmental setting has the potential to unravel earliest evolution photosynthesis. An ideal place to tackle this issue is the Paleoarchean (~3.22 Ga) Moodies Group of the Barberton Greenstone Belt, South Africa, which contains widespread remains of remarkably well-preserved microbial mats and sedimentary structures in shallow-water sandstones.

In the Saddleback Syncline of the central BGB, kerogenous laminae representing fossilized microbial mats occur abundantly in a ~1000-m-thick succession of fine- to coarse-grained sandstones and conglomerates, which can be traced laterally for >15 km. Microbial mats were thriving in coastal floodplain, inter-, and supratidal paleoenvironments. In situ $\delta^{13}C_{PDB}$ measurements of the kerogen range from -32.3‰ to -21.3‰ and are consistent with a biogenic origin. The exclusive occurrence of mats in shallow-water, high-energy setting, and their tufted micro-morphology suggest that they were photosynthetic and most likely build by ancestral cyanobacteria. However, the ultimate question whether the microbes were producing free oxygen or not still needs to be resolved. The identification of cavity-dwelling microbial communities beneath these microbial mats, has extended the geological record of coelobionts by ~500 Ma, while the occurrence of microbial mats in fluvial-alluvial conglomerates and sandstones extends the record of terrestrial life by ~400 Ma.

Table of contents

List of figures

Acknowledgement

This research was made possible through the financial support of the Deutsche Forschungsgemeinschaft (DFG grant He2418/13-1). In the following, I would like to express my gratitude to several people who supported me during my stay at the Freie Universität in various ways.

First of all, I am grateful to Prof. Dr. Christoph Heubeck for giving me the opportunity to do research on one of Earth's oldest well-preserved sedimentary succession, the Moodies Group, with the goal to unravel more secrets of his beloved "crinklies", a.k.a. microbial mats. I am thankful for three outstanding field seasons in South Africa and Swaziland and the chance to attend national and international conferences around the world: Sediment (Leipzig, 2011); Geosynthesis (Cape Town, 2011); AAPG (Milan, 2011); GAC-MAC (St. John's, 2012); GRC Geobiology (Ventura, 2013); Goldschmidt (Florence, 2013); Sediment (Tübingen, 2013); Life-Origins (Porto, 2015); and finally GeoBerlin 2015, which gave me the opportunity to meet and discuss with some of the leading scientist in the thrilling field of Archean research. Thank you for your constant motivation and advice, for supporting me in the writing process on the first and following manuscripts, your constant trust in me and universal truths like: "Geld wächst nach, Zeit nicht."

Secondly, I am thankful to Prof. Dr. Alessandro Airo. It was a blessing that you came back to the FU Berlin the same year as I started my PhD project. You were actually the first person I met who had previously worked on thrombolites. After I managed to convince you of the biogenicity of the Moodies microbial mats, or "biomats" as you like to call them, we never had a serious scientific disagreement again. Thank you for all your support and effort during the writing process, for convincing me to join you on the Great Basin fieldtrip, and for all our fruitful discussions. There are more to come!

Furthermore, I am indebted to many others. Jonathan Engelhardt, Sami Nabhan, Danielle Zentner, Laura Stutenbecker, Nadja Drabon, Tim Luber, Saskia Bläsing, Marc Grund, and Paul Fugmann for field assistance and their pleasant companionship in the field and beyond. Anna Giribaldi is thanked for (polished) thin section preparation, Jan Evers for assistance with the SEM, Martina Grundman for IT support and a constant flow of good coffee: $E = MC^2$ (Energy = milk*coffee^2), Britta Ernst for updating the website. Silvia Favaro, Xiaojuan Sun and Andreas Scharf are the best office mates ever. Eline Le Breton, Mark Handy, Jörg Giese, and Jan Pleuger are thanked for coffee table conversations about e.g. the excellent quality of the mensa food.

Micha, Stefan, Lukas, and Marco you are the best. Marco; thanks for sending me all the inaccessible publications. Max^1 – Greifswald! Max^2 – Garbage am↯dm! To the entire Nevada gang: thanks for resurrecting me – in dust we trust! Claire, Hanne & Jerry – c'est la blague! Fred & Gwen – thanks for having us! Telfords – DB! GiGi & Flavia ❤ Finally, I would like to thank my parents and my grandfather for their constant support, motivation, and love.

Thank you all so much!

Structure of this thesis

This thesis is publication-based and consists of five chapters and three appendixes. Chapter I introduces the subject and provides an overview of the content. Chapters II, III, and IV are individual manuscripts published in or in preparation for submission to peer-reviewed scientific journals, respectively. Chapter V provides overall conclusions. Brief outlines of the three manuscripts and of the contributions of the co-authors are given below. The three appendices include (A1) a short entry in the Encyclopedia of Astrobiology, (A2) a description of a series of microbial mat growth experiments and comparisons of modern microbial mats of Tunisia with Archean microbial structures, and (A3) results of Rock-Eval pyrolysis of kerogenous material of the Moodies microbial mats.

Chapter II

Morphological adaptations of 3.22 Ga tufted microbial mats to Archean coastal habitats (Moodies Group, Barberton Greenstone Belt, South Africa)

Martin Homann, Christoph Heubeck, Alessandro Airo, Michael M. Tice

Precambrian Research, 2015, 266, 47-64

This chapter describes the stratigraphic and depositional context of fossil microbial mats preserved in the siliciclastic Moodies Group. During three field seasons 2011-2013, high-resolution stratigraphic sections were logged and samples were collected and analyzed at the FU Berlin. The manuscript includes a paleoenvironmental reconstruction of the depositional environment and describes distinct morphological adaptations of the microbial mats to different paleoenvironmental settings.

The first author (Martin Homann) carried out fieldwork. The second author (Christoph Heubeck) introduced, assisted, advised and helped with the revisions of the manuscript. The third author (Alessandro Airo) significantly improved the style of the manuscript and contributed some biogeochemical aspects. The fourth author (Michael M. Tice) supervised the XRF measurements of our samples at his lab at Texas A&M University, improved the discussion section and had useful comments concerning the grain size distribution and flow velocity analysis and their interpretation. The first author drafted all the figures and tables, which were discussed and improved through the input of all co-authors.

Chapter III

Evidence for cavity-dwelling microbial life in 3.22 Ga tidal deposits

Martin Homann, Christoph Heubeck, Tomaso R.R. Bontognali, Lukas Baumgartner, Alessandro Airo

Geology, 2016, v. 44, no. 1, p. 51–54

This chapter comprises a detailed, petrographic and geochemical study of Earth's earliest cavity-dwelling microbial communities, extending their geological record for ~500 Ma.

The first author (Martin Homann) carried out fieldwork and collected the analyzed samples in 2012 and 2013. The second author (Christoph Heubeck) conducted Raman spectroscopy measurements. The third author (Tomaso R.R. Bontognali) organized the in situ carbon isotope measurements at the University of Lausanne. All co-authors significantly improved previous versions of the manuscript and helped with constructive criticism. The first author drafted all figures and tables, which were refined by comments from all co-authors.

Chapter IV

The conquest of land: Terrestrial microbial mats at 3.22 Ga

Martin Homann, Christoph Heubeck, Martin Van Kranendonk, Alessandro Airo

In preperation

This manuscript describes an occurrence of microbial mats in the BGB within high-energetic conglomerates of the Moodies Group, which extends the temporal record of microbial ecosystems in terrestrial aquatic environments by ~400 Ma into the past.

The first author (Martin Homann) carried out fieldwork, measured stratigraphic sections, collected samples and drafted the figures. The co-authors commented on various aspects of this work, revised the manuscript, and substantially improved it.

I.

Introduction

I.1 Life in the Archean

If you could travel back in time to the Archean Earth, you would probably not recognize it as the green planet we inhabit today. Damaging UV radiation and the temperature were significantly higher than today, and the reducing atmosphere, which lacked free oxygen but contained high levels of carbon dioxide, some methane, ammonia, and other gases would have been hostile to most present-day life forms (Kasting, 1993). The close orbit of the moon likely caused a much higher tidal range and enormously wide tidal environments fringing the first small continental land masses.

More than sixty years after the discovery of fossil microorganisms in ~1.9 Ga cherts of the Gunflint Formation in Canada, interest in the history of life on Earth and on other planets in our solar system continues unabated (Tyler and Barghoorn, 1954; Lanier, 1989; Westall, 2005; Shapiro and Konhauser, 2015). On the one hand this is driven by the relatively new research fields of Astrobiology and Geobiology, and on the other hand by the development of sophisticated analytical techniques, which allow analyses on the nanoscale. Additionally, the discoveries of NASA's and ESA's Mars exploration programs (e.g. Pathfinder 1997, Phoenix 2008, Curiosity 2013) have raised the awareness of these topics in the research community and gained significant media attention. The early Earth was supposedly similar to Early Mars in some aspects, hence analog studies of the Earth are of paramount importance. However, the Archean rock record on Earth and its traces of early life are sparse, fragmentary, and largely metamorphosed; thus, the identification of microbial remains and the reconstruction of their metabolic pathways is challenging. Lithified aquatic sediments are considered the most suitable archive of remains of microbial life, because water is a fundamental requirement for life. Earth's oldest putative geochemical signs of life are based on information from one single zircon from Jack Hills, Western Australia, which has an age of 4.1 Ga and contains carbonaceous inclusions of potentially biogenic origin (Bell et al., 2015). An earlier study of ~3.8 Ga zircons from the Isua greenstone belt in southwest Greenland yielded similar results; however, the host rocks are highly metamorphosed and the traces of life are controversial (Mojzsis et al., 1996; Lepland et al., 2005). Actually, there are only two outcrop locations known worldwide where Archean rocks of unequivocal sedimentary origin are preserved with low-grade metamorphic overprint: The Barberton Greenstone Belt (BGB, 3.5 - 3.2 Ga) in the Kaapvaal craton of southern Africa and the greenstone belts of the Pilbara craton of Western Australia (3.5 - 3.0 Ga; Fig. I.1).

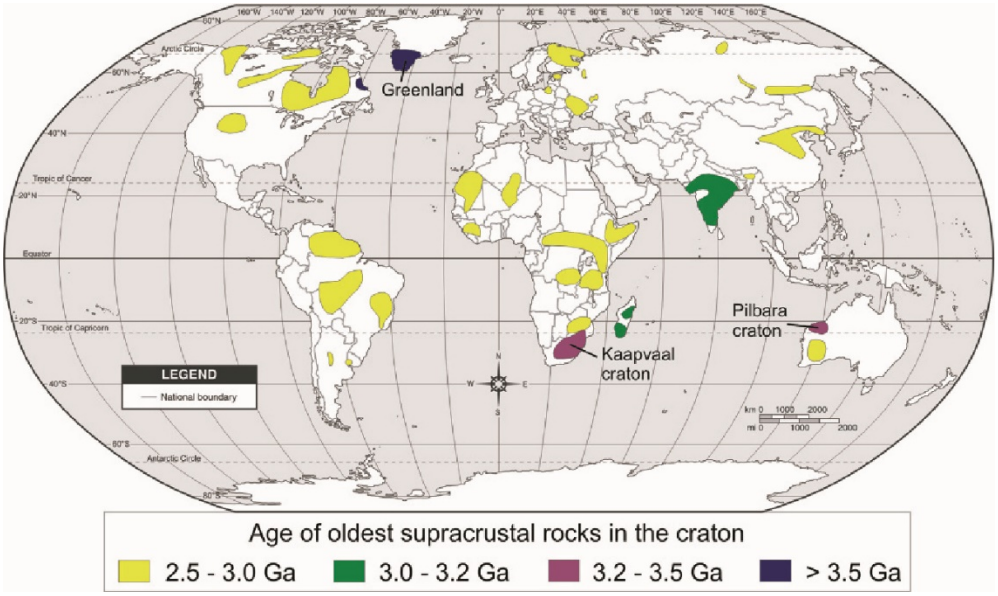

Figure I. 1: *Distribution of preserved remains of Archean cratons exposed at the Earth's surface (Wacey, 2009).*

For a long period, early life studies focused on the search of fossil cyanobacteria, but for the last decade investigations have moved to more fundamental questions: (1) What is the nature of Earth's earliest preserved microbes?; (2) In which environments were they thriving?; and (3) How does one distinguish the morphological and biogeochemical signatures of life from those produced by abiogenic processes (Nisbet, 1985; Nisbet and Sleep, 2001; Westall, 2005)?

In the past, siliciclastic lithologies were commonly bypassed by the early life studies in favor of the more promising stromatolites, but the past decade has seen an increasing number of publications on microbial mats in ancient shallow-water siliciclastic settings (Tice and Lowe, 2004; Noffke et al., 2006; Dornbos et al., 2007; Heubeck, 2009; Noffke, 2009; Eriksson et al., 2010; Wacey et al., 2011; Gamper et al., 2012; Homann et al., 2015). These deposits contain multiple lines of evidence suggesting an abundance of microbial life in a range of paleoenvironments and imply that microbial life may have developed the ability to thrive as complex communities with advanced metabolisms well prior to 3.5 Ga. The world's oldest-known convincing record of microbial mats in a siliciclastic tidal deposit comes from the 3.22 Ga Moodies Group of the Barberton Greenstone Belt. It is the prime objective of this thesis.

I.2 Evolution of oxygenic photosynthesis

The most dramatic geochemical change in Earth's history was caused by the evolution of oxygenic photosynthesis by cyanobacteria, which evolved this sophisticated metabolism to obtain energy from sunlight while releasing free oxygen as a metabolic byproduct (Buick, 2008; Farquhar et al., 2011; Schopf, 2011; Lyons et al., 2014). The onset of oxygenic photosynthesis triggered the Great Oxidation Event (GOE) ~2.4 - 2.3 Ga ago and is responsible for the accumulation of free oxygen in the atmosphere and shallow

oceans (Fig.I.2). The current trend in the literature records a continuous backdating of the first occurrence of free oxygen on Earth by yearly about 100 Ma. This trend is based on a growing amount of evidence for "whiffs of oxygen" prior to the GOE, suggesting the presence of locally oxygenated environments, starting at 3 Ga or earlier (Eigenbrode and Freeman, 2006; Anbar et al., 2007; Bosak et al., 2009; Crowe et al., 2013; Czaja et al., 2013; Planavsky et al., 2014; Stueken et al., 2015). Such "oxygen oases" emerged around shallow marine and possibly even terrestrial microbial mats that were capable of performing oxygenic photosynthesis, but the amount of released oxygen was insufficient to cause a global change in oxidation state (Kasting, 1993; Eigenbrode and Freeman, 2006; Olson et al., 2013; Riding et al., 2014; Lalonde and Konhauser, 2015).

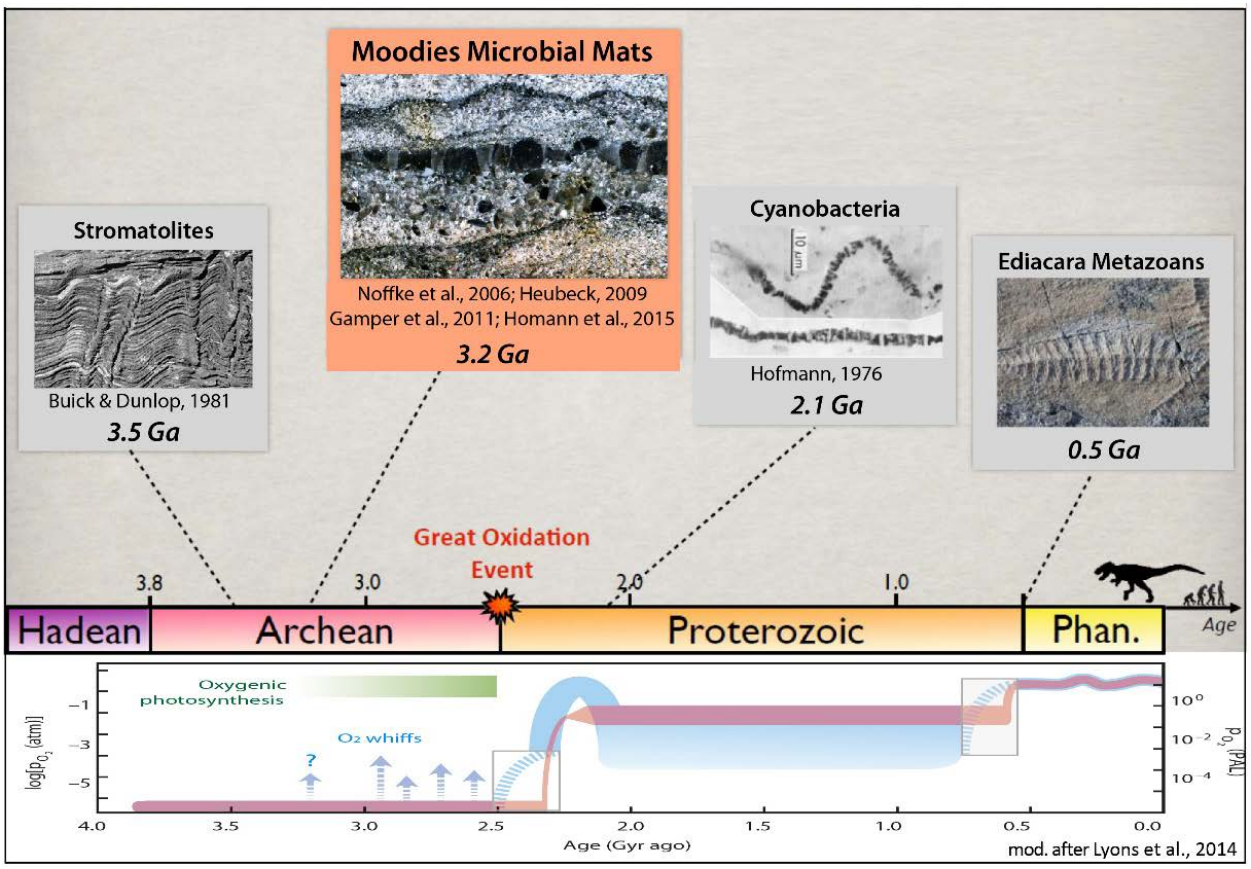

Figure I. 2: *Geological time scale showing major events and the evolution of Earth's oxygen content. Stromatolites represent Earth's oldest macroscopic traces of microbial life. After the Great Oxidation Event, atmospheric oxygen first rose globally, but evidence for several "whiffs of oxygen" have been reported in >2.5 Ga sediments, indicating the invention of oxygenic photosynthesis and the presence of cyanobacteria. With an age of ~3.2 Ga, the Moodies Group microbial mats belong to Earth's oldest and best preserved microbial remains. Note that the oldest unequivocal cyanobacterial microfossils are 2.1 Ga, whereas more complex multicellular organisms first appear at the beginning of the Phanerozoic.*

It is generally assumed that the earliest microbial communities, in which the last universal common ancestor (LUCA) lived, were chemotrophic hyperthermophiles thriving in the vicinity of widespread hydrothermal activity (Nisbet and Sleep, 2001; Westall et al., 2015), but evidence for the existence of hydrothermal vents are lacking in the Archean geological record (Lowe and Byerly, 2007). Microfossils (Knoll, 1992),

stromatolites (Walter et al., 1976; Buick and Dunlop, 1981; Hofmann et al., 1999) and geochemical evidence (Lyons et al., 2014) all suggest that also photosynthetic, mat-forming microorganisms existed already in the Archean (Fig. I.2). However, unequivocal evidence that they were cyanobacteria has still to be documented (Brasier et al., 2002). The oldest claims of putative fossil cyanobacteria come from Schopf (1993), who interpreted filamentous microstructures in black chert veins within the 3.46 Ga Apex Basalt in the Pilbara Craton of Western Australia as "probable cyanobacteria" (Schopf and Packer, 1987; Schopf, 1993; Schopf, 2006; Schopf et al., 2007; Schopf and Kudryavtsev, 2009; Schopf and Kudryavtsev, 2012). The evidence of Schopf's initial interpretation was questioned by Brasier et al. (2002), who concluded that the microstructures solely represent carbonaceous wisps, arranged in filamentous patterns around crystal boundaries (Brasier et al., 2002; Brasier et al., 2005; Brasier et al., 2006; Brasier et al., 2015). This view is also supported by extensive investigations of these microstructures conducted by Wacey et al., (2015) in which they conclude that the structures actually represent mineral artefacts produced during phyllosilicate exfoliation. Therefore, the Apex chert microfossil debate, one of the longest running paleobiological controversies, seems to be finally solved. All too commonly, previous early life studies too readily took the co-occurrence of micromorphology and carbonaceous composition as sufficient evidence of biogenicity. A positive side effect of the Apex microfossil debate was the establishment of a checklist of criteria to test the biogenicity of putative microfossils (Schopf, 2004; Brasier et al., 2006; Wacey, 2009):

(1) Provenance: Is the geological context of the microfossils-containing rocks firmly established?
(2) Age: Is the age known with appropriate precision?
(3) Indigenousness: Are the features indigenous to the rock?
(4) Syngenicity: Is the metamorphic degree of the structures the same as the surrounding host rock?
(5) Biogenicity: Are the features assuredly of biological origin?

These criteria need to be evaluated for virtually any claim of early life; usually, several lines of evidence are required to falsify the "null hypothesis" of a non-biological origin. Fortunately, the development of high-precision analytical technologies has significantly enhanced the quality of early life studies.

The finding that 2α-methylhopanoids constitute a distinct biomarker for cyanobacteria (Summons et al., 1999) and their documentation in 2.7 Ga shales of the Pilbara Craton (Brocks, 1999) was thought to be a major breakthrough in documenting the antiquity of oxygenic photosynthesis. However, this interpretation was rejected by (Rasmussen et al., 2008) who showed that the initial results of Brocks et al. (1999) were inconsistent and that the identified biomarkers were not indigenous to the host rock but likely represented contamination. It is generally accepted that the oldest morphological fossils of clearly cyanobacterial affinity are ~2.15 Ga old (Hofmann, 1976; Brocks et al., 2003; Rasmussen et al., 2008). Nevertheless, cyanobacteria evidently evolved long before this time, but it remains challenging to find reliable macroscopic traces in the sedimentary record.

I.3 Microbial mats

Microbial mats develop from thin biofilm coatings into millimeter- to centimeter-thick, laminated, carpet-like structures that typically grow at the sediment-water-interface and may cover many kilometers of tidal, lagoonal, and continental shelf deposits (Krumbein et al., 1994; Noffke, 2010). They are commonly stratified in several layers dominated by specific types of microorganisms with different metabolisms and close ecological relationships (Canfield and Des Marais, 1993; Konhauser, 2007). In aqueous photic-zone environments, the upper mat layers are mostly dominated by cyanobacteria performing oxygenic photosynthesis, while the lower layers are generally dominated by anaerobic communities such as sulfate-reducing bacteria, and by methanogenic or methanotrophic archaea. Microbial mats are cohesive and attached to their substrate (e.g. sediment grains) by mucilaginous extracellular polymeric substances (EPS). The sugar- and protein-rich EPS are secreted by the microorganisms and form a protective and adhesive matrix in which the microbes are embedded (Decho, 2010; Decho, 2013; Noffke et al., 2013). In siliciclastic environments, fossilized microbial mats can be preserved as 'biolaminates' interbedded with sand (Gerdes et al., 2000), whereas rigid build-ups composed of mineralized multilayered microbial mats and trapped sediment are known as microbialites and commonly occur in chemically-dominated aqueous environments nearly free of siliciclastic input (Fig. I.3; Noffke and Awramik, 2011). Microbialites can be subdivided in two main endmember groups: stromatolites (layered fabric), which belong to Earth's oldest macroscopic traces of life, and thrombolites (clotted fabric). They lithify due to in situ precipitation of carbonate or silica minerals that are either induced by the metabolic activity of the mat-building microbes or triggered by chemical oversaturation of the ambient water in the vicinity of the cell walls (Dupraz et al., 2009).

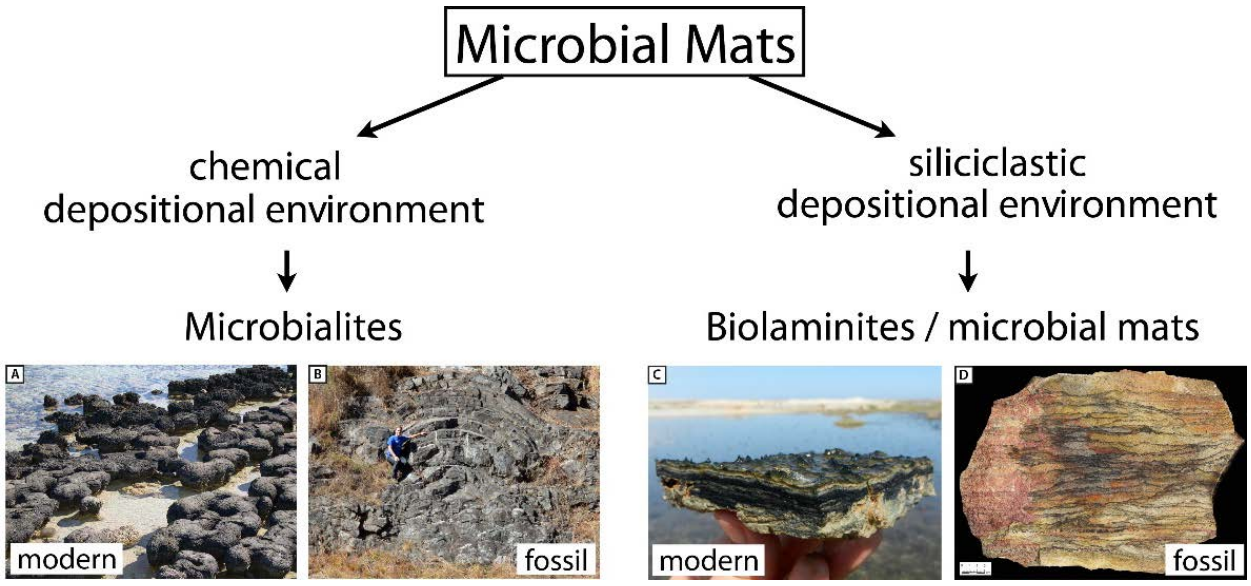

Figure I. 3: *Microbial mats are constructed by microbes and form either mineralized microbialites or densely biolaminated structures depending on the depositional environment. (A) Modern microbialites from Shark Bay, Australia. (B) Stromatolites of the Malmani Group (~2.5 Ga) near Nelspruit, South Africa. (C) Modern microbial mats of the Bahar Alouane tidal channel, southern Tunisia. (D) Microbial mats of the Moodies Group, Barberton Greenstone Belt, South Africa (~3.2 Ga).*

I.4 References

Anbar, A.D., Duan, Y., Lyons, T.W., Arnold, G.L., Kendall, B., Creaser, R., Kaufman, A.J., Gordon, G.W., Scott, C., Garvin, J., and Buick, R., 2007, A whiff of oxygen before the great oxidation event? Science (New York, N.Y.), v. 317, no. 5846, p. 1903–6, doi: 10.1126/science.1140325.

Bell, E.A., Boehnke, P., Harrison, T.M., and Mao, W.L., 2015, Potentially biogenic carbon preserved in a 4.1 billion-year-old zircon: PNAS, , no. 20, p. 1–4, doi: 10.1073/pnas.1517557112.

Bosak, T., Liang, B., Sim, M.S., and Petroff, A.P., 2009, Morphological record of oxygenic photosynthesis in conical stromatolites.: Proceedings of the National Academy of Sciences of the United States of America, v. 106, no. 27, p. 10939–10943, doi: 10.1073/pnas.0900885106.

Brasier, M.D., Antcliffe, J., Saunders, M., and Wacey, D., 2015, Changing the picture of Earth's earliest fossils (3.5–1.9 Ga) with new approaches and new discoveries: Proceedings of the National Academy of Sciences, v. 112, no. 16, p. 4859–4864, doi: 10.1073/pnas.1405338111.

Brasier, M., Green, O.R., Jephcoat, A.P., Kleppe, A.K., Van Kranendonk, M., Lindsay, J.F., Steele, A., and Grassineau, N.V., 2002, Questioning the evidence for Earth's oldest fossils: Nature, v. 416, no. March, p. 76–81.

Brasier, M., Green, O., Lindsay, J.F., McLoughlin, N., Steele, A., and Stoakes, C., 2005, Critical testing of Earth's oldest putative fossil assemblage from the ~3.5Ga Apex chert Australia: Precambrian Research, v. 140, no. 1-2, p. 55–102, doi: 10.1016/j.precamres.2005.06.008.

Brasier, M., McLoughlin, N., Green, O., and Wacey, D., 2006, A fresh look at the fossil evidence for early Archaean cellular life: Philosophical transactions of the Royal Society of London. Series B, Biological sciences, v. 361, no. 1470, p. 887–902, doi: 10.1098/rstb.2006.1835.

Brocks, J.J., 1999, Archean Molecular Fossils and the Early Rise of Eukaryotes: Science, v. 285, no. 5430, p. 1033–1036, doi: 10.1126/science.285.5430.1033.

Brocks, J.J., Buick, R., Summons, R.E., and Logan, G.A., 2003, A reconstruction of Archean biological diversity based on molecular fossils from the 2.78 to 2.45 billion-year-old Mount Bruce Supergroup, Hamersley Basin, Western Australia: Geochimica et Cosmochimica Acta, v. 67, no. 22, p. 4321–4335, doi: 10.1016/S0016-7037(03)00209-6.

Buick, R., 2008, When did oxygenic photosynthesis evolve? Philosophical transactions of the Royal Society of London. Series B, Biological sciences, v. 363, no. 1504, p. 2731–43, doi: 10.1098/rstb.2008.0041.

Buick, R., Dunlop, J.S.R., and Groves, D.I., 1981, Stromatolite recognition in ancient rocks: an appraisal of irregularly laminated structures in an Early Archaean chert-barite unit from North Pole, Western Australia: Alcheringa: An Australasian Journal of Palaeontology, v. 5, no. 3, p. 161–181, doi: 10.1080/03115518108566999.

Canfield, D.E., and Des Marais, D.J., 1993, Biogeochemical cycles of carbon, sulfur, and free oxygen in a microbial mat: Geochimica et Cosmochimica Acta, v. 57, no. 16, p. 3971–3984, doi: 10.1016/0016-7037(93)90347-Y.

Crowe, S.A., Døssing, L.N., Beukes, N.J., Bau, M., Kruger, S.J., Frei, R., and Canfield, D.E., 2013,

Atmospheric oxygenation three billion years ago.: Nature, v. 501, no. 7468, p. 535–8, doi: 10.1038/nature12426.

Czaja, A.D., Johnson, C.M., Beard, B.L., Roden, E.E., Li, W., and Moorbath, S., 2013, Biological Fe oxidation controlled deposition of banded iron formation in the ca. 3770Ma Isua Supracrustal Belt (West Greenland): Earth and Planetary Science Letters, v. 363, p. 192–203, doi: 10.1016/j.epsl.2012.12.025.

Decho, A.W., 2010, Overview of biopolymer-induced mineralization: What goes on in biofilms? Ecological Engineering, v. 36, no. 2, p. 137–144, doi: 10.1016/j.ecoleng.2009.01.003.

Decho, A.W., 2013, The EPS matrix as an adaptive bastion for biofilms: Introduction to special issue: International Journal of Molecular Sciences, v. 14, no. 12, p. 23297–23300, doi: 10.3390/ijms141223297.

Dornbos, S.Q., Noffke, N., and Hagadorn, J.W., 2007, Mat-decay features, *in* Schieber, J., Bose, P.K., Eriksson, P.., Banerjee, S., Sarkar, S., Altermann, W., and Catuneanu, O. eds., Atlas of microbial mats features …, Elsevier, Amsterdam, p. 106–110.

Dupraz, C., Reid, R.P., Braissant, O., Decho, A.W., Norman, R.S., and Visscher, P.T., 2009, Processes of carbonate precipitation in modern microbial mats: Earth-Science Reviews, v. 96, no. 3, p. 141–162, doi: 10.1016/j.earscirev.2008.10.005.

Eigenbrode, J.L., and Freeman, K.H., 2006, Late Archean rise of aerobic microbial ecosystems.: Proceedings of the National Academy of Sciences, v. 103, no. 43, p. 15759–15764, doi: 10.1073/pnas.0607540103.

Eriksson, P.G., Sarkar, S., Banerjee, S., Porada, H., Catuneanu, O., and Samanta, P., 2010, Paleoenvironmental context of microbial mat-related structures in siliciclastic rocks — examples from the Proterozoic of India and South Africa, *in* Seckbach, J. and Oren, A. eds., Microbial Mats: Modern and Ancient Microorganisms in Stratified Systems, Springer, Berlin, p. 73–108.

Farquhar, J., Zerkle, A.L., and Bekker, A., 2011, Geological constraints on the origin of oxygenic photosynthesis.: Photosynthesis research, v. 107, no. 1, p. 11–36, doi: 10.1007/s11120-010-9594-0.

Gamper, A., Heubeck, C., Demske, D., and Hoehse, M., 2012, Composition and Microfacies of Archean Microbial Mats (Moodies Group, ca. 3.22 Ga, South Africa), *in* Noffke, N. and Chafetz, H.S. eds., Microbial Mats in Silicilastic Depositional Systems Through Time, SEPM, Tulsa, p. 65–74.

Gerdes, G., Klenke, T., and Noffke, N., 2000, Microbial signatures in peritidal siliciclastic sediments: a catalogue: Sedimentology, v. 47, p. 279–308.

Heubeck, C., 2009, An early ecosystem of Archean tidal microbial mats (Moodies Group, South Africa, ca. 3.2 Ga): Geology, v. 37, no. 10, p. 931–934, doi: 10.1130/G30101A.1.

Hofmann, H.J., 1976, Precambrian Microflora, Belcher Islands , Canada : Significance and Systematics: Journal of Paleontology, v. 50, no. 6, p. 1040–1073.

Hofmann, H.J., Grey, K., Hickman, A.H., and Thorpe, R.I., 1999, Origin of 3.45 Ga coniform stromatolites in Warrawoona Group, Western Australia: Geological Society of America Bulletin, v. 111, no. 8, p. 1256–1262, doi: 10.1130/0016-7606(1999)111<1256:OOGCSI>2.3.CO;2.

Homann, M., Heubeck, C., Airo, A., and Tice, M.M., 2015, Morphological adaptations of 3.22 Ga-old tufted microbial mats to Archean coastal habitats (Moodies Group, Barberton Greenstone Belt, South Africa): Precambrian Research, v. 266, p. 47–64, doi: 10.1016/j.precamres.2015.04.018.

Kasting, J.F., 1993, Earth's Early Atmosphere: Science, v. 259, no. 5097, p. 920–926.

Knoll, A., 1992, The early evolution of eukaryotes: a geological perspective: Science, v. 256, no. 5057, p. 622–627, doi: 10.1126/science.1585174.

Konhauser, K., 2007, Introduction to Geomicrobiology: Blackwell Science.

Krumbein, W.E., Paterson, D.M., and Stal, L.J. (Eds.), 1994, Biostabilization of Sediments: BIS, Oldenburg.

Lalonde, S. V., and Konhauser, K.O., 2015, Benthic perspective on Earth's oldest evidence for oxygenic photosynthesis: Proceedings of the National Academy of Sciences, v. 112, p. 995–1000, doi: 10.1073/pnas.1415718112.

Lanier, W.P., 1989, Interstitial and peloid microfossils from the 2.0 Ga Gunflint Formation: Implications for the paleoecology of the Gunflint Stromatolites: Precambrian Research, v. 45, no. 4, p. 291–318, doi: http://dx.doi.org/10.1016/0301-9268(89)90067-3.

Lepland, A., van Zuilen, M.A., Arrhenius, G., Whitehouse, M.J., and Fedo, C.M., 2005, Questioning the evidence for Earth's earliest life—Akilia revisited: Geology, v. 33, no. 1, p. 77–79, doi: 10.1130/G20890.1.

Lowe, D.R., and Byerly, G.R., 2007, Ironstone bodies of the Barberton greenstone belt, South Africa: Products of a Cenozoic hydrological system, not Archean hydrothermal vents! GSA Bulletin, v. 119, no. 1-2, p. 65–87, doi: 10.1130/b25997.1.

Lyons, T.W., Reinhard, C.T., and Planavsky, N.J., 2014, The rise of oxygen in Earth's early ocean and atmosphere.: Nature, v. 506, no. 7488, p. 307–15, doi: 10.1038/nature13068.

Mojzsis, S.J., Arrhenius, G., McKeegan, K.D., Harrison, T.M., Nutman, a P., and Friend, C.R., 1996, Evidence for life on Earth before 3,800 million years ago.: Nature, v. 384, no. 6604, p. 55–59, doi: 10.1038/384055a0.

Nisbet, E.G., 1985, The geological setting of the earliest life forms: Journal of Molecular Evolution, v. 21, no. 3, p. 289–298, doi: 10.1007/BF02102361.

Nisbet, E.G., and Sleep, N.H., 2001, The habitat and nature of early life.: Nature, v. 409, no. 6823, p. 1083–1091, doi: 10.1038/35059210.

Noffke, N., 2010, Microbial Mats in Sandy Deposits from the Archean to Today: Springer, Heidelberg.

Noffke, N., 2009, The criteria for the biogeneicity of microbially induced sedimentary structures (MISS) in Archean and younger, sandy deposits: Earth-Science Reviews, v. 96, no. 3, p. 173–180, doi: 10.1016/j.earscirev.2008.08.002.

Noffke, N., and Awramik, S.M., 2011, Stromatolites and MISS — Differences between relatives: GSA Today, v. 23, no. 9, p. 4–9, doi: 10.1130/GSATG187A.1.Figure.

Noffke, N., Decho, A.W., and Stoodle, P., 2013, Slime Through Time: the Fossil Record of Prokaryote

Evolution: Palaios, v. 28, no. 1, p. 1–5, doi: 10.2110/palo.2013.SO1.

Noffke, N., Eriksson, K.A., Hazen, R.M., and Simpson, E.L., 2006, A new window into Early Archean life: Microbial mats in Earth's oldest siliciclastic tidal deposits (3.2 Ga Moodies Group, South Africa): Geology, v. 34, no. 4, p. 253, doi: 10.1130/G22246.1.

Olson, S.L., Kump, L.R., and Kasting, J.F., 2013, Quantifying the areal extent and dissolved oxygen concentrations of Archean oxygen oases: Chemical Geology, v. 362, p. 35–43, doi: 10.1016/j.chemgeo.2013.08.012.

Planavsky, N.J., Asael, D., Hofmann, A., Reinhard, C.T., Lalonde, S.V., Knudsen, A., Wang, X., Ossa Ossa, F., Pecoits, E., Smith, A.J.B., Beukes, N.J., Bekker, A., Johnson, T.M., Konhauser, K.O., et al., 2014, Evidence for oxygenic photosynthesis half a billion years before the Great Oxidation Event: Nature Geoscience, v. 7, no. 4, p. 283–286, doi: 10.1038/ngeo2122.

Rasmussen, B., Fletcher, I.R., Brocks, J.J., and Kilburn, M.R., 2008, Reassessing the first appearance of eukaryotes and cyanobacteria.: Nature, v. 455, no. 7216, p. 1101–1104, doi: 10.1038/nature07381.

Riding, R., Fralick, P., and Liang, L., 2014, Identification of an Archean marine oxygen oasis: Precambrian Research, v. 251, p. 232–237, doi: 10.1016/j.precamres.2014.06.017.

Schopf, J.W., 2006, Fossil evidence of Archaean life.: Philosophical transactions of the Royal Society of London. Series B, Biological sciences, v. 361, no. 1470, p. 869–85, doi: 10.1098/rstb.2006.1834.

Schopf, J.W., 2004, Geochemical and submicron-scale morphologic analyses of individual Precambrian microorganisms: The Geochemical Society Special Publications, , no. 9, p. 365–375.

Schopf, J.. W., 1993, Microfossils of the Early Archean Apex Chert: New Evidence of the Antiquity of Life: S, v. 260, no. 5108, p. 640–646.

Schopf, J.W., 2011, The paleobiological record of photosynthesis: Photosynthesis Research, v. 107, p. 87–101, doi: 10.1007/s11120-010-9577-1.

Schopf, J.W., and Kudryavtsev, A.B., 2012, Biogenicity of Earth's earliest fossils: A resolution of the controversy: Gondwana Research, v. 22, no. 3-4, p. 761–771, doi: 10.1016/j.gr.2012.07.003.

Schopf, J.W., and Kudryavtsev, A.B., 2009, Confocal laser scanning microscopy and Raman imagery of ancient microscopic fossils: Precambrian Research, v. 173, no. 1-4, p. 39–49, doi: 10.1016/j.precamres.2009.02.007.

Schopf, J.W., Kudryavtsev, A.B., Czaja, A.D., and Tripathi, A.B., 2007, Evidence of Archean life: Stromatolites and microfossils: Precambrian Research, v. 158, no. 3-4, p. 141–155, doi: 10.1016/j.precamres.2007.04.009.

Schopf, J.W., and Packer, B.M., 1987, Early archean (3.3-billion to 3.5-billion-year-old) microfossils from Warrawoona Group, Australia: Science, v. 237, no. 4810, p. 70–73.

Shapiro, R.S., and Konhauser, K.O., 2015, Hematite-coated microfossils: primary ecological fingerprint or taphonomic oddity of the Paleoproterozoic? Geobiology, v. 13, p. 209–224, doi: 10.1111/gbi.12127.

Stueken, E.E., Buick, R., and Anbar, A.D., 2015, Selenium isotopes support free O2 in the latest Archean: Geology, v. 43, no. 3, p. 259–262, doi: 10.1130/G36218.1.

Summons, R.E., Jahnke, L.L., Hope, J.M., and Logan, G.A., 1999, 2-Methylhopanoids as biomarkers for cyanobacterial oxygenic photosynthesis.: Nature, v. 400, no. 6744, p. 554–557, doi: 10.1038/23005.

Tice, M.M., and Lowe, D.R., 2004, Photosynthetic microbial mats in the 3 , 416-Myr-old ocean fluorescence at the Geoanalytical Laboratory , Washington State University (Pullman ,: Nature, v. 431, no. September, p. 549–552, doi: 10.1038/nature02920.1.

Tyler, S.A., and Barghoorn, E.S., 1954, Occurrence of Structurally Preserved Plants in Pre-Cambrian Rocks of the Canadian Shield.: Science (New York, N.Y.), v. 119, no. 3096, p. 606–8, doi: 10.1126/science.119.3096.606.

Wacey, D., 2009, Early Life on Earth. A Practical Guide: Springer.

Wacey, D., Saunders, M., Brasier, M.D., and Kilburn, M.R., 2011, Earliest microbially mediated pyrite oxidation in ~3.4 billion-year-old sediments: Earth and Planetary Science Letters, v. 301, no. 1-2, p. 393–402, doi: 10.1016/j.epsl.2010.11.025.

Wacey, D., Saunders, M., Kong, C., Brasier, A., and Brasier, M., 2015, 3.46Ga Apex chert “microfossils” reinterpreted as mineral artefacts produced during phyllosilicate exfoliation: Gondwana Research, , no. AUGUST, doi: 10.1016/j.gr.2015.07.010.

Walter, M.R., Bauld, J., and Brock, T.D., 1976, Microbiology and morphogenesis of columnar stromatolites (Conophyton, Vacerrila) from hot springs in Yellowstone National Park, *in* Walter, M.R. ed., Stromatolites, Elsevier, New York, p. 273–310.

Westall, F., 2005, Life on the Early Earth: A Sedimentary View: Science, v. 308, no. 5720, p. 366–367, doi: 10.1126/science.1107227.

Westall, F., Campbell, K. a., Breheret, J.G., Foucher, F., Gautret, P., Hubert, a., Sorieul, S., Grassineau, N., and Guido, D.M., 2015, Archean (3.33 Ga) microbe-sediment systems were diverse and flourished in a hydrothermal context: Geology, v. 43, no. 7, p. 615–618, doi: 10.1130/G36646.1.

II.

Morphological adaptations of 3.22 Ga tufted microbial mats to Archean coastal habitats (Moodies Group, Barberton Greenstone Belt, South Africa)

Martin Homann[1], Christoph Heubeck[2], Alessandro Airo[1], Michael M. Tice[3]

Precambrian Research, 2015, 266, 47-64, doi:10.1016/j.precamres.2015.04.018

[1]Institute of Geological Sciences, Freie Universität Berlin

[2]Department of Geosciences, Friedrich-Schiller-Universität Jena

[3]Department of Geology & Geophysics, Texas A&M University

II.1 Abstract

Microbial life was well established and widespread by the Paleoarchean; however, the degree of evolutionary advancement such as microbial motility, intra- and inter-species interactions, phototropism, or oxygenic photosynthesis by that time remains highly debated. The 3.22 Ga Moodies Group in the Barberton Greenstone Belt (BGB, South Africa) are Earth's oldest well-preserved siliciclastic tidal deposits. They exhibit a unique assemblage of microbial mats, providing an excellent opportunity to decipher the morphological adaptations of microbial communities to different paleoenvironmental settings. The fossil mats are preserved as kerogenous laminations (0.5 - 1 mm thick) that can be traced laterally for ~15 km in a ~1000 m-thick succession of fine- to coarse-grained tidal sandstones and conglomerates. We here present a detailed stratigraphic and depositional facies analysis, documenting the association of the three principal mat morphotypes with specific environmental settings: (1) planar-type in coastal floodplain, (2) wavy-type in intertidal, and (3) tufted-type in upper inter- to supratidal facies. All mat types indicate a flourishing phototrophic biota; moreover, the tufted morphology suggests an intricate level of coordinated growth commonly known from cyanobacterial mats in modern environments.

II.2 Introduction

The study of the diversity and setting of early Archean ecosystems is essential for unraveling the phyolgenetic tree of life and the onset of oxygenic photosynthesis, the principal source of free oxygen in the atmosphere. Although the atmospheric oxygen concentration first rose globally and permanently during the 'Great Oxidation Event' (GOE), 2.5 - 2.3 Ga ago, several recent geochemical studies suggest a prolonged and dynamic transition from anoxic conditions, starting 3 Ga ago or even earlier (Holland, 2002, 2006; Anbar et al., 2007; Buick, 2008; Farquhar et al., 2011; Crowe et al., 2013; Lyons et al., 2014; Mukhopadhyay et al., 2014; Planavsky et al., 2014; Lalonde and Konhauser, 2015).Studies aiming to investigate the structure and diversity of early microbial communities are essentially restricted to two locations worldwide in which sedimentary rocks have escaped regional high-grade metamorphism and penetrative deformation: the Pilbara Craton of Western Australia and the Barberton Greenstone Belt (BGB) of the Kaapvaal Craton of southern Africa. In the strata of the BGB, a variety of microbial traces are preserved, e.g., carbonaceous chert containing filamentous, coccoidal and spindle-shaped microfossils (Walsh and Lowe, 1985, 1999; Walsh, 1992; Westall et al., 2006), planar microbial mats (Tice et al., 2004; Tice and Lowe, 2006; Tice, 2009), pseudocolumnar, stromatolite-like structures (Byerly et al., 1986; Walsh and Westall, 2003 and references therein), and organic-walled, spheroidal microfossils (Javaux et al., 2010). Moreover, the BGB includes the world's oldest known regionally mappable record of microbial mats in a siliciclastic tidal setting, exposed in the 3.22 Ga, and remarkably well-preserved Moodies Group (Noffke et al., 2006; Heubeck, 2009; Gamper et al., 2012).

Initially, the macroscopic laminations described here were interpreted as shale partings in horizontally bedded sandstones (Visser, 1956; Eriksson, 1977); however, Heubeck and Lowe (1994a) noted that the laminae were anastomosing in cross-section and exhibited mushroom-shaped protrusions. Subsequently, Noffke et al. (2006), Heubeck (2009), and Gamper et al. (2012) established their biogenicity, based on carbonaceous composition, sedimentary environment, negative $\delta^{13}C$ values (-22.5‰ to -20.1‰), and specific local textures such as eroded microbial mat fragments and fluid-escape structures. We here present the first detailed characterization of the paleoenvironmental context of the Moodies mats, and discuss the environmental adaptation of the mats in comparison with modern microbial ecosystems.

II.3 Regional geology

The Barberton Greenstone Belt (3.57 to ca. 3.22 Ga) of South Africa and Swaziland is located at the eastern margin of the Kaapvaal Craton (Fig.II.1) and represents one of world's oldest Archean greenstone belts. The greenstone belt fill (the Barberton Supergroup, formerly Swaziland Supergroup) is subdivided into (1) the ~8 - 10 km thick, ca. 3.57 - 3.30 Ga volcanic-dominated Onverwacht Group (Viljoen and Viljoen, 1969; Anhaeusser, 1976; Lowe and Byerly, 2007; De Wit et al., 2011); (2) the up to 3 km thick, ca. 3.55 - 3.25 Ga

Fig Tree Group, which includes mostly shale, banded iron-formation (BIF), and volcaniclastic sediments (Heinrichs and Reimer,1977; Condie, 1997; Lowe and Byerly, 1999; Hofmann, 2005); and (3) the up to 3.7 km thick, coarse siliciclastic Moodies Group (Eriksson, 1977; Heubeck and Lowe, 1994a, 1994b, 1999). All BGB strata experienced several phases of major deformation during which they were extensively folded, faulted and altered (De Ronde and De Wit, 1994; Lowe and Byerly, 1999). A major fault system, the Inyoka Fault, transects the greenstone belt approximately medially. The dominant large-scale orogeny of the BGB took place contemporaneously with deposition of the Moodies Group at 3.225 - 3.215 Ma (Lamb and Paris, 1988; Heubeck et al., 2013).

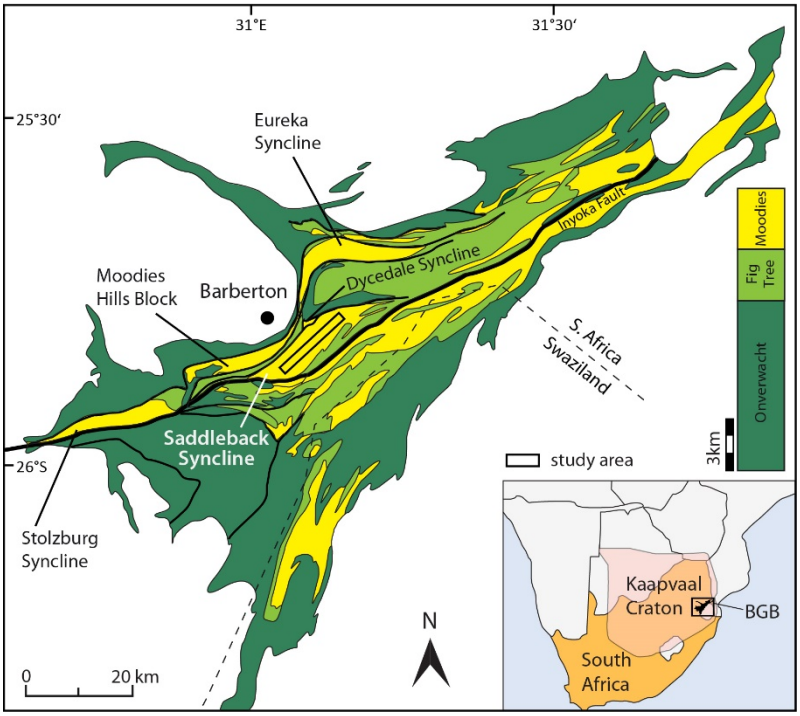

Figure II. 1: *Simplified geological map of the Barberton Greenstone Belt (BGB) of South Africa and Swaziland, comprising the Onverwacht, Fig Tree and Moodies groups, in the eastern part of the Kaapvaal Craton. Moodies strata crop out in five synclines north of the Inyoka Fault: the Stolzburg Syncline, the Moodies Hills Block, the Eureka Syncline, the Dycedale Syncline and the Saddleback Syncline as well as in synclines to the South of the Inyoka Fault. The boxed area shows the study area in the Saddleback Syncline.*

II.4. The Moodies Group

Strata of the Moodies Group are laterally traceable and can be subdivided stratigraphically, allowing the identification of distinct facies and their transitions (Hall, 1918; Visser, 1956; Anhaeusser, 1976; Eriksson, 1977, 1978, 1979, 1980; Heubeck and Lowe, 1994a, 1994b, 1999; Eriksson and Simpson, 2000; Eriksson et al., 2006; Heubeck, 2009; Simpson et al., 2012). Moodies Group strata north of the Inyoka Fault are preserved in several, commonly northward-overturned synclines that are tectonically separated by major

faults (Fig.II.1). Strata there are dominated by fine- to coarse-grained, quartz-rich sandstones that are locally interbedded with conglomerates and were deposited in alluvial, fluvial, possibly aeolian, deltaic, tidal, and subtidal paleoenvironments (Anhaeusser, 1976; Eriksson, 1977, 1979; Heubeck and Lowe, 1999, 1994a; Eriksson and Simpson, 2000; Eriksson et al., 2006; Simpson et al., 2012). Minor components include shales, siltstones, BIF, thin tuffs, and a single basaltic lava (Bontognali et al., 2013; Heubeck et al., 2013). Moodies Group strata south of the Inyoka Fault are dominated by coarse-grained, gravelly sandstones that lack feldspar and marker units and have not been correlated with the strata north of the fault (Heubeck and Lowe, 1994a). The Moodies Group north of the Inyoka Fault was subdivided in several informal lithostratigraphic members and in three formally defined formations (Joe's Luck, Clutha, and Baviaanskop) by Visser (1956) and Anhaeusser (1976), respectively; Eriksson (1977) suggested an alternative subdivision in five fining-upward sequences (MD1 through MD5). Petrofacies trends in sandstone composition in the lower Moodies Group were interpreted by Heubeck and Lowe (1994a) as indicative of an extensional setting, while the architecture and composition of the upper Moodies Group indicated a response to syndepositional shortening along the northern margin of the greenstone belt and incipient basin uplift. The best-preserved and strain-free Moodies sandstones are silicified and occur in the interior of the central BGB, distant from major fault zones, BGB-marginal strain, and fold hinges. Based on isotopic resetting in barites and carbonates, the regional heating of the BGB was estimated to have reached a minimum temperature of ~200°C (De Ronde et al., 1991; Toulkeridis et al., 1998; Tice et al., 2004). The age of the Moodies Group is constrained by stratiform dacitic tuff beds and felsic dikes radiating from the Kaap Valley Tonalite (KVT) that crosscut beds of the Moodies Hills Block and Eureka Syncline along the northern margin of the BGB (Layer et al., 1996; Heubeck et al., 2013). Depositional ages of the volcanic beds throughout the Moodies Group, obtained through single-zircon U-Pb dating, indicate that deposition began ~3223 ± 1 Ma and had ended by ~3219 ± 9 Ma (De Ronde and Kamo, 2000; Heubeck et al., 2013). Consequently, the >3 km thick Moodies succession was deposited and deformed within <1 - 14 Ma and with that represents a unique, very-high-resolution archive of Archean surface and sedimentation processes, comparable in spatial and temporal resolution to many Quaternary sections.

One of the most intriguing features of Moodies sandstones is the occurrence of locally abundant, macroscopically visible, microbial mats and associated structures, preserved in exquisite detail, which are the focus of this work. Mapping and regional field studies demonstrate that these are preserved best in the overturned limb of the Saddleback Syncline in the central BGB in a ca. 3 km-thick succession of subvertically dipping, laterally continuous and unfaulted strata (Figs. II.1 and II.2). For the current study, we investigated strata of the lower section of this succession, which are equivalent to units MdB and MdQ1 of Anhaeusser (1976) and to unit MD1 and MD3 of (Eriksson, 1977); they reach approximately 1350 m thick (Fig. II.2). Over large parts of this area, the very resistant, quartz-cemented sandstones are exposed in large tilted rock faces that allow detailed observations from the sub-mm to km scale.

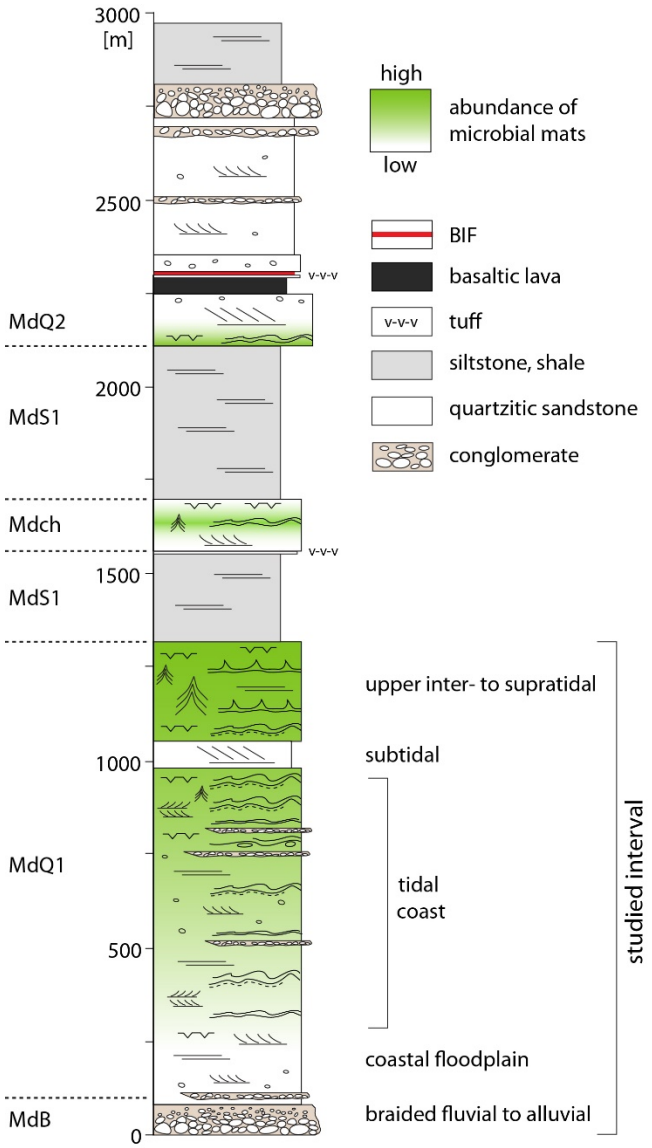

Figure II. 2: *Generalized stratigraphy of the Moodies Group in the Saddleback Syncline in the central BGB. Note that microbial mats in the studied interval are clearly restricted to peritidal, shallow-water paleoenvironments. Stratigraphic abbreviations follow Anhaeusser (1976) and Lowe et al. (2012); MdB = Moodies basal conglomerate, MdQ1 = Moodies medium- to coarse-grained quarzitic sandstone, MdS1 = Moodies fine-grained sand- and siltstones, MdCh = Moodies sandstone with cherty lithic grains, MdQ2 = Moodies coarse-grained quartz arenite. For explanation of symbols and signatures in the column, see legend of Fig. II.3.*

II.5 Data and methods

We measured and correlated eighteen detailed stratigraphic sections of 50 - 700 m length on the southern, overturned limb of the Saddleback Syncline along approx. 15 km strike length (Fig. II.3). At several locations, we constructed facies maps. Approximately fifty slabbed and polished samples supplemented the field observations and were used for detailed observations, thin sectioning, and photography of microbial mat textures and morphologies.

Paleocurrent data were mainly measured on planar and trough-cross stratified sandstones; data from clast imbrication and ripple crest orientation were used only in a few cases. All measurements were corrected for tectonic fold plunge and tilt of bedding using the structural parameters listed by Heubeck and Lowe (1994a). Rose diagrams were constructed using Stereonet 8.9.1 (Allmendinger et al., 2012). Grain size measurements of polished thin sections were performed by using the software ImageJ 1.49n. Relative coordinates, orientation, and the apparent long and short axis length of each resolvable grain were recorded for more than 3000 grains. Elemental mapping of polished rock chips was performed using a Horiba XGT-7000 X-ray fluorescence microanalyzer with a spatial resolution of 10 µm at Texas A&M University.

II.6 Stratigraphy and facies of the Saddleback Syncline

The investigated strata expose a variety of abundant and well-preserved sedimentary structures which allow interpretation of hydrodynamic processes and detailed reconstruction of paleoenvironments. They show only minor and localized brittle deformation and are crosscut by diabase dikes dated at ca. 2950 Ma (Klausen et al., 2010) and one prominent postdepositional strike-slip fault with an estimated offset of approx. 600 m (Fig. II.3). Based on lithological composition, characteristic sedimentary structures and textures, internal and external geometries and vertical facies relationships, five major depositional facies can be distinguished (Fig. II.3, Table 1). All following descriptions and interpretations refer to the Saddleback Syncline.

II.6.1 Facies 1: braided fluvial to alluvial

II.6.1.1 Description

The Moodies basal conglomerate (MdB) overlies felsic volcanic and volcaniclastic rocks of the Schoongezicht Formation of the Fig Tree Group with gradational contact and thins to the southwest (Heubeck and Lowe, 1994a). It is a polymict, clast-supported, pebble-and-cobble conglomerate, commonly interbedded with lenses of sand-matrix-supported conglomerate and gravelly sandstone, which increase toward the top of this unit (Heubeck and Lowe, 1994b; Fig. II.4A). Dominant sedimentary structures include clast imbrication and horizontal stratification.

II.6.1.2 Interpretation

The low compositional and textural maturity of this conglomerate and its rapid lateral changes in composition and thickness point to a proximal origin and indicate deposition in a braided fluvial to alluvial environment (Eriksson, 1978, 1980; Heubeck and Lowe, 1994a).

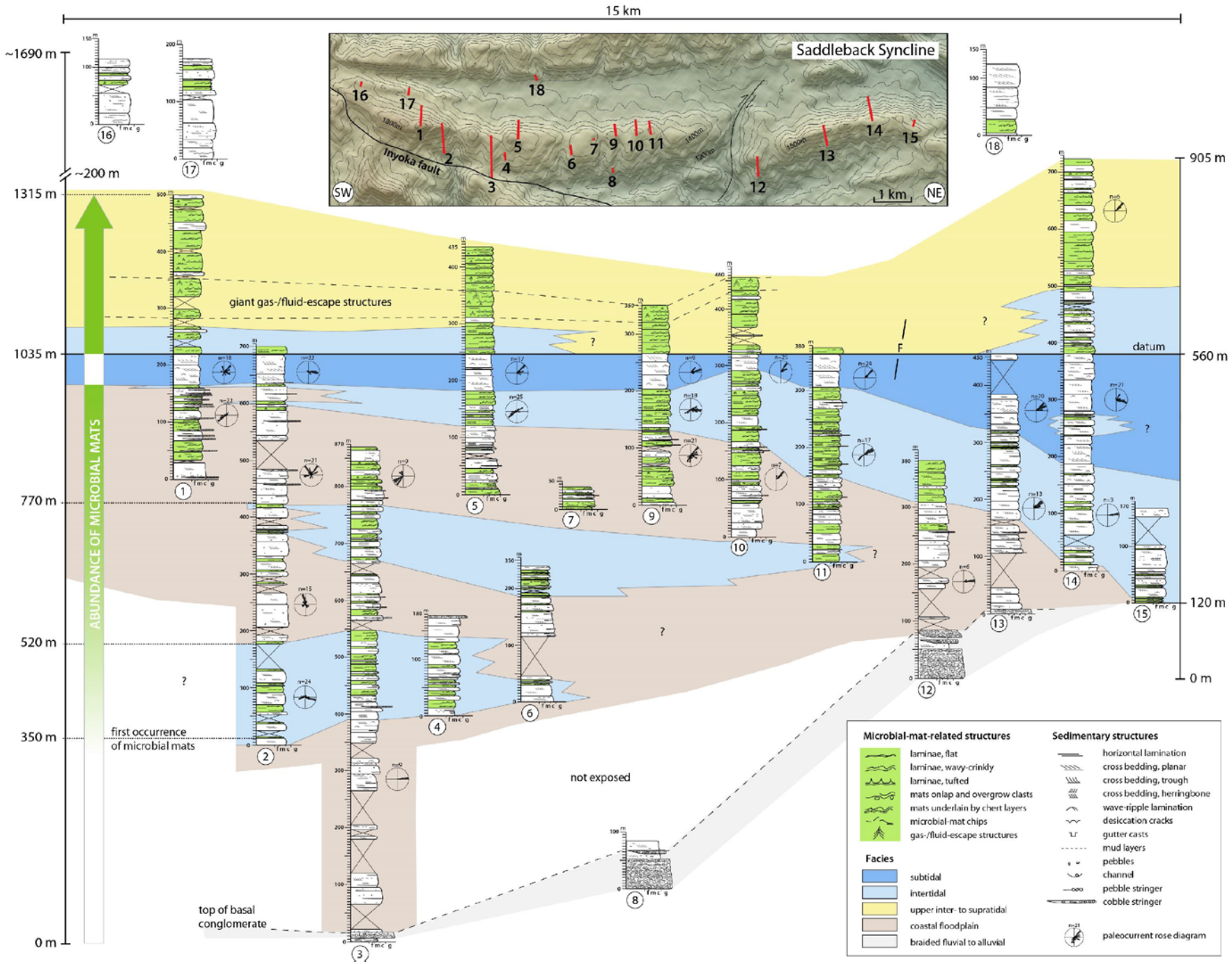
15 km
~1690 m
~200 m
1315 m
1035 m
770 m
520 m
350 m
0 m
905 m
560 m
120 m
0 m
datum
Saddleback Syncline
Inyoka fault
SW
NE
1 km
giant gas-/fluid-escape structures
ABUNDANCE OF MICROBIAL MATS
first occurrence
of microbial mats
top of basal
conglomerate
not exposed
Microbial-mat-related structures
laminae, flat
laminae, wavy-crinkly
laminae, tufted
mats onlap and overgrow clasts
mats underlain by chert layers
microbial-mat chips
gas-/fluid-escape structures
Facies
subtidal
intertidal
upper inter- to supratidal
coastal floodplain
braided fluvial to alluvial
Sedimentary structures
horizontal lamination
cross bedding, planar
cross bedding, trough
cross bedding, herringbone
wave-ripple lamination
desiccation cracks
gutter casts
mud layers
pebbles
channel
pebble stringer
cobble stringer
paleocurrent rose diagram

◄ ***Figure II. 3:*** *Integrated stratigraphic and depositional facies correlation of measured sections in the Saddleback Syncline. Locations of each section are indicated in the topographic map (inset). Microbial mats and related structures (highlighted in green) appear confined to the coastal floodplain, supra- and intertidal paleoenvironments and are absent in the subtidal zone. Note the interval with giant gas-/fluid-escape structures that spans over 7 km in the upper parts of the studied succession in the upper inter- to supratidal facies. Paleoflow is mainly bidirectional and oriented towards the NE and SW in the intertidal and coastal floodplain facies; it appears unidirectional towards the NE in the subtidal facies. For a detailed description of the lithofacies, see Table II.1.*

Table II.1

Facies description and interpretation of the studied succession in the Saddleback Syncline.

Lithofacies	Lithologic description	Microbial-mat-related structures	Depositional environment	Water depth
basal conglomerate	polymict pebble-cobble conglomerate, clast supported interbedded with gravelly sandstone	not observed	*braided fluvial to alluvial* (Eriksson, 1978, 1980; Heubeck and Lowe, 1994a)	0 - 1 m
poorly-sorted, medium- to coarse-grained sandstone with gravel beds	planar and trough cross bedding (up to 0.3 m); gravelly beds extend ~150 m along strike local erosive channels (50 cm-wide) common desiccation cracks	planar microbial laminae pebble-cobble overgrowth rare chert layers, mat chips gas-/fluid-escape structures (~0.2 m)	*coastal floodplain* paleoflow direction mainly to the NE or SW	0 - 2m
medium-sorted, medium- to coarse-grained sandstone and minor mudstone	horizontal bedding abundant desiccation cracks	microbial mats with tufts (0.3 - 1 cm, when vertically stacked up to 2 cm), filled with nodular chert concretions common chert layers mat chips, shrinkage cracks large gas-/fluid-escape structures (0.5 - 6 m in height), polygonal cracks gas domes, fenestral fabric	*upper inter- to supratidal*	0 - 3 m
medium-sorted, medium- to coarse-grained sandstone with pebble beds	herringbone cross bedding, sigmoidal foreset bundles (up to 0.5 m), mud drapes reactivation surfaces rare desiccation cracks sinuous-crested ripples small channels (10 - 20 cm wide) pebbly conglomerate stringers	wavy-crinkly microbial laminae with small microbial domes abundant chert layers and mat chips gas-/fluid-escape structures (~0.4 m)	*intertidal* bidirectional paleoflow towards the NE and SW	0 - 5 m
well-sorted, medium-grained, intensely silicified sandstone	large-scale, low-angle, planar foresets (up to 4 m); rare trough cross bedding (20 - 40 cm) straight-crested ripples; gutter casts	not observed	*subtidal* unidirectional paleoflow to the NE and E	5 - 15 m

II.6.2 Facies 2: coastal floodplain

II. 6.2.1 Description

Medium-bedded, poorly sorted, medium-to coarse-grained sandstones are confined to the lower part of the studied succession. Low-angle planar and trough cross bedding in which foresets reach up to 0.3 m in preserved height is abundant. Sandstones are commonly pebbly or cobbly. Wedge-shaped conglomerates (single-clast to <0.6 m thick), predominantly composed of black or black-and-white-layered chert, but felsic porphyry clasts, altered ultramafic volcanic rock and BIF also occur (Fig. II.4B). These units can be followed laterally for up to 150 m. Clast diameter ranges between 0.5 and 16.5 cm with a mean value of 6 cm (n=148). The conglomeratic sandstones are locally associated with desiccation cracks on thin, discontinuous mudstone partings (Fig. II.7A). Minor erosional channels up to 50 cm wide and up to 20 cm deep are filled by basal pebble lags overlain by trough-cross-bedded sandstone (Fig. II.4C). Paleocurrent measurements yield mainly directions oriented towards the NE or SW (Fig. II.3).

II.6.2.2 Interpretation

Low-angle cross-stratification in sandstone and lenticular conglomerates suggest dominant upper flow-regime conditions under high shear stress and high to medium current velocities. Rare desiccation cracks indicate ponding of shallow bodies of standing water and subaerial exposure. Altogether, these are common features on unvegetated coastal floodplains (Long, 2004; Heubeck, 2009; Fralick and Zaniewski, 2012). This facies is overlain and interfingers towards the northeast with intertidal deposits (Fig. II.3).

II.6.3 Facies 3: upper intertidal to supratidal

II.6.3.1 Description

Thin-bedded, poorly sorted, medium- to coarse-grained sandstone occurs widely in the upper part of the studied strata. These are commonly subhorizontally laminated, weather recessively and occasionally show a fenestral fabric (Fig.II. 4D). This fabric is characterized by isolated, empty or chert-filled cavities, usually 1 - 20 mm across, which are commonly elongated parallel to bedding. Desiccation cracks on thin discontinuous mudstone partings, filled with coarse-grained sandstone, are also common (Fig. II.4E).

II.6.3.2 Interpretation

Abundant desiccation cracks indicate that these strata were deposited in shallow to very shallow water in a low-energetic environment with occasional subaerial exposure. This may have occurred in an upper intertidal to supratidal setting which was periodically inundated (Terwindt, 1988). Fenestral fabrics commonly form in these environments e.g. due to entrapment of gas in the sediment, produced by the decay of buried organic matter (Gerdes, 2007, see section 6.4)

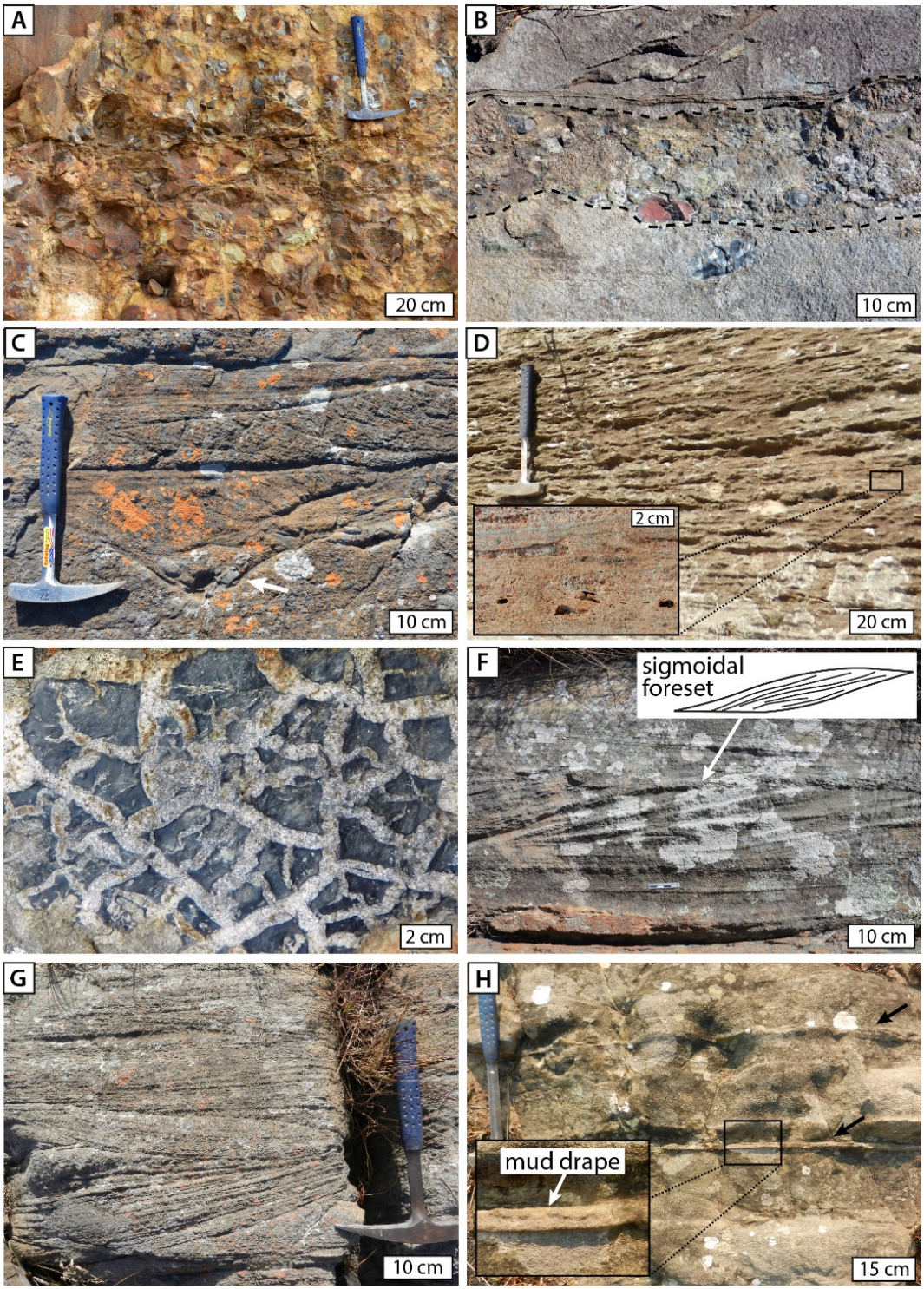

Figure II. 4: *Field photographs of sedimentary structures from the braided fluvial-alluvial (A), coastal floodplain (B and C), upper inter- to supratidal (D and E), and intertidal facies (F - H) in the lower half of the Saddleback Syncline stratigraphy. (A) Cross-section view of polymict, clast-supported conglomerate from the basal Moodies Group. (B) Cross-section view of erosive pebble-cobble bed (in dashed lines). (C) Cross-section view of erosional channel filled with trough-cross-bedded sandstone and lag deposit at the base (arrow). (D) Cross-section view of subhorizontally-laminated sandstone with fenestral fabric. (E) Desiccation cracks on thin mudstone partings filled with coarse-grained sandstone (bedding plane view). (F) Cross-section view of a sigmoidal-shaped foreset and simplified sketch. (G) Bidirectionally-oriented foresets interpreted as herring bone cross stratification. (H) Cross-section view of planar foresets with mud drapes (arrows).*

II.6.4 Facies 4: intertidal

II.6.4.1 Description

Sandstones of this facies are moderately to poorly sorted, medium-to coarse-grained, rarely interbedded with pebble stringers and single pebbles, and commonly form sigmoidal foreset bundles (Fig. II.4F) and sinuous-crested ripples. Small erosive channels of 10 - 20 cm in width and a few cm in depth, reactivation surfaces and herringbone cross stratification are also common (Fig. II.4G). Individual foresets may be mud-draped and reach a maximum height of 0.5 m (Fig. II.4H). Desiccation cracks are less abundant. The foresets show consistent bidirectional paleocurrent directions towards the NE and SW (Fig. II.3).

II.6.4.2 Interpretation

Reversing currents, sigmoidal-shaped foresets, highly varying flow velocities at shallow water depths and channelization are indicative of intertidal settings (Alam et al., 1985; Kreisa and Moila, 1986; Terwindt, 1988; Eriksson and Simpson, 2004). Mud drapes, formed due to slack-water deposition during current reversals, also are good indicators for tidally-influenced environments (Eriksson et al., 2006; Nichols, 2009).

II.6.5 Facies 5: subtidal

II.6.5.1 Description

The deposits of this facies are represented widely by resistantly weathering, thick-bedded, moderately to well sorted, medium-grained sandstones. The top of this facies was selected as the datum for correlation of the measured stratigraphic sections because the contact is readily recognizable in the field and has excellent lateral continuity (Fig. II.3). Large-scale, low-angle planar foresets up to 4 m in preserved thickness (Fig. II.5A) are characteristic; trough cross bedding (0.2 - 0.4 m) is less common. Paleocurrent directions indicate an unidirectional flow to the NE and were reconstructed based on the orientation of foresets and straight-crested symmetrical- to asymmetrical ripples (Figs. II.3 and II.5B and C). Steep-sided symmetrical depressions, approximately 4 cm deep and 10 cm wide, are rare (Fig. II.5D).

II.6.5.2 Interpretation

The large-scale foresets represent remnants of unidirectionally-migrating dunes forming sand ridges in the subtidal shoreface zone (Desjardins et al., 2012; Nichols, 2009). Such large, elongated sand bodies are usually oriented obliquely to the coastline and often generated near shorelines that experience strong tidal currents and storms (Stubblefield et al., 1984). Small and steep erosional depressions are tentatively interpreted as gutter casts, which form in shallow-marine environments due to unidirectional current flow, often triggered by storms, or by the passing of a tidal bore (Allen, 1984; Myrow, 1992; Johnson and Baldwin, 1996; Archer, 2013). Although the size and uniformity of the foresets could also be expected from an aeolian dune setting, the absence of diagnostic aeolian features such as inversely graded foresets, pin

stripe lamination, low-angle truncation surfaces, interdune deposits or desiccation cracks make this interpretation unlikely (Fryberger and Schenk, 1988; Eriksson and Simpson, 1998; Simpson et al., 2012).

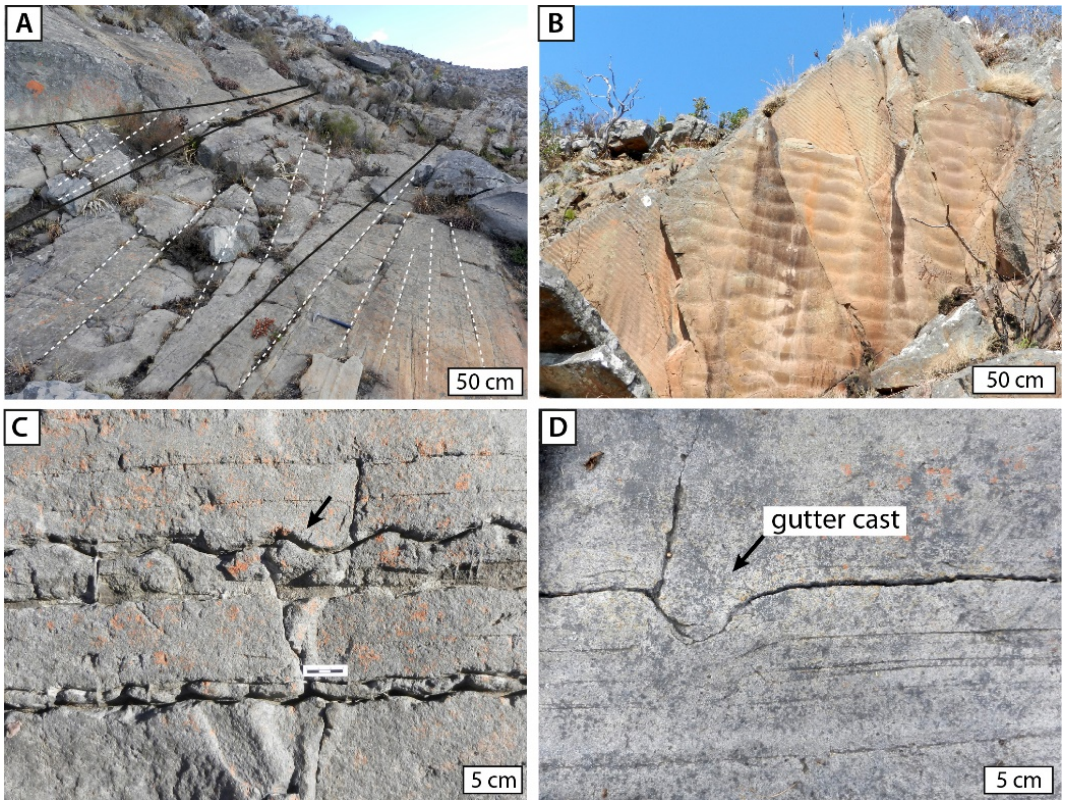

Figure II. 5: *Field photographs of common sedimentary structures in the subtidal sand ridge deposits. (A) Low angle planar foresets showing almost 4 m of preserved thickness. (B) Bedding plane view of asymmetrical ripples. (C) Cross-section view of straight-crested, symmetrical ripples (arrow). (D) Erosional depression in cross-section view, interpreted as gutter cast.*

II.7 Identification and classification of microbial mats

The biomass of microbial mats is inevitably subject to degradation upon burial. If the decomposition of the organic matter remains incomplete, carbonaceous material (kerogen) will remain and delineate the former location of the mat as a lamina. However, commonly, no organic material is preserved. In such cases, the former presence of a microbial mat can only be inferred indirectly through physical or chemical properties of the sediment, e.g., indications of resistance to erosion, cohesiveness, modified permeability and mat-related mineralization (Schieber, 1999, 2004; Schieber et al., 2007; Gerdes et al., 2000; Noffke et al., 2001a; Noffke, 2010). The resulting tell-tale sedimentary features, such as a lamina-specific sorting, shrinkage cracks, microbial sand chips or gas domes, are commonly referred to as microbially-induced sedimentary structures (MISS; Noffke et al., 2001a; Gingras, 2002) or mat-related structures (MRS; Schieber et al., 2007; Eriksson et al., 2010). In the Moodies Group, microbial lamination occurs as black, dark green weathering, erosion-resistant, densely spaced, subparallel crinkly laminae. They show, as detailed below, specific

surface textures and mat morphotypes, evidence of enhanced cohesiveness, and various features indicative of mat destruction, decay and mineralization. The two stratigraphically lowest occurrences of microbial mats occur ~350 m and ~190 m, respectively, above the top of the basal conglomerate in the southwestern and northeastern part of the Saddleback Syncline (Fig. II.3). The overlying sedimentary succession, ~1000 m thick, contains rare to abundant, macroscopically visible microbial mats. The best exposed and laterally most continuous outcrops are found in the upper 700 m of this succession (Figs. II.2 and II.3). Two additional units with widespread, well-developed microbial mats occur in the stratigraphically higher units MdCh of Lowe et al. (2012) and at the base of unit MdQ2 of Anhaeusser (1976) in the upper part of the Moodies Group in the Saddleback Syncline (Fig. II.2). In the following, we will limit our description to the main occurrences of microbial mats showing the most continuous lateral exposure. These largely coincide with the informal lithostratigraphic unit MdQ1 of Anhaeusser (1976).

II.7.1 Kerogenous laminae

II.7.1.1 Description

Black to dark green, 0.5 to 1 mm thick, wavy-crinkly laminations are spaced vertically several millimeters to centimeters apart, separating individual sandstone sets (Fig. II.6A). The green weathering color of the kerogenous laminae is due to minor admixtures of fine-grained chlorite which forms, along with carbonate and quartz, the most abundant minerals in the thick siltstones of the Moodies Group (Fig. II.2). The seemingly homogenous appearance of the laminae can be resolved at microscopic scale into individual, interweaving strands of black carbonaceous matter (Figs. II.6B and C). Where not modified by subsequent early postdepositional processes, the laminae coat sandy and gravelly sedimentary structures including horizontal lamination, individual foresets, sand ripple packages and individual conglomerate clasts (Figs. II.6A and II.7A). Laminations are occasionally cracked and their margins bent upward. They are laterally continuous at outcrop-scale and consistently interbedded with fine- to coarse-grained, occasionally gravelly sandstones, rarely also with conglomerate stringers. Granulometric analysis demonstrates that detrital sand particles are typically fine- to medium-grained below a lamina, fine-grained within it, and medium- to coarse-grained above (Figs. II.6B and C and Fig. II.S1). Particle long-axes within the laminations are usually oriented parallel to bedding, whereas grains below and above the lamination are dominantly randomly oriented. Fine-grained heavy minerals, such as zircon and rutile or anatase are commonly enriched within the lamina (Fig. II.6D). Notable is the near-complete absence of shale.

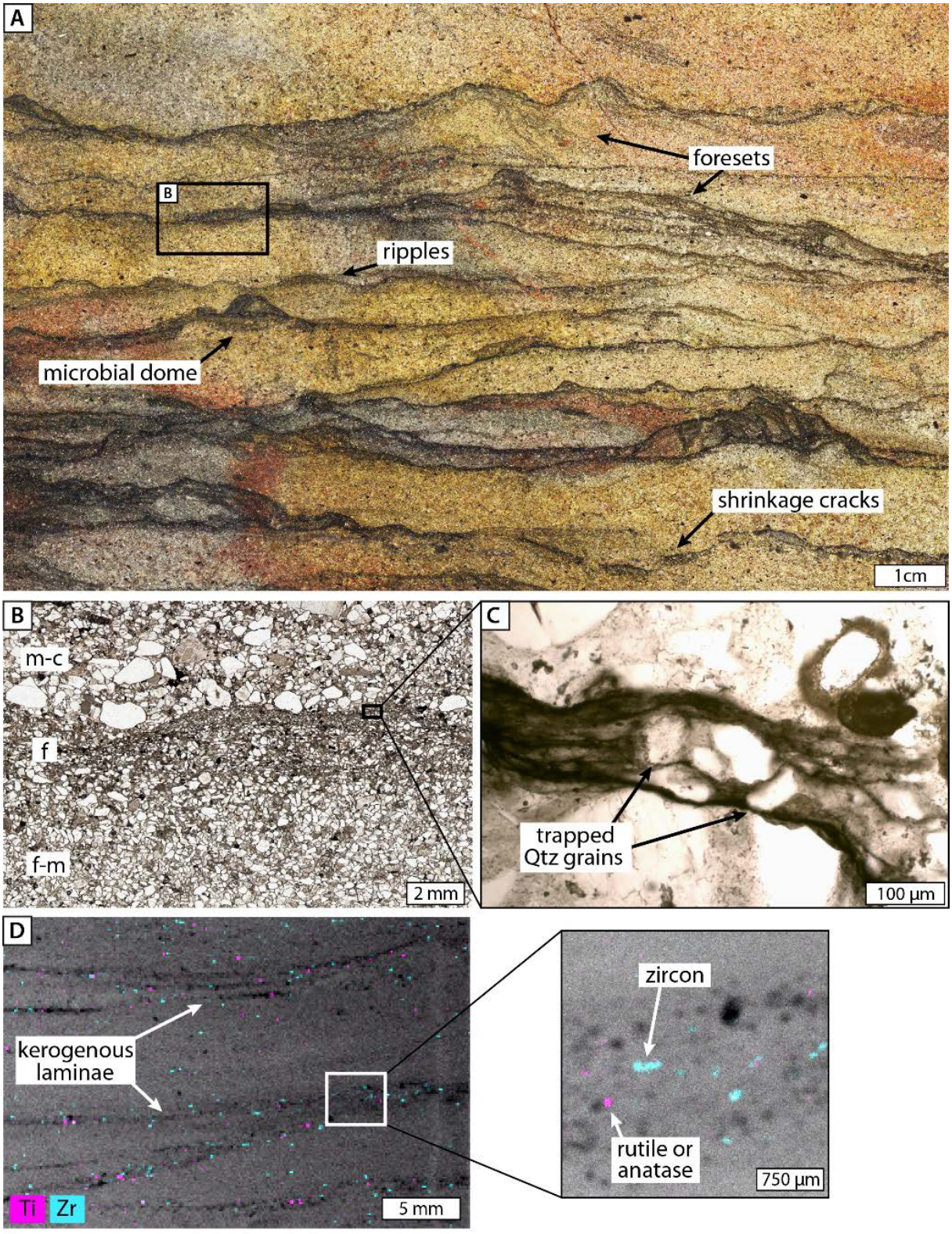

Figure II. 6: *(A) Photograph of polished slab (cross-section view) containing abundant remnants of microbial mats (dark wavy laminae) which coat sand ripples, foresets, form small domes and shrinkage cracks. (B) Transmitted light photomicrograph (of boxed area in A) showing that detrital sand particles are commonly fine- to medium-grained (f-m) below a lamina, fine-grained (f) within and medium-to-coarse-grained (m-c) above a lamina. (C) Close-up view of undulatory kerogenous laminae with fine-grained-sand and silt-sized particles. (D) Trans-X-ray elemental maps of Ti (purple) and Zr (cyan) show the preferential enrichment of zircon and rutile or anatase in the dark microbial laminae.*

II.7.1.2 Interpretation

The morphological similarity of the wavy-crinkly laminae to modern and other fossil microbial mat laminae, their facies setting and the reported negative $\delta^{13}C$ isotope ratios of -22.5‰ to -20.1‰ PDB (Noffke et al., 2006) obtained from these kerogenous laminations are indicative of, and consistent with, a biogenic origin (Schidlowski, 2001). Negative $\delta^{13}C$ values can also be produced by abiotic processes, e.g., through Fischer-Tropsch-type reactions in hydrothermal environments or during the decomposition of siderite under metamorphic conditions (McCollom and Seewald, 2006, and references therein). However, the study area lacks any evidence for hydrothermal activity such as chert veining. The difference in grain size above and below the microbial lamina indicate changes in current velocity which may correspond to periods of enhanced mat growth during phases of reduced water flow velocity and clastic deposition (Noffke et al., 1997; Noffke, 2010). For the grain size distributions determined in thin section, the minimum flow velocities are approximately 0.08 m/s before, 0.06 m/s during, and 0.09 m/s after mat growth (calculated after Williams et al., 2013; Tables II.S1 and II.S2, Fig. II.S1. Observations of modern mat growth suggest that the development of thick mats is usually preceded by the establishment of biofilms during times of low hydrodynamic energy (Krumbein et al., 1994; Noffke et al., 1997). However, it is conceivable that a permanent sediment bypass was occurring during mat growth and only fine-sized particles and heavy mineral grains were trapped within the mat fabric. In contrast, the coarser-grained and poorly sorted sand layers immediately overlying the mats likely reflect depositional events in which current velocities were sufficiently high to transport them but not high enough to erode the mats. During subsequent periods of relative quiescence, the deposited sand was recolonized by microbes which either originated from the water column or migrated upwards from the buried mat over a distance of millimeters to few centimeters (Noffke, 2010). Most laminae represent the rare case of in situ preserved microbial mats which were partly degraded, dehydrated and early cemented, but being only minimally compacted. The accumulation of detrital heavy minerals within the mat fabric, caused by microbial baffling and trapping, is common in epibenthic microbial mats (Gerdes et al., 2000). Consequently, heavy mineral laminations can be indicative of ancient mats and thus could serve as biosignatures where no organic matter has been preserved (Noffke, 2010).

II.7.2 Mat morphotypes and their relationship to siliciclastic facies

II.7.2.1 Description

Environmental parameters inferred from physical sedimentary structures (Table 1) constrain the habitat and biological affinity of the microbial community. Based on our field observations, microbial mats can be assigned to three different paleoenvironments, each associated with a specific mat morphotype:

(1) Planar microbial mats, without any significant morphological relief, are typical of the coastal floodplain zone (section II.6.2; Fig. II.7A). Vertically-oriented growth structures (e.g., microbial domes) are absent. However, laminae occasionally onlap, drape and overgrow thin pebble and cobble conglomerate beds and may occur a few millimeters above and below thin, desiccation-cracked bedding planes (Fig. II.7A).

(2) Wavy-crinkly microbial mats, which are commonly associated with bedding-plane-parallel chert layers, dominate the intertidal zone (section II.6.4; Fig. II.7B). These layers widely contain remnants of carbonate minerals (see description below in section II.7.5). Microbial laminae coat sand ripples and cross-laminations and occasionally form small, isolated microbial domes showing increased lamina density. These preferentially develop on minor topographic highs (Fig. II.8A). Small channels filled by coarse-grained sandstone fill the relief defined by microbial domes (Heubeck, 2009).

(3) Tufted microbial mats are exclusively present in strata that are inferred to represent upper inter- to supratidal facies (section II.6.3; Fig. II.7C). The tufts are typically 0.3 - 1 cm in height but can attain up to 2 cm where they are vertically stacked in cones (Fig. II.7C). Tufts are spaced several centimeters apart and are laterally supported by draping laminae (Figs. II.8B and D). Tufts are sub-circular in horizontal section (Fig. II.8E) and internally filled with fine-grained sediment. Some, however, are filled by nodular microcrystalline quartz (Figs. II.8B and F and II.9A). The density of the kerogenous lamina seemingly increases within the silicified tuft (Figs. II.8D and F).

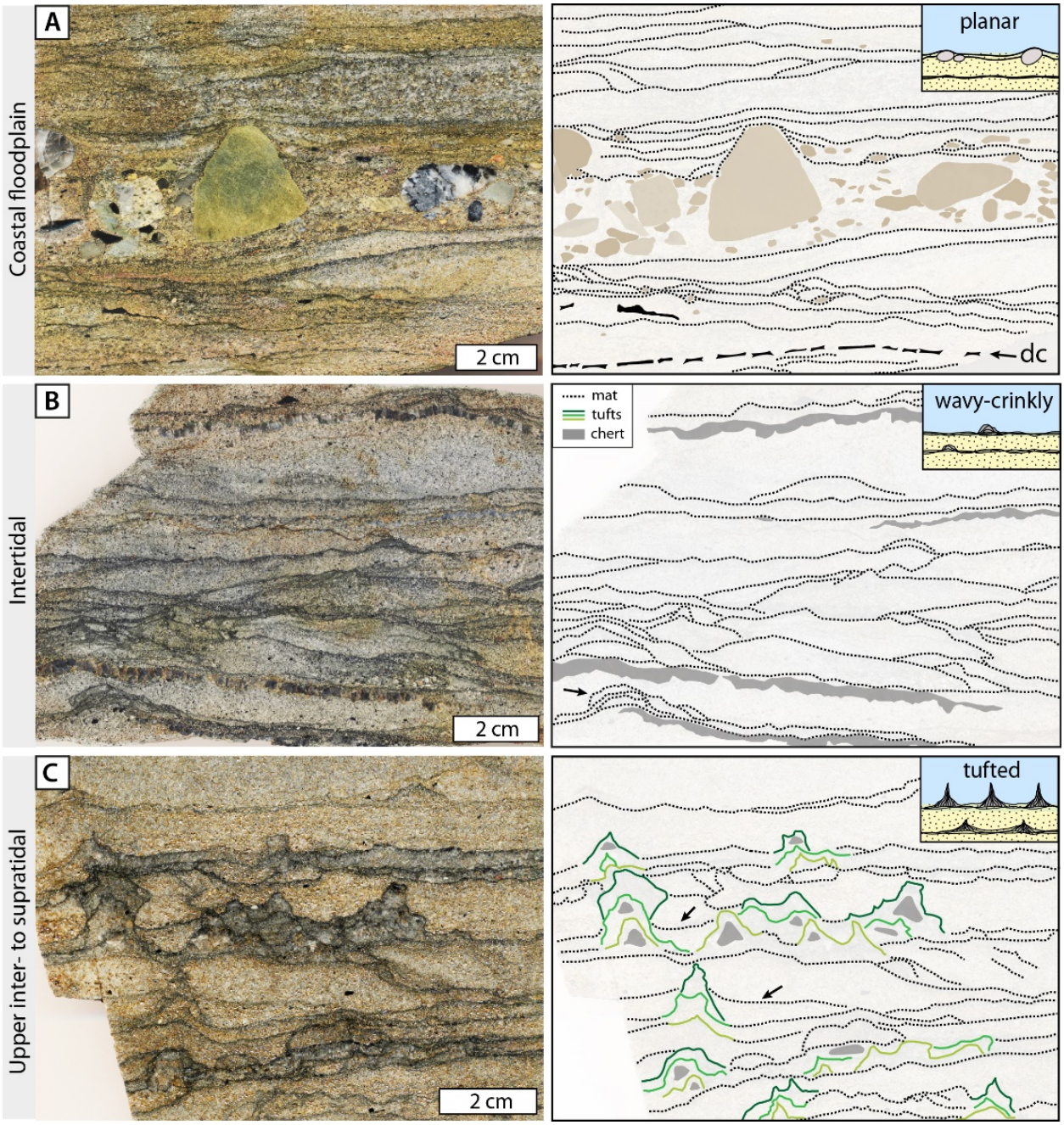

Figure II. 7: *Photographs of polished sandstone slabs (cross-section view) and corresponding sketches, highlighting the mat morphotypes of each paleoenvironment. Reconstructed mat morphologies are indicated in the simplified sketch (top right) for each facies. (A) Planar mats that cover former sedimentary surfaces and occasionally onlap and drape pebbly conglomerate layers; dc = desiccation cracks. (B) Wavy-crinkly mats and small microbial domes (arrow), commonly underlain by bedding-plane-parallel layers of chert. Note that the upper contact of these layers is straight or gently undulating, whereas the lower part is commonly more irregular. (C) Tufted microbial mats with vertically stacked cones that are partially filled with chert and supported by draping laminae (arrows). The successive growth stages of the tufts are depicted by different shades of green.*

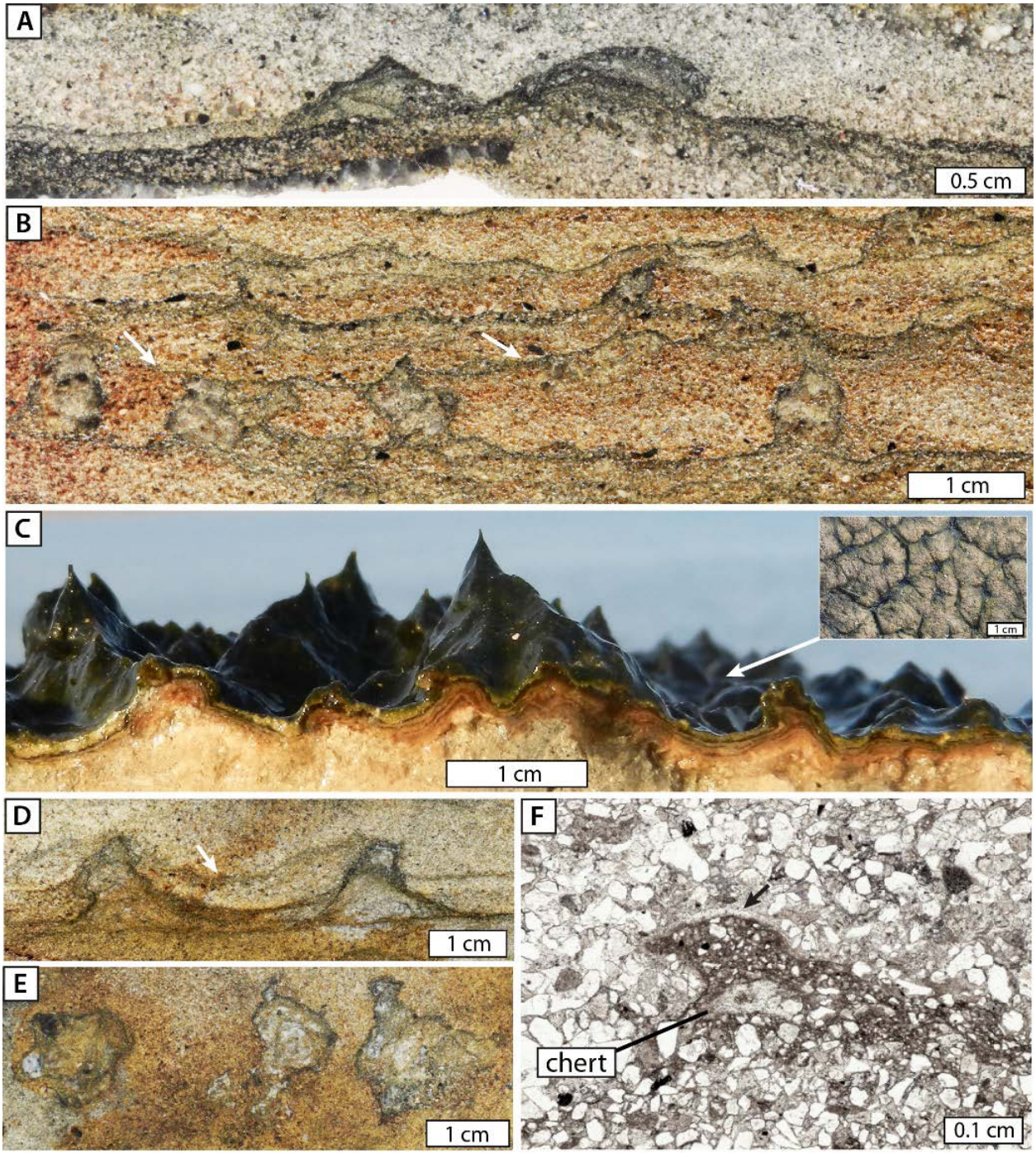

Figure II. 8: *Photographs of polished slabs of microbial tufts and domes and comparison with modern analog. (A) Cross-section view of microbial domes that preferentially develop on small topographic highs and may represent initial growth stages of tufts. (B) Cross-section view of a microbial mat showing closely spaced tufts, interconnected by draping laminae (arrows). The tufts are internally partly filled by chert. (C) Cross-section view of tufted microbial mat from Bahar Alouane (Tunisia) built by vertically oriented bundles of filamentous cyanobacteria. These mats commonly show polygonal patterns of reticulate ridges (arrow) with tufts at ridge junctions in plan view. (D) Cross-section view of two single tufts laterally linked by microbial lamina (arrow). (E) Horizontal section through a tuft layer reveals their sub-circular structure. (F) Transmitted light photomicrograph of a silicified microbial tuft (arrow) with trapped fine-grained sediment. Note the chert-filled void in the central part of the tuft.*

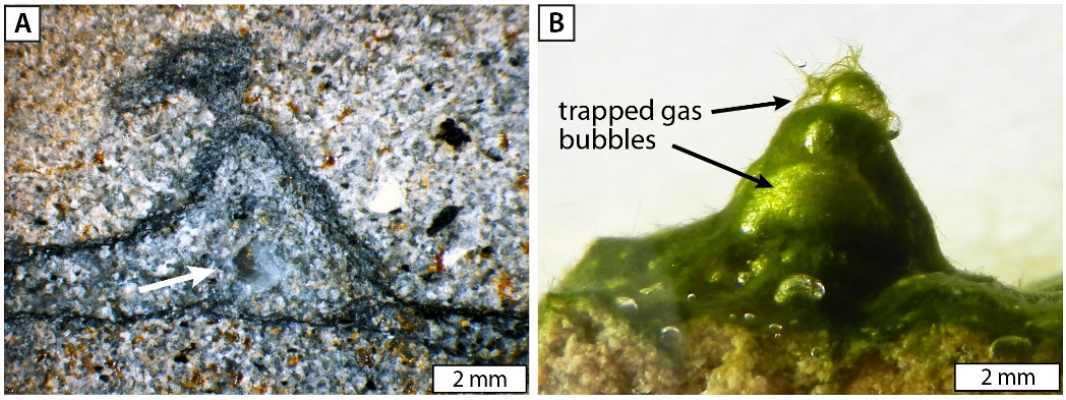

Figure II. 9: *Morphological similarities of gas bubbles trapped in modern tuft from Bahar Alouane, Tunisia in comparison with fossil microbial tuft of the Moodies Group. (A) Polished slab photograph of a tuft with chert-filled void in the central part interpreted as former gas bubble (arrow). (B) Modern tuft with trapped oxygen-rich bubbles enmeshed by filamentous cyanobacteria.*

II.7.2.2 Interpretation

The growth of these three distinct mat morphotypes presumably represents a morphological response of mat-building microbial communities to changing physicochemical conditions (Gerdes et al., 1993, 2000; Battin et al., 2003; Eriksson et al., 2010). The tufted mats, in particular, resemble closely modern tufted microbial mats from Bahar Alouane (Tunisia) that are dominantly built by filamentous cyanobacteria that intertwine and form durable networks of reticulate ridges on the sediment surface (Fig. II.8C, see discussion below in section II.8.4). The nodular chert in the interior of some tufts most likely represent the fill of former gas bubbles that were trapped within the mat fabric, which is well-known from modern cyanobacterial mats that produce oxygen-rich bubbles with strikingly similar morphologies (Figs. II.8F and II.9A and B; Bosak et al., 2010). Microbial tufts and domes in the studied Moodies strata occur confined to the tidally-influenced facies and exhibit almost vertical structures, well above the critical angle of repose for sand grains. These delicate vertical structures appear to have been solely formed and structurally supported by biomass but probably would not have been preserved without early silicification.

II.7.3 Mat destruction and cohesiveness

II.7.3.1 Description

Microbial mat-covered sediment surfaces in the upper inter- to supratidal facies occasionally show polygonal or incomplete networks of cracks with slightly upward-curved margins and sand-filled openings which can be traced over several cm length (Fig. II.10A). These cracks are commonly associated with, but distinct from, more prominent desiccation-cracked mudstone layers (compare Figs. II.6A and II.10B). Occasionally, eroded fragments of mat-bound sediment are incorporated in the shallow and wide channels between cross-bedded sandstones as 1 - 5 mm-thick, ~2 - 9-cm-long, ridged and slightly curved clasts (Figs. II.10C, D and E), forming microbial-sand-chip conglomerates (Pflüger and Gresse, 1996; Eriksson et al., 2007).

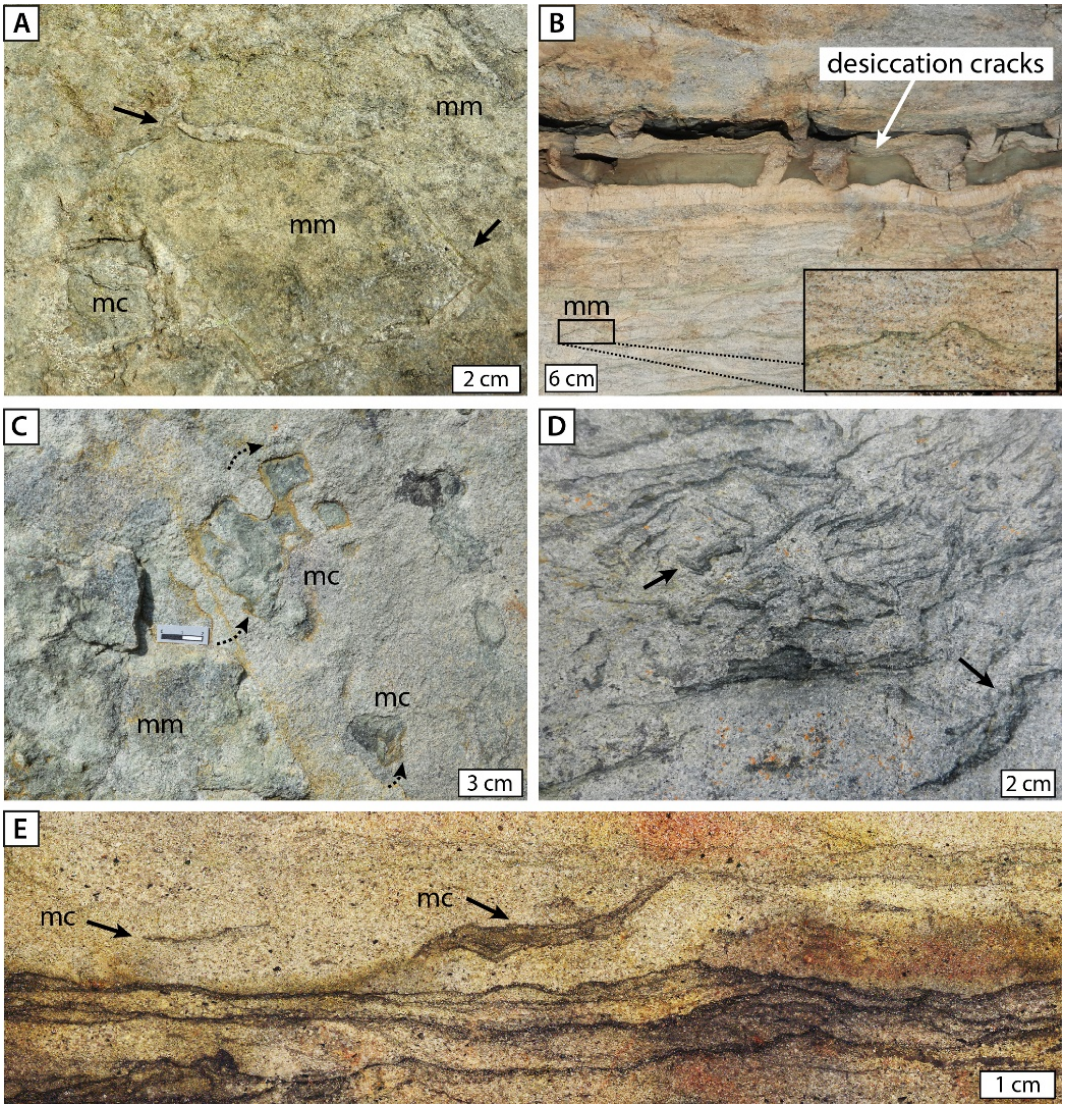

Figure II. 10: *Field and polished slab photographs of cohesive microbial mats from inter- to supratidal paleo-environments that experienced periods of subaerial exposure, dehydration, erosion and redeposition. (A) Bedding plane view of a microbial mat-covered surface (mm) with shrinkage cracks exhibiting a polygonal pattern (arrows). Microbial mat chips (mc) are visible adjacent to these cracks. Note that shrinkage cracks are associated with – but distinct from – desiccation-cracked bedding planes. (B) Cross-section view of microbial-mat-bearing sandstone (mm) intersected by a prominent horizon of desiccation-cracked mudstones. (C) Bedding plane view of microbial mats (mm) associated with microbial mat chips (mc) that presumably were eroded from the edges of the mat (dotted arrows). (D) Eroded mat fragments forming a microbial-sand-chip conglomerate. Note the slightly curved ends of some of the chips (arrows). (E) Cross-section view of densely laminated microbial mats with eroded mat chips (mc) above that presumably had a rigid, cohesive consistency.*

II.7.3.2 Interpretation

Periods of persistent subaerial exposure dehydrate mats, leading to their shrinkage and cracking. The resulting microbial mat chips easily peel off the sandy substrate, are transported by wind or reworked by flowing water and redeposited during flood events (Noffke, 1999; Schieber, 2004; Bouougri and Porada, 2012). Curved and upturned ends of some chips indicate a moderate elasticity while desiccating; however, roll-up structures noted by Noffke et al. (2006) have not been observed. Apparently, the mat chips had a

high rigidity even under turbulent flow. These observations indicate a tough, perhaps leather- or rubber-like consistency, possibly enhanced by early silicification (Schieber, 2004; Tice et al., 2011).

II.7.4 Mat decay

II.7.4.1 Description

In some sandstone beds, microbial mats are disrupted and bent upwards along subvertical linear structures that trend perpendicular to bedding and reach dm to m in height (Fig. II.11A). These structures occur throughout the studied succession are laterally unevenly spaced, but are restricted to microbial mat-bearing sandstones (Fig. II.3). They are particularly common in a ~50-m-thick, densely microbial-mat-laminated section in the upper parts of the MdQ1 unit which can be traced for >7 km in strike length in strata interpreted as upper inter- to supratidal facies (Fig. II.3). In this section, the vertical linear structures occur in medium- to coarse-grained, thin-bedded sandstone. The central area of the subvertical channels shows thread-like, disrupted dark, carbonaceous material and occasionally nodular chert (Fig. II.11A and Fig. II.S2.). Where the linear structures intersect bedding planes, they form a pattern of polygonal cracks of 1 - 5 cm width and several dm length, bordered by two parallel running ridges (Fig. II.11B). The mean vertical extent of 62 surveyed structures in the upper inter- to supratidal facies of the study area is 2.1 m, the maximum height is 6.1 m. The structures are less common in the coastal floodplain and intertidal facies and also smaller. There they reach mean heights of only 0.2 and 0.4 m, respectively (Table II.S1). Subcircular, ~1 - 2 cm-high and ~2 - 8 cm-wide mounds with a prominent central depression locally appear on microbial-mat-covered bedding planes in sandstones with common fenestral fabric, assigned to the supratidal facies (Fig. II.11C).

II.7.4.2 Interpretation

The vertical linear structures bordered by upward-curved mats are best explained as gas- or fluid-escape structures formed in mat-bound sediment in a postdepositional, but early diagenetic stage, indicated by the plastic behavior of the unconsolidated sediment and by the absence of mud (Lowe, 1975; Eriksson, 1979; Heubeck, 2009). Experimental studies of Frey et al. (2009) define a key morphological difference between gas- and water-escape structures: laminations warp downward when deformed by water fluidization but upward when disturbed by gas fluidization as is the case in the examples studied here. The circular mounds with the central depression likely represent smaller, ruptured gas domes and should not be confused with sand volcanoes which are the result of purely physical processes, occuring e.g. during the rising flood in supratidal settings (Dornbos et al., 2007; Taj et al., 2014). Surface sealing by mats which hinder the escape of biogenic gas that either developed from buried organic matter, or was related to metabolic effects of live microbial mats, can trigger the formation of fenestral fabric, gas domes and escape structures (Gerdes et al.,

1993, 2000; Gerdes, 2007; Noffke et al., 2001a; Bose and Chafetz, 2009). However, fluid escape due to the dewatering of compacting mats and sediment cannot be ruled out. The cracks observed on mat-covered bedding planes may form part of larger polygonal crack networks in brittle, superficially cemented sediment through which gas or water escaped. Similar polygonal crack patterns are common in modern upper inter- to supratidal mats (Noffke et al., 2001b; Gerdes, 2007; Noffke, 2010; Bouougri and Porada, 2007; Bose and Chafetz, 2009).

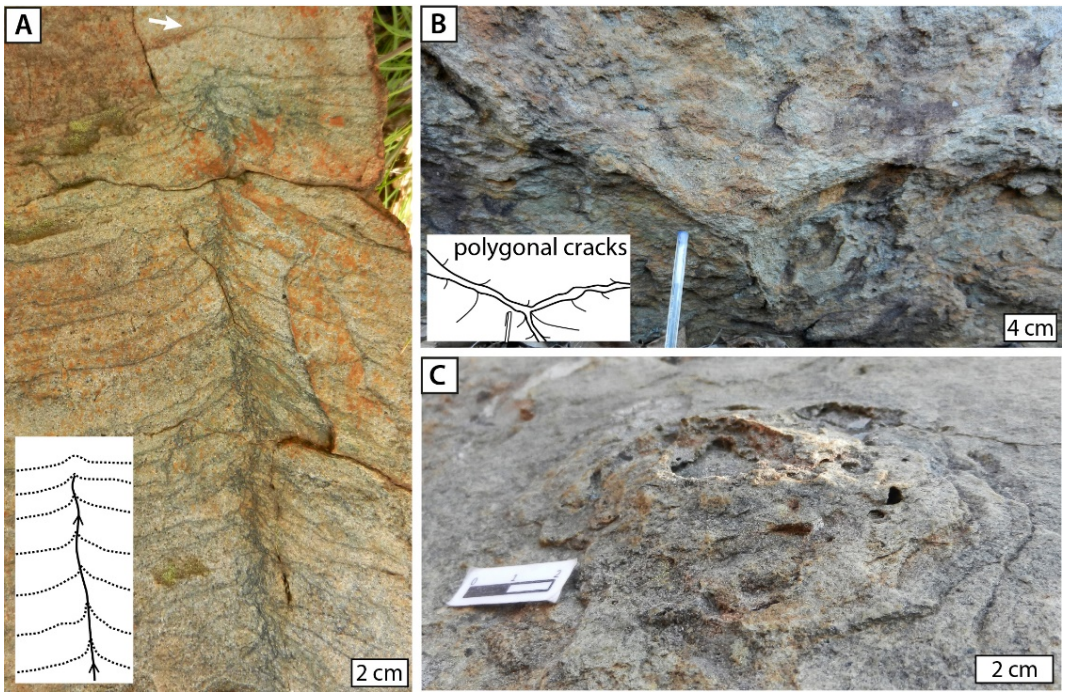

Figure II. 11: *Field photographs of structures related to gas or fluid escape in densely microbial mat-laminated sandstone of the supratidal facies. (A) Cross-section view and simplified sketch of a vertical-oriented gas- or fluid-escape structure bordered by upward-curved microbial mats. The central channel shows a high concentration of carbonaceous material that was probably concentrated in the waning flow. Note the domed mat in the upper part (arrow). (B) Linear cracks on mat-covered bedding plane that may form part of a larger polygonal crack networks. (C) Ruptured gas dome with central depression on a well-preserved bedding plane.*

II.7.5 Mat-associated mineralization

II.7.5.1 Description

Microbial mats in the intertidal zone are widely underlain by bedding-plane-parallel chert layers that are a few mm thick, up to 80 cm long and gradually thin laterally (Figs. II.7B and II.12A and B). In cross- section, these layers show gently undulating upper contacts whereas the contact with the underlying sediment is commonly more irregular (Fig. II.7B). The chert layers are never eroded nor erosive and contain remnants of carbonate minerals. In places, ferroan dolomite makes up more than half of the layers (Figs. II.12A and B). It clearly displays corroded and undulatory grain boundaries, and truncated dolomite twin lamellae, as

well as abundant nucleation centers of chert (Fig. II.12C). Gamper et al. (2012) also described undulating wisps of kerogenous laminations within the chert layers.

II.7.5.2 Interpretation

The occurrence of chert layers a few mm underneath the microbial mats indicates that their formation may be related. Because chert layers are never eroded nor reworked, they likely formed post-depositionally in the shallow subsurface. Hence, the previous interpretation, namely, that these chert layers formed at the sediment-water or sediment-atmosphere interface and may represent very-early-mineralized, patchy microbial mats (suggested by Heubeck, 2009, and by Gamper et al., 2012) now appears less likely. The apparent replacement of carbonate by chert rather suggests that primary carbonates had precipitated

in synsedimentary cavities that developed beneath the microbial mats and were dissolved when pore waters became acidic, which promoted the precipitation of silica. Both processes would also explain the excellent preservation of the delicate microbial tufts. Carbonate precipitation is common in modern photosynthetic mats and is frequently interpreted to be induced through metabolic activity and/or templating of nucleation (Burne and Moore, 1987; Reid et al., 2000; Dupraz et al., 2009; Decho, 2010).

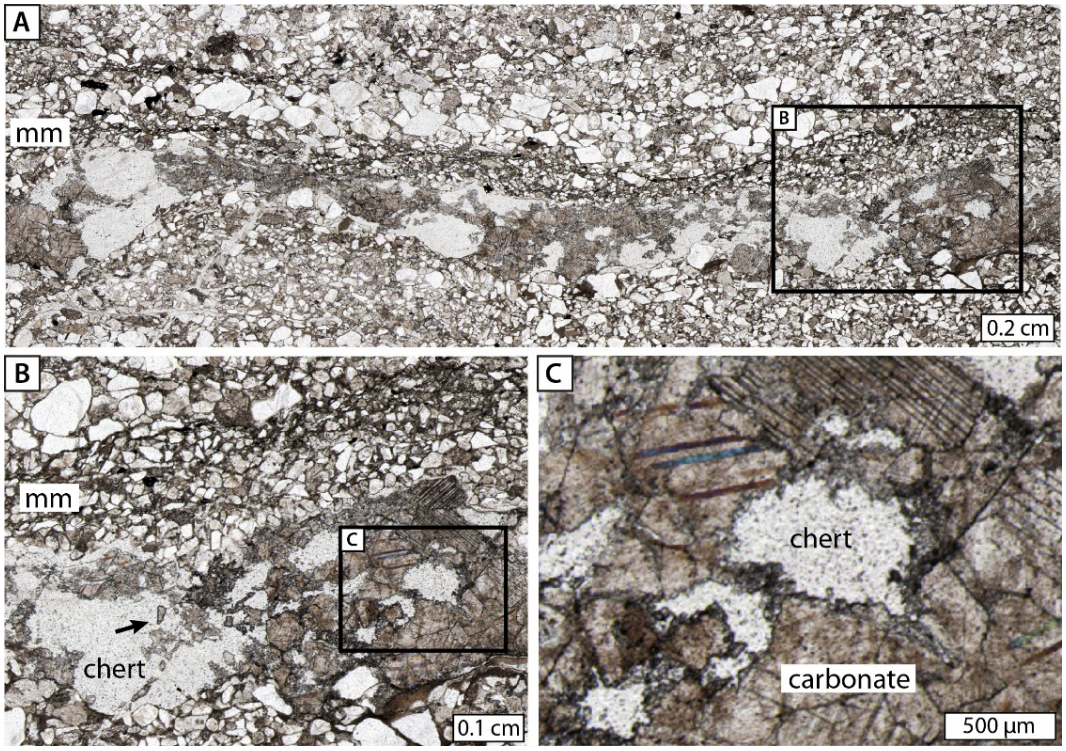

Figure II. 12: *Transmitted light photomicrographs of chert layers underlying microbial mats in cross-section. (A) Microbial mat (mm) underlain by bedding-plane-parallel, up to 4 mm thick chert layer with patchy remnants of carbonates. (B) Close-up view of the boxed area in A, documenting the partial replacement of carbonate by chert. Note small carbonate remnants within chert (arrow). (C) Close-up view of the boxed area in B, showing corroded and undulatory grain boundaries (arrow), and truncation of dolomite twin lamellae, as well as several nucleation centers of chert.*

II.8 Discussion

II.8.1 Facies

Paleoenvironmental reconstructions and facies analysis of Archean depositional systems are often hampered by poor preservation, diagenetic, and metamorphic overprint or post-depositional tectonics (Eriksson et al., 1998; Altermann and Corcoran, 2002; Donaldson et al., 2004; Embry et al., 2004; Van Kranendonk et al., 2007; Wacey, 2009).

In the Saddleback Syncline of the central BGB, however, the outstanding exposure, abundant well-preserved sedimentary structures, high temporal resolution, excellent lateral continuity and only minor metamorphic and tectonic overprint provide a reliable basis for paleoenvironmental reconstructions of Moodies strata, which record the transition from alluvial-braided fluvial to a peritidal shoreline setting, followed by subtidal, then upper inter- to supratidal depositional environments. Two vertical facies trends can be noted in this succession: a deepening- and fining-upward trend from alluvial to subtidal facies, followed by an aggradational, largely shallow-marine upper inter- to supratidal facies. Correlation of measured sections indicates only minor lateral facies changes in the plane of exposure; rather, the overall horizontal superposition of strata reflects an overall aggradational stacking pattern in which subsidence and sediment supply were well balanced.

The most prominent change along strike is a decrease in the number and thickness of thin conglomeratic stringers towards the NE, concomitant with an increase in the thickness of the subtidal facies. This may indicate a southwestern provenance of these sediments. Measured paleocurrents are mostly oriented towards the NE and SW in tidally-influenced strata, and towards the NE and E in the subtidal facies (Fig. II.3). The predominant transport direction of the investigated sandstone succession in the lower half of the Saddleback Syncline is directed towards the NE (Fig. II.3). These observations disagree with previous paleoflow reconstructions of Heubeck and Lowe (1994a, 1999), which had indicated an overall SW-oriented transport direction in the Saddleback Syncline.

A possible explanation for the observed lack of significant lateral facies changes is that the subvertical dip allows easy recognition of foresets indicating sediment transport subparallel to depositional strike but makes it difficult to recognize across-strike transport facies change. The apparent low variability in facies changes also indicates that the sedimentary basin(s) of early Moodies time and north of the Inyoka Fault, was (or were) only poorly confined by the present tectonic boundaries; they presumably extended well beyond the present-day boundaries of the BGB (Heubeck and Lowe, 1999). A generalization of the observation would suggest that Archean continents and their shelves may have been covered for several tens of kilometers by extensive coastal zones due to an overall low topographic gradient, combined with low continental freeboard (Eriksson, 1999; Eriksson et al., 2004). Consequently, substantial lateral facies changes in the terrestrial, coastal, and nearshore zones could only be observed at a large scale.

II.8.2 Biogenicity

Decades of research and the development of sophisticated techniques have led to the establishment of a number of solid criteria for assessing the biogenicity and syngenicity of purported evidence of life (Schopf, 1993, 2004, 2006; Brasier et al., 2002, 2006; Schopf and Kudryavtsev, 2005, 2009; Wacey, 2009; Wacey et al., 2010, 2012, 2014). Below, we will follow mainly those laid down by Schopf (2004) and Brasier et al. (2006). Geological context, age, facies, and provenance of the microbial mat-bearing sandstones of the Moodies Group are reasonably well constrained (Heubeck and Lowe, 1994a; Heubeck, 2009; Heubeck et al., 2013). The observations described above document a close interaction between the kerogenous laminae and associated small- and medium-scale sedimentary structures in Moodies sandstones, reflecting also facies changes. The syndepositional origin of the laminae is unquestionable (Schieber, 2004). At outcrop scale, changes in dominant mat morphotype correlate well with changes in clastic facies, which suggests an adaptation of the microbial mats to the environment and therefore serve as a biogenicity indicator (Allwood et al., 2006; Brasier et al., 2006). At microscale, negative $\delta^{13}C$ values of the kerogen and associated filamentous microstructures are indicative of a microbial origin (Noffke et al., 2006; Gamper et al., 2012; Homann et al., 2013). Consequently, the laminae do not represent abiogenic deposits of organic matter on the sedimentary surface, e.g., by fall-out deposits from atmospheric haze or marine colloids that were subsequently concentrated and deformed during early diagenesis (Wells, 1998; Trainer et al., 2006). No known abiological process can explain the systematic variations and observed correlations between the kerogenous laminations and their surrounding siliciclastic substrate. Rather, the steepness of the near-vertical, up to 1 cm-high microbial tufts and the widespread occurrence of the kerogenous laminae is consistent with a primary, microbially-mediated, erosion-resistant relief on the paleosurface, subsequently locally deformed by upward-migrating gases and/or fluids, or locally eroded and incorporated in mat-chip conglomerates.

II.8.3 Biostratigraphy and paleoecology

Biostratigraphy based on microbial-mat morphology, associated mat-related structures, and comparisons with modern analogs allows to spatially refine paleoenvironmental interpretations (Table 1; Banerjee et al., 2014; Sarkar and Banerjee, 2014). Similar approaches have been conducted on the basis of morphological differences of stromatolites, providing a more precise interpretation of their paleoenvironmental context (Schopf, 1977; Bertrand-Sarfati and Walter, 1981; Allwood et al., 2006; Grey et al., 2011; Jahnert and Collins, 2012, 2013). Morphological relief does not necessarily correlate with an increased bioproductivity, however, it can be assumed that it indicates an increased biomass accumulation. Large amount of biomass accumulation could either indicate high bioproductivity or low biomass degradation.

Microbial mats of the Moodies Group are morphologically most prominent and show the highest topographic relief in the *upper inter- to supratidal facies*, suggesting optimal growth conditions and bioproductivity there. Tufted microbial mats are widespread in this facies and occur in association with gas domes, giant gas- or fluid-escape structures, and shrinkage cracks. In contrast, tufts, gas domes, and shrinkage cracks are mostly absent in the adjacent *intertidal facies*, which are dominated by wavy-crinkly mat morphologies and relatively small microbial domes. Their wavy morphology could have been enhanced by a preexisting topography such as, e.g., ripples and forests. A subsequent and repeated mat overgrowth of topographic highs could have caused the development of microbial domes that might represent initial growth stages of tufts. Mats in this facies are typically associated with abundant mat chips and chert layers while gas-/or fluid-escape structures are distinctly subordinate. In the *coastal floodplain facies* only a small variety of mat-related structures has been observed. Mats typically display a planar and generally less complex morphology which is likely a morphological adaptation to high hydrodynamic shear stress (Fig. II.S2). We have not identified microbial mats or mat-related structures either in the *braided fluvial to alluvial facies* or *subtidal facies* of the Moodies Group, which might be either due to reduced preservation potential and poorer development there or due to the primary absence of microbial mats.

A similar distribution pattern of mat-related structures and mat morphotypes, especially tufted mats, have been reported from other siliciclastic strata of Precambrian age (Banerjee et al., 2014) as well as from modern environments (Gerdes et al., 2000; Cuadrado et al., 2011; Bose and Chafetz, 2009; Sarkar and Banerjee, 2014). Mat morphotypes described above likely represent an active adaptation by the microbial community to environmental factors such as sedimentation rate, hydrodynamic regime, and the availability of nutrients and light (e.g., Gerdes et al., 2000). It is important to note that these adaptations are not found at point sources such as hydrothermal vents but occur regionally and developed exclusively in the shallow- and very shallow-water photic zone of the Moodies Group under conditions of moderate to high water agitation. This not only indicates that this environment represented an ecological optimum for the growth and preservation of the mats but also strongly suggests that these communities were phototrophic and able to sustain the presumably high UV radiation (Phoenix et al., 2001). The reported $\delta^{13}C$ values of -22.5‰ to -20.1‰ (Noffke et al., 2006) are in the range of cyanobacteria, however, similar values can also be produced by anoxygenic phototrophs or methanogens (Schidlowski, 2001; Schopf, 2011). A methanotrophic-bacteria-dominated community is rather unlikely because their $\delta^{13}C$ values would be significantly more negative.

II.8.4 Tufted microbial mats

Tufted mats of the inferred upper inter- to supratidal zone in the Moodies Group are strikingly similar to modern tufted mats, which are predominantly built by filamentous cyanobacteria and described, e.g., from Bahar Alouane, Tunisia (Fig. II.8C; Gerdes et al. 2000; Gerdes, 2007), Shark Bay, Australia (Jahnert and

Collins, 2013), Texas Gulf Coast, USA (Bose and Chafetz, 2009), and the Red Sea of Saudi Arabia (Taj et al., 2014). Polygonal patterns of reticulate ridges with tufts at ridge junctions are a well known surface texture in modern (e.g., Gerdes, 2007; Shepard and Sumner, 2010) and some Archean tufted mats (Beukes, 1987; Sumner, 1997; Flannery and Walter, 2011). Due to the steep dip throughout the study area, only a limited amount of bedding planes are exposed. However, tufts in cross-section view can be seen to be laterally connected by draping lamina which either represent ridges or a transect through a continuous mat cover (Fig. II.8B and D).

The process of tuft formation in modern settings is not entirely understood. It is thought to require gliding motility and tangling behavior of the mat-building filaments. Tufts and cones have been interpreted to indicate microbial phototactic behavior but this process remains debated (Castenholz, 1968, 1967; Walter et al., 1976; Shepard and Sumner, 2010; Bosak et al., 2012; Sim et al., 2012; Reyes et al., 2013). Morphogenetic mechanisms such as photo- and chemotaxis, competition for space, potentially mediated by quorum sensing may also be involved (Petroff et al., 2010; Decho, 2010). Tuft formation may be a communal microbial strategy to penetrate the laminar boundary layer in the flowing medium above the substrate, gaining access to the overlying, more nutrient-laden turbulent layer (Tice et al., 2011). To date, the oldest fossil tufted microbial mats are reported from the 2.7 Ga Tumbiana Fm., Australia (Flannery and Walter 2011). The putative micro-tufted structures described by Noffke et al. (2013) from the 3.48 Ga Dresser Fm., Australia, reach only 25 - 50 µm in height (Fig. 6 of Noffke et al., 2013), are thus at another scale of observation and therefore, in our opinion, not comparable with the macroscopic, 0.3-to-1 cm-high microbial tufts (Fig. II.8) preserved in Moodies sandstones. Hence, the Moodies Group contains the oldest known convincing macro-tufted microbial mats in the geological record.

High resistance and adaptability to environmental stresses, high productivity, and the ability to form and sustain complex vertical structures only supported by biomass is an almost unique trait of cyanobacteria (Lyons and Kolter, 2015). Phylogenetic analysis suggest that the ancestor to most extant cyanobacteria evolved between 2.4 and 3.1 Ga or even earlier (Schirrmeister et al., 2013). Bosak et al. (2009) linked the formation of oxygen-rich bubbles in modern cyanobacterial cones with fossil gas bubbles present in the central zone of 2.7 Ga conical stromatolites and concluded that fossil gas bubbles may be used as an indicator for oxygenic photosynthesis. Moreover, experiments with laboratory-grown cyanobacterial mats propose that tufted structures can serve as morphological indicator of oxygenated Archean environments (Sim et al., 2012). Therefore, in the absence of preserved biomarkers in the Moodies Group the morphological attributes of the microbial mats may be the principal clue to constrain the microbial metabolism(s). If cyanobacteria were indeed the only microorganisms with the ability to form macroscopic tufts, their first appearance in the geological record would set a minimum age for the origin of cyanobacteria. This reasoning has been previously made by Flannery and Walter (2011) and would now place their origin to at least 700 Ma prior to the GOE.

II.8.5 Regional and stratigraphic distribution

Fossilized microbial mats appear to be absent in shallow-water paleoenvironments of other large Moodies synclines north of the Inyoka Fault, such as the Eureka Syncline, the Moodies Hills Block, and the Stolzburg Syncline, even though we conducted careful dedicated searches in stratigraphically equivalent units there; microbial mats have been found only in the Saddleback and Dycedale Synclines and possibly thin and poorly developed ones in the Stolzburg Syncline. Microbial mats have not been documented from the quartzose sandstones of the Moodies Group south of the Inyoka Fault. This apparent absence is puzzling because the abundant sedimentary structures and common sandy, silty, and gravelly lithologies in the stratigraphically equivalent units in these tectonic regions strongly suggest equivalent facies, ranging between braided-stream and prodelta. The absence of microbial mats may be explained by either one or a combination of two hypotheses: (1) Mats did not form elsewhere because environmental conditions there were subtly different and growth conditions unfavorable to allow macroscopic accumulation; (2) microbial mats were not preserved elsewhere because only the Moodies strata in the central Saddleback Syncline in the interior of the BGB experienced the proper combination of very early silicification, low tectonic strain and low hydrothermal overprint, thus preserving the organic matter.

II.9 Conclusions

Microbial mats of the 3.22 Ga Moodies Group, exposed on the overturned limb of the Saddleback Syncline, represent one of Earth's oldest, macroscopically visible, large-scale and mappable Archean ecosystem. The fossil mats are preserved as kerogenous laminations and are particularly unique due to their excellent preservation and large extent over approx. 15 km strike length in a stratigraphically coherent interval of roughly 1000 m thickness. Microbial mat biostratigraphy based on (1) mat morphology (planar, wavy, and tufted), (2) the association and distribution pattern of distinct microbial-mat-related structures, and (3) comparisons with modern analogs was applied for spatially refining the paleoenvironmental settings. In the coastal floodplain zone, mats are typically planar, whereas the association of more complex wavy-crinkly mat morphotypes, small microbial domes, and mat chips is characteristic for the intertidal zone. Tufted microbial mats are exclusively present in the upper inter- to supratidal zone and are commonly associated with shrinkage cracks, gas domes, and extensive gas- or fluid-escape structures. These three distinct mat morphotypes are interpreted to represent an adaptation of the phototrophic microbial communities to changing physiochemical conditions, furthermore, the tufted microbial mats were perhaps build by ancestral cyanobacteria. These microbial communities had optimum growth conditions in the photic zone under moderate water agitation and persisted within mechanically abrasive, high-energy shoreline environments.

II.10 Acknowledgements

Research was supported by DFG grant He2418/13-1. CH was partially supported by the EU COST Action "Life-ORIGINS" (TD1308). MH and CH thank Jonathan Engelhardt, Laura Stutenbecker, Nadja Drabon, Sami Nabhan, Danielle Zentner and Lizzy Trower Stefurak for assistance in the field. The authors are grateful to Sappi Limited and their forestry managers for permission to access private forest roads. We thank Don Lowe, Gary Byerly, Martin Van Kranendonk, Kurt Konhauser, Bill Schopf, Jian Gong, David Flannery, and Tomaso Bontognali for constructive discussions and comments on various aspects of this work. The Nel family provided help and hospitality. Anna Giribaldi, FU Berlin, prepared thin sections; Tim Luber and Markus Gogouvitis are thanked for helping with sample preparation; Daniel Korb and Oliver Burkhardt assisted in the grain size analysis. Thoughtful and constructive reviews by Martin Van Kranendonk and an anonymous reviewer significantly improved the manuscript.

II.11 Supplementary data

Table II.S1

Assumed hydraulic parameters

Location	Sediment density, ρ_s	Fluid density, ρ	D_{50}	D_{84}	critical Shields		slope	g
	kg/m^3	kg/m^3	m	m	min	max		m/s^2
all	3000	1000			0.03	0.07	0.1	9.81
above			0.00017	0.00033				
within			0.00008	0.00012				
below			0.00015	0.00024				

Table II.S2

Computed hydraulic parameters for slope values 0.01

Location	critical Shields	u* (m/s)	ū (m/s)	Ø (m/s)
above	0.03	0.01	0.06	0.09
above	0.07	0.015	0.12	
within	0.03	0.007	0.04	0.06
within	0.07	0.01	0.08	
below	0.03	0.01	0.06	0.08
below	0.07	0.014	0.11	

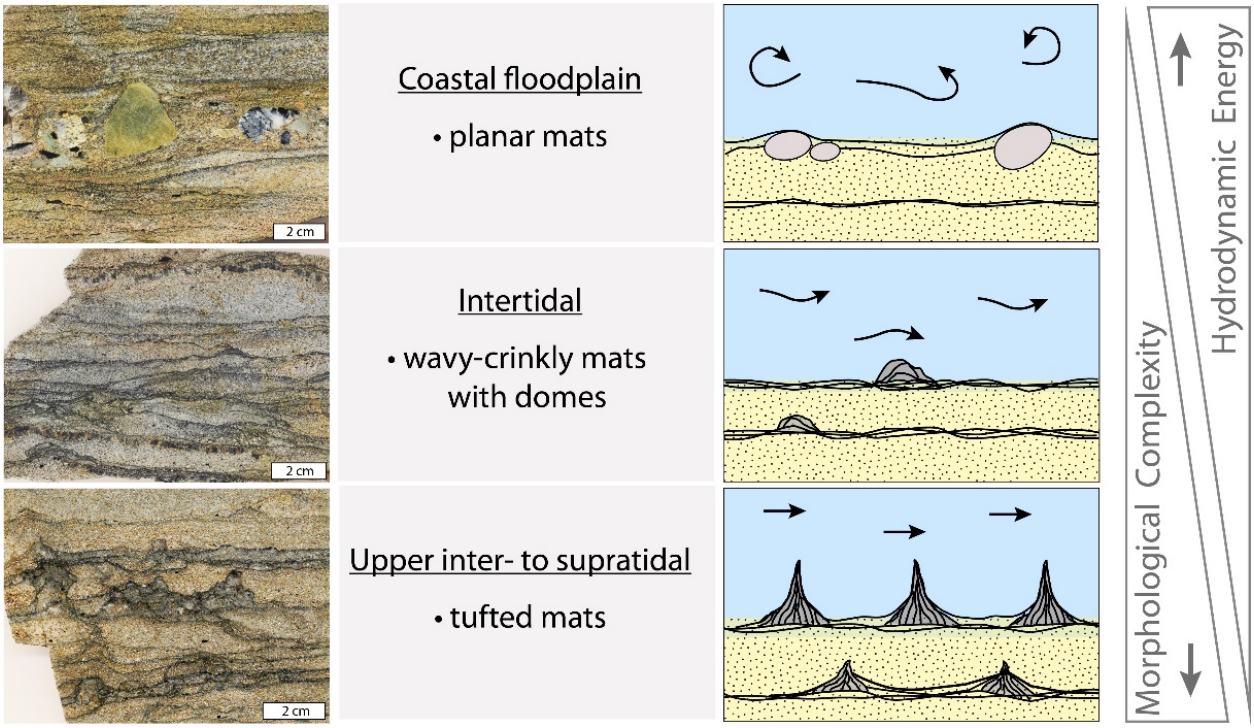

Figure II.S 1: *Graphical abstract highlighting the morphological adaptation of microbial communities to different paleo-environmental settings, which are characterized by variable current energy.*

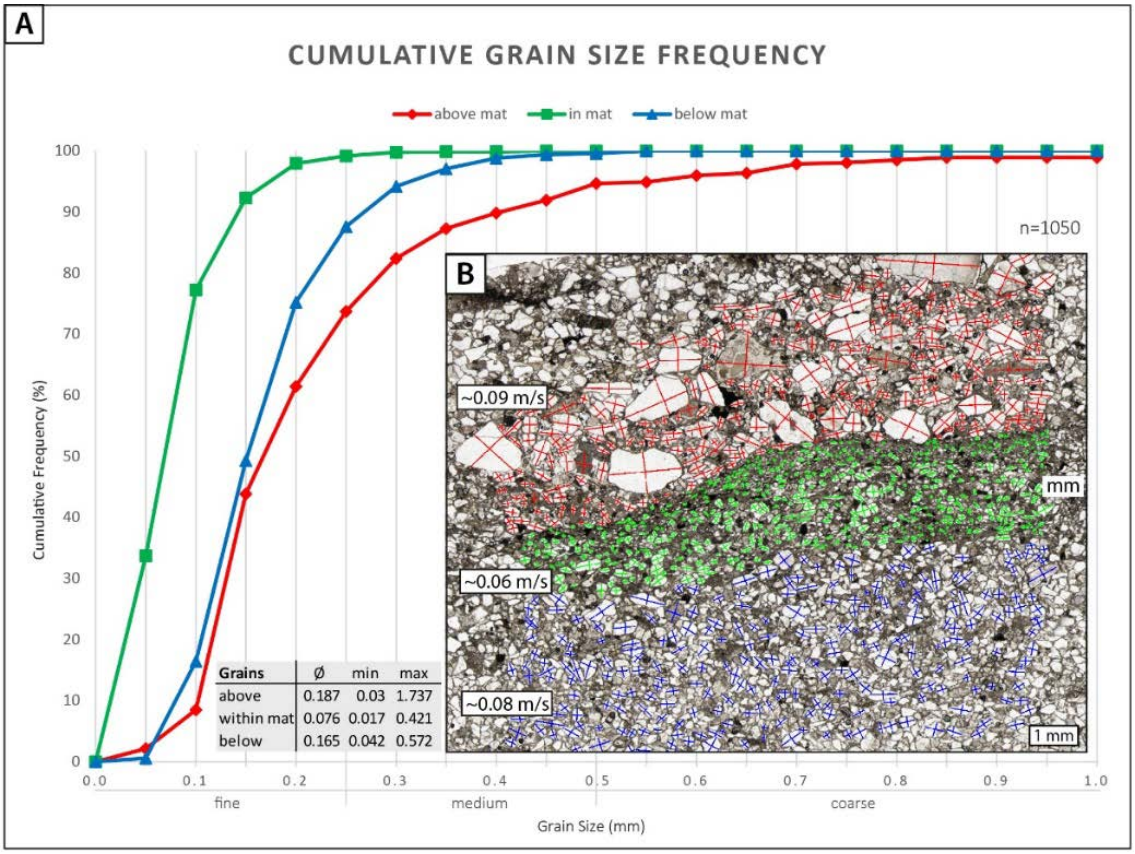

Figure II.S 2: *Cumulative grain size frequency plot of detrital grains below (blue), within (green), and above a microbial mat (red) and corresponding thin section. (A) The grain size distribution of the three measured areas shows that particles are fine- to medium-grained below, fine-grained within, and medium- to coarse-grained above the mat. Sorting is less in the grains overlying the mat. (B) Transmitted light photomicrograph of the analyzed sandstone sample in cross section view with calculated current velocities. The remains of a former microbial mat (mm) are visible in the central part. Colors correspond to the cumulative frequency curves.*

Figure II.S 3: *Polished slab photograph of microbial mats (dark laminae) in cross-section view. Mats are vertically disrupted by a gas- or fluid-escape structure (arrows). Note that the mats are bent upwards and partly dragged into the subvertical linear channel.*

II.12 References

Alam, M.M., Crook, K.A.W., Taylor, G., 1985. Fluvial herring-bone cross-stratification in a modern tributary mouth bar, Coonamble, New South Wales, Australia. Sedimentology 32, 235–244. doi:10.1111/j.1365-3091.1985.tb00506.x

Allen, J.R.L., 1984. Sedimentary structures: their character and physical basis, in: Developments in Sedimentology 30. Elsevier, Amsterdam, p. 663.

Allmendinger, R.W., Cardozo, N.C., Fisher, D., 2012. Structural Geology Algorithms: Vectors & Tensors, Structural Geology Algorithms. Cambridge University Press, Cambridge.

Allwood, A.C., Walter, M.R., Kamber, B.S., Marshall, C.P., Burch, I.W., 2006. Stromatolite reef from the Early Archaean era of Australia. Nature 441, 714–8. doi:10.1038/nature04764

Altermann, W., Corcoran, P.L., 2002. Precambrian Sedimentary Environments: A modern approach to ancient depositional systems. Blackwell Science (Special publication number 33 of the International Association of Sedimentologists), Oxford.

Anbar, A.D., Duan, Y., Lyons, T.W., Arnold, G.L., Kendall, B., Creaser, R., Kaufman, A.J., Gordon, G.W., Scott, C., Garvin, J., Buick, R., 2007. A whiff of oxygen before the great oxidation event? Science 317, 1903–6. doi:10.1126/science.1140325

Anhaeusser, C.R., 1976. The geology of the Sheba Hills area of the Barberton Mountain Land, South Africa: with particular reference to the Eureka Syncline. Trans. Geol. Soc. S. Afr 79, 253–280.

Archer, A.W., 2013. World's highest tides: Hypertidal coastal systems in North America, South America and Europe. Sediment. Geol. 284-285, 1–25. doi:10.1016/j.sedgeo.2012.12.007

Banerjee, S., Sarkar, S., Eriksson, P.G., 2014. Palaeoenvironmental and biostratigraphic implications of microbial mat-related structures: Examples from the modern Gulf of Cambay and the Precambrian Vindhyan. J. Palaeogeogr. 3, 127–144. doi:10.3724/SP.J.1261.2014.00048

Battin, T.J., Kaplan, L.A., Newbold, J.D., Hansen, C.M.E., 2003. Contributions of microbial biofilms to ecosystem processes in stream mesocosms. Nature 439–442.

Bertrand-Sarfati, J., Walter, M.R., 1981. Stromatolite biostratigraphy. Precambrian Res. 15, 353–371.

Beukes, N.J., 1987. Facies relations, depositional environments and diagenesis in a major Early Proterozoic stromatolitic carbonate platform to basinal sequence, Campbellrand Supergroup, Transvaal Supergroup, Souhhern Africa. Sediment. Geol. 54, 1–46.

Bontognali, T.R.R., Fischer, W.W., Föllmi, K.B., 2013. Siliciclastic associated banded iron formation from the 3.2Ga Moodies Group, Barberton Greenstone Belt, South Africa. Precambrian Res. 226, 116–124. doi:10.1016/j.precamres.2012.12.003

Bosak, T., Bush, J.W.M., Flynn, M.R., Liang, B., Ono, S., Petroff, a. P., Sim, M.S., 2010. Formation and stability of oxygen-rich bubbles that shape photosynthetic mats. Geobiology 8, 45–55. doi:10.1111/j.1472-4669.2009.00227.x

Bosak, T., Liang, B., Sim, M.S., Petroff, A.P., 2009. Morphological record of oxygenic photosynthesis in conical stromatolites. Proc. Natl. Acad. Sci. U. S. A. 106, 10939–10943. doi:10.1073/pnas.0900885106

Bosak, T., Liang, B., Wu, T.-D., Templer, S.P., Evans, A., Vali, H., Guerquin-Kern, J.-L., Klepac-Ceraj, V., Sim, M.S., Mui, J., 2012. Cyanobacterial diversity and activity in modern conical microbialites. Geobiology 10, 384–401. doi:10.1111/j.1472-4669.2012.00334.x

Bose, S., Chafetz, H.S., 2009. Topographic control on distribution of modern microbially induced sedimentary structures (MISS): A case study from Texas coast. Sediment. Geol. 213, 136–149. doi:10.1016/j.sedgeo.2008.11.009

Bouougri, E., Porada, H., 2007. Complex structures associated with siliciclastic biolaminites, in: Schieber, J., Bose, P.K., Eriksson, P.., Banerjee, S., Sarkar, S., Altermann, W., Catuneanu, O. (Eds.), Atlas of Microbial Mat Features Preserved within the Siliciclastic Rock Record. Elsevier, Amsterdam, pp. 111–115.

Bouougri, E., Porada, H., 2012. Wind-induced mat deformation structures in recent tidal flats and sabkhas of SE-Tunisia and their significance for environmental interpretation of fossil structures. Sediment. Geol. 263-264, 56–66. doi:10.1016/j.sedgeo.2011.12.011

Brasier, M., Green, O.R., Jephcoat, A.P., Kleppe, A.K., Van Kranendonk, M., Lindsay, J.F., Steele, A., Grassineau, N.V., 2002. Questioning the evidence for Earth's oldest fossils. Nature 416, 76–81.

Brasier, M., McLoughlin, N., Green, O., Wacey, D., 2006. A fresh look at the fossil evidence for early Archaean cellular life. Philos. Trans. R. Soc. Lond. B. Biol. Sci. 361, 887–902. doi:10.1098/rstb.2006.1835

Buick, R., 2008. When did oxygenic photosynthesis evolve? Philos. Trans. R. Soc. Lond. B. Biol. Sci. 363, 2731–43. doi:10.1098/rstb.2008.0041

Burne, R.V.R. V, Moore, L.S.L.S., 1987. Microbialites : Organosedimentary Deposits of Benthic Microbial Communities. Palaios 2, 241–254.

Byerly, G.R., Lowe, D.R., Walsh, M.M., 1986. Stromatolites from the 3,300–3,500-Myr Swaziland Supergroup, Barberton Mountain Land, South Africa. Nature 319, 489–491.

Castenholz, R.W., 1967. Aggregation in a thermophilic Oscillatoria. Nature 215, 1285–1286.

Castenholz, R.W., 1968. The behavior of Oscillatoria terebriformis in hot springs. J. Phycol. 4, 132–139.

Condie, K.C., 1997. Plate Tectonics and Crustal Evolution, 4th ed. Butterworth-Heinemann, Oxford.

Crowe, S.A., Døssing, L.N., Beukes, N.J., Bau, M., Kruger, S.J., Frei, R., Canfield, D.E., 2013. Atmospheric oxygenation three billion years ago. Nature 501, 535–8. doi:10.1038/nature12426

Cuadrado, D.G., Carmona, N.B., Bournod, C., 2011. Biostabilization of sediments by microbial mats in a temperate siliciclastic tidal flat, Bahia Blanca estuary (Argentina). Sediment. Geol. 237, 95–101. doi:10.1016/j.sedgeo.2011.02.008

De Ronde, C.E.J., De Wit, M.J., 1994. Tectonic history of the Barberton Greenstone Belt, South Africa: 490 million years of Archaean evolution. Tectonics 983–1005.

De Ronde, C.E.J., Hall, C.M., York, D., Spooner, E.T.C., 1991. Laser step-heating 40Ar/39Ar age spectra from Early Archean (~3.5 Ga) Barberton greenstone belt sediments: A technique for detecting cryptic tectono-thermal events. Geochim. Cosmochim. Acta 55, 1933–1951.

De Ronde, C.E.J., Kamo, S.L., 2000. An Archaean arc-arc collisional event: A short-lived (ca 3 Myr) episode, Weltevreden area, Barberton greenstone belt, South Africa. J. African Earth Sci. 30, 219–248. doi:10.1016/S0899-5362(00)00017-8

De Wit, M.J., Furnes, H., Robins, B., 2011. Geology and tectonostratigraphy of the Onverwacht Suite, Barberton greenstone belt, South Africa. Precambrian Res. 186, 1–27.

Decho, A.W., 2010. Overview of biopolymer-induced mineralization: What goes on in biofilms? Ecol. Eng. 36, 137–144. doi:10.1016/j.ecoleng.2009.01.003

Desjardins, P.R., Buatois, L.A., Ma, M.G., 2012. Tidal Flats and Subtidal Sand Bodies, in: Knaust D., Bromley R. (Eds.), Trace Fossils as Indicators of Sedimentary Environments. Elsevier, pp. 529–561.

Donaldson, J.A., Aspler, L.B., Chiarenzelli, J.R., 2004. Sedimentary Structures: An essential key for interpreting the Precambrian rock record, in: Eriksson, P.G., Altermann, W., Nelson, D.R., Mueller, W.U., Catuneanu, O. (Eds.), The Precambrian Earth: Tempos and Events. Elsevier (Developments in Precambrian Geology), Amsterdam, pp. 602–612.

Dornbos, S.Q., Noffke, N., Hagadorn, J.W., 2007. Mat-decay features, in: Schieber, J., Bose, P.K., Eriksson, P.., Banerjee, S., Sarkar, S., Altermann, W., Catuneanu, O. (Eds.), Atlas of Microbial Mats Features …. Elsevier, Amsterdam, pp. 106–110.

Dupraz, C., Reid, R.P., Braissant, O., Decho, A.W., Norman, R.S., Visscher, P.T., 2009. Processes of carbonate precipitation in modern microbial mats. Earth-Science Rev. 96, 141–162. doi:10.1016/j.earscirev.2008.10.005

Embry, A.F., Catuneanu, O., Eriksson, P.G., 2004. Sequence stratigraphy and the Precambrian, in: Eriksson, P.G., Altermann, W., Nelson, D.R., Mueller, W.U., Catuneanu, O. (Eds.), The Precambrian Earth: Tempos and Events. Elsevier (Developments in Precambrian Geology), Amsterdam, pp. 681–684.

Eriksson, K.A., 1977. Tidal deposits from the Archaean Moodies Group, Barberton Mountain Land, South Africa. Sediment. Geol. 18, 257–281.

Eriksson, K.A., 1978. Alluvial and destructive beach facies from the Archaean Moodies Group, Barberton Mountain Land, South Africa and Swaziland, in: Miall, A.D. (Ed.), Fluvial Sedimentology. Can. Soc. Petrol. Geol., Mem. 5, pp. 287–311.

Eriksson, K.A., 1979. Marginal marine depositional processes from the Archaean Moodies Group, Barberton Mountain Land; South Africa: Evidence and significance. Precambrian Res. 8, 153–182.

Eriksson, K.A., 1980. Transitional sedimentation styles in the Fig Tree and Moodies Group, Barberton Mountain Land, South Africa: evidence favouring an Atlantic or Japan sea-type Archaean continental margin. Precambrian Res. 12, 141–160.

Eriksson, K.A., Simpson, E.L., 1998. Controls on spatial and temporal distribution of Precambrian eolianites. Sediment. Geol. 120, 275–294. doi:10.1016/S0037-0738(98)00036-0

Eriksson, K.A., Simpson, E.L., 2000. Quantifying the oldest tidal record: The 3.2 Ga Moodies Group, Barberton Greenstone Belt, South Africa. Geology 28, 831. doi:10.1130/0091-7613(2000)28<831:QTOTRT>2.0.CO;2

Eriksson, K.A., Simpson, E.L., 2004. Precambrian tidalites: recognition and significance, in: Eriksson, P.G., Altermann, W., Nelson, D.R., Mueller, W.U., Catuneanu, O. (Eds.), The Precambrian Earth: Tempos and Events. Elsevier (Developments in Precambrian Geology), Amsterdam, pp. 631–642.

Eriksson, K.A., Simpson, E.L., Mueller, W.U., 2006. An unusual fluvial to tidal transition in the mesoarchean Moodies Group, South Africa: A response to high tidal range and active tectonics. Sediment. Geol. 190, 13–24. doi:10.1016/j.sedgeo.2006.05.011

Eriksson, P.G., 1999. Sea level changes and the continental freeboard concept: general principles and application to the Precambrian. Precambrian Res. 97, 143–154. doi:10.1016/S0301-9268(99)00029-7

Eriksson, P.G., Bumbb, A.J., Mostert, P., 2004. Early precambrian epeiric seas, in: Eriksson, P.G., Altermann, W., Nelson, D.R., Mueller, W.U., Catuneanu, O. (Eds.), The Precambrian Earth: Tempos and Events. Elsevier (Developments in Precambrian Geology), Amsterdam, pp. 657–660.

Eriksson, P.G., Condie, K.C., Tirsgaard, H., Mueller, W.U., Altermann, W., Miall, a. D., Aspler, L.B., Catuneanu, O., Chiarenzelli, J.R., 1998. Precambrian clastic sedimentation systems. Sediment. Geol. 120, 5–53. doi:10.1016/S0037-0738(98)00026-8

Eriksson, P.G., Porada, H., Banerjee, S., Bouougri, E., Sarkar, S., Bumbb, A.J., 2007. Mat-destruction features, in: Schieber, J., Bose, P.K., Eriksson, P.., Banerjee, S., Sarkar, S., Altermann, W., Catuneanu, O. (Eds.), Atlas of Microbial Mat Features Preserved within the Siliciclastic Rock Record. Elsevier, Amsterdam, pp. 76–105.

Eriksson, P.G., Sarkar, S., Banerjee, S., Porada, H., Catuneanu, O., Samanta, P., 2010. Paleoenvironmental context of microbial mat-related structures in siliciclastic rocks — examples from the Proterozoic of India and South Africa, in: Seckbach, J., Oren, A. (Eds.), Microbial Mats: Modern and Ancient Microorganisms in Stratified Systems. Springer, Berlin, pp. 73–108.

Farquhar, J., Zerkle, A.L., Bekker, A., 2011. Geological constraints on the origin of oxygenic photosynthesis. Photosynth. Res. 107, 11–36. doi:10.1007/s11120-010-9594-0

Flannery, D.T., Walter, M.R., 2011. Archean tufted microbial mats and the Great Oxidation Event: new insights into an ancient problem. Aust. J. Earth Sci. 59, 1–11. doi:10.1080/08120099.2011.607849

Fralick, P., Zaniewski, K., 2012. Sedimentology of a wet, pre-vegetation floodplain assemblage. Sedimentology 59, 1030–1049. doi:10.1111/j.1365-3091.2011.01291.x

Frey, S.E., Gingras, M.K., Dashtgard, S.E., 2009. Experimental Studies of Gas-Escape and Water-Escape Structures: Mechanisms and Morphologies. J. Sediment. Res. 79, 808–816. doi:10.2110/jsr.2009.087

Fryberger, S.G., Schenk, C.J., 1988. Pin stripe lamination: a distinctive feature of modern and ancient eolian sediments. Sediment. Geol. 55, 1–15.

Gamper, A., Heubeck, C., Demske, D., Hoehse, M., 2012. Composition and Microfacies of Archean Microbial Mats (Moodies Group, ca. 3.22 Ga, South Africa), in: Noffke, N., Chafetz, H.S. (Eds.), Microbial Mats in Silicilastic Depositional Systems Through Time. SEPM, Tulsa, pp. 65–74. doi:10.2110/sepmsp.101.065

Gerdes, G., 2007. Structures Left by Modern Microbial Mats in Their Host Sediments, in: Schieber, J., Bose, P.K., Eriksson, P.., Banerjee, S., Sarkar, S., Altermann, W., Catuneanu, O. (Eds.), Atlas of Microbial Mat Features Preserved within the Siliciclastic Rock Record. Elsevier, Amsterdam, pp. 5–38. doi:10.1016/S1574-1966(07)02001-9

Gerdes, G., Claes, M., Dunajtschik-Piewak, K., Riege, H., Krumbein, W.E., H.E., R., 1993. Contribution of microbial mats to sedimentary surface structures. Facies 61–74.

Gerdes, G., Klenke, T., Noffke, N., 2000. Microbial signatures in peritidal siliciclastic sediments: a catalogue. Sedimentology 47, 279–308.

Gingras, M.K., 2002. Microbially Induced Sedimentary Structures - A New Category within the Classification of Primary Sedimentary Structures - Discussion. J. Sediment. Res. 72, 587–588.

Grey, K., Hill, A.C., Calver, C., 2011. Biostratigraphy and stratigraphic subdivision of Cryogenian successions of Australia in a global context, in: Arnoud, E., Halverson, G.P., Shields-Zhou, G. (Eds.), The Geological Record of Eoproterozoic Glaciations. Geological Society Memoirs, 36, London, pp. 113–134. doi:10.1144/M36.8

Hall, A.L., 1918. The geology of the Barberton gold mining district. Geol. Surv. South Africa Mem. 1–324.

Heinrichs, T.K., Reimer, T.O., 1977. A sedimentary baryte deposit from the Archean Fig Tree Group of the Barberton Mountain Land (South Africa). Econ. Geol. 72, 1426–1441.

Heubeck, C., 2009. An early ecosystem of Archean tidal microbial mats (Moodies Group, South Africa, ca. 3.2 Ga). Geology 37, 931–934. doi:10.1130/G30101A.1

Heubeck, C., Engelhardt, J., Byerly, G.R., Zeh, A., Sell, B., Luber, T., Lowe, D.R., 2013. Timing of deposition and deformation of the Moodies Group (Barberton Greenstone Belt, South Africa): Very-high-resolution of Archaean surface processes. Precambrian Res. 231, 236–262. doi:10.1016/j.precamres.2013.03.021

Heubeck, C., Lowe, D.R., 1994a. Depositional and tectonic setting of the Archean Moodies Group, Barberton greenstone belt, South Africa. Precambrian Res. 68, 257–290.

Heubeck, C., Lowe, D.R., 1994b. Late syndepositional deformation and detachment tectonics in the Barberton Greenstone Belt, South Africa. Tectonics 13, 1514–1536.

Heubeck, C., Lowe, D.R., 1999. Sedimentary petrography and provenance of the Archean Moodies Grou, Barberton Greenstone Belt, in: Lowe, D.R., Byerly, G.R. (Eds.), Geologic Evolution of the Barberton Greenstone Belt, South Africa. Geological Society of America Special Paper 329, pp. 259–286.

Hofmann, A., 2005. The geochemistry of sedimentary rocks from the Fig Tree Group, Barberton greenstone belt: Implications for tectonic, hydrothermal and surface processes during mid-Archaean times. Precambrian Res. 143, 23–49. doi:10.1016/j.precamres.2005.09.005

Holland, H., 2002. Volcanic gases, black smokers, and the Great Oxidation Event. Geochim. Cosmochim. Acta 66, 3811–3826.

Holland, H.D., 2006. The oxygenation of the atmosphere and oceans. Philos. Trans. R. Soc. Lond. B. Biol. Sci. 361, 903–15. doi:10.1098/rstb.2006.1838

Homann, M., Heubeck, C., Airo, A., Tice, M.M., Nabhan, S., 2013. Microbially-induced carbonate precipitation, Moodies Group (3.2 Ga, BGB, South Africa), in: Mineralogical Magazine. p. 1316. doi:10.1180/minmag.2013.077.5.8

Jahnert, R.J., Collins, L.B., 2012. Characteristics, distribution and morphogenesis of subtidal microbial systems in Shark Bay, Australia. Mar. Geol. 303-306, 115–136. doi:10.1016/j.margeo.2012.02.009

Jahnert, R.J., Collins, L.B., 2013. Controls on microbial activity and tidal flat evolution in Shark Bay, Western Australia. Sedimentology 60, 1071–1099. doi:10.1111/sed.12023

Javaux, E.J., Marshall, C.P., Bekker, A., 2010. Organic-walled microfossils in 3.2-billion-year-old shallow-marine siliciclastic deposits. Nature 463, 934–8. doi:10.1038/nature08793

Johnson, H.D., Baldwin, C.T., 1996. Shallow siliciclastic seas, in: Reading, H.G. (Ed.), Sedimentary Environments; Processes, Facies and Stratigraphy. Blackwell Science, Cambridge, p. 688.

Klausen, M.B., Söderlund, U., Olsson, J.R., Ernst, R.E., Armoogam, M., Mkhize, S.W., Petzer, G., 2010. Petrological discrimination among Precambrian dyke swarms: Eastern Kaapvaal craton (South Africa). Precambrian Res. 183, 501–522. doi:10.1016/j.precamres.2010.01.013

Kreisa, R.D., Moila, R.J., 1986. Sigmoidal tidal bundles and other tidegenerated sedimentary structures of the Curtis Formation. GSA Bull. 97, 381–387.

Krumbein, W.E., Paterson, D.M., Stal, L.J. (Eds.), 1994. Biostabilization of Sediments. BIS, Oldenburg.

Lalonde, S. V., Konhauser, K.O., 2015. Benthic perspective on Earth's oldest evidence for oxygenic photosynthesis. Proc. Natl. Acad. Sci. 112, 995–1000. doi:10.1073/pnas.1415718112

Lamb, S., Paris, I., 1988. Post-onverwacht group stratigraphy in the SE part of the Archaean Barbeton greenstone belt. J. African Earth Sci. (and Middle East) 7, 285–306. doi:10.1016/0899-5362(88)90074-7

Layer, P.W., Kroner, A., McWilliams, M., 1996. An Archean Geomagnetic Reversal in the Kaap Valley Pluton, South Africa. Science 273, 943–946.

Long, D.G.F., 2004. Precambrian rivers, in: Eriksson, P.G., Altermann, W., Nelson, D.R., Mueller, W.U., Catuneanu, O. (Eds.), The Precambrian Earth: Tempos and Events. Elsevier (Developments in Precambrian Geology), Amsterdam, pp. 660–663.

Lowe, D.R., 1975. Water escape structures in coarse-grained sediments. Sedimentology 22, 157–204.

Lowe, D.R., Byerly, G.R., 1999. Stratigraphy of the west-central part of the Barberton Greenstone Belt, South Africa, in: Lowe, D.R., Byerly, G.R. (Eds.), Geologic Evolution of the Barberton Greenstone Belt, South Africa. Geological Society of America Special Paper 329, pp. 1–36.

Lowe, D.R., Byerly, G.R., 2007. An overview of the geology of the Barberton Greenstone Belt and vicinity: implications for early crustal development., in: Van Kranendonk, M.J.; Smithies, R.H.; Bennett, V.H. (Ed.), Earth's Oldest Rocks. Elsevier (Developments in Precambrian Geology), Amsterdam, pp. 481–526.

Lowe, D.R., Byerly, G.R., Heubeck, C., 2012. Geologic Map of the west-central Barberton Greenstone Belt, in: South Africa, Scale 1:25,000. Geological Society of America Map and Chart Series No. 103, Boulder. doi:10.1130/2012. MCH103

Lyons, N.A., Kolter, R., 2015. On the evolution of bacterial multicellularity. Curr. Opin. Microbiol. 24, 21–28. doi:10.1016/j.mib.2014.12.007

Lyons, T.W., Reinhard, C.T., Planavsky, N.J., 2014. The rise of oxygen in Earth's early ocean and atmosphere. Nature 506, 307–15. doi:10.1038/nature13068

McCollom, T.M., Seewald, J.S., 2006. Carbon isotope composition of organic compounds produced by abiotic synthesis under hydrothermal conditions. Earth Planet. Sci. Lett. 243, 74–84. doi:10.1016/j.epsl.2006.01.027

Mukhopadhyay, J., Crowley, Q.G., Ghosh, S., Ghosh, G., Chakrabarti, K., Misra, B., Heron, K., Bose, S., 2014. Oxygenation of the Archean atmosphere: New paleosol constraints from eastern India. Geology 42, 923–926. doi:10.1130/G36091.1

Myrow, P.M., 1992. Pot and gutter casts from the Chapel Island Formation, southeast Newfoundland. J. Sediment. Petrol. 62, 992–1007.

Nichols, G., 2009. The Marine Realm: Morphology and Processes, in: Sedimentology and Stratigraphy. Wiley-Blackwell, pp. 163–178.

Noffke, N., 1999. Erosional remnants and pockets evolving from biotic–physical interactions in a Recent lower supratidal environment. Sediment. Geol. 123, 175–181. doi:10.1016/S0037-0738(98)00135-3

Noffke, N., 2010. Microbial Mats in Sandy Deposits from the Archean to Today. Springer, Heidelberg.

Noffke, N., Christian, D., Wacey, D., Hazen, R.M., 2013. Microbially induced sedimentary structures recording an ancient ecosystem in the ca. 3.48 billion-year-old Dresser Formation, Pilbara, Western Australia. Astrobiology 13, 1103–24. doi:10.1089/ast.2013.1030

Noffke, N., Eriksson, K.A., Hazen, R.M., Simpson, E.L., 2006. A new window into Early Archean life: Microbial mats in Earth's oldest siliciclastic tidal deposits (3.2 Ga Moodies Group, South Africa). Geology 34, 253. doi:10.1130/G22246.1

Noffke, N., Gerdes, G., Klenke, T., Krumbein, W., 1997. A microscopic sedimentary succession of graded sand and microbial mats in modem siliciclastic tidal flats. Sediment. Geol. 110, 1–6.

Noffke, N., Gerdes, G., Klenke, T., Krumbein, W., 2001a. Microbially induced sedimentary structures - A new category within the classification of primary sedimentary structures. J. Sediment. Res. 71, 649–656.

Noffke, N., Gerdes, G., Klenke, T., Krumbein, W.E., 2001b. Microbially induced sedimentary structures indicating climatological, hydrological and depositional conditions within Recent and Pleistocene coastal facies zones (Southern Tunesia). Facies 49, 23–30.

Petroff, A.P., Sim, M.S., Maslov, A., Krupenin, M., Rothman, D.H., Bosak, T., 2010. Biophysical basis for the geometry of conical stromatolites. Proc. Natl. Acad. Sci. U. S. A. 107, 9956–61. doi:10.1073/pnas.1001973107

Pflüger, F., Gresse, P.G., 1996. Microbial sand chips- a non-actualistic sedimentary structure. Sediment. Geol. 102, 263–274.

Phoenix, V.R., Konhauser, K.O., Adams, D.G., Bottrell, S.H., 2001. Role of biomineralization as an ultraviolet shield: Implications for Archean life. Geology 29, 823–826. doi:10.1130/0091-7613(2001)029<0823:ROBAAU>2.0.CO

Planavsky, N.J., Asael, D., Hofmann, A., Reinhard, C.T., Lalonde, S.V., Knudsen, A., Wang, X., Ossa Ossa, F., Pecoits, E., Smith, A.J.B., Beukes, N.J., Bekker, A., Johnson, T.M., Konhauser, K.O., Lyons, T.W., Rouxel, O.J., 2014. Evidence for oxygenic photosynthesis half a billion years before the Great Oxidation Event. Nat. Geosci. 7, 283–286. doi:10.1038/ngeo2122

Reid, R.P., Visscher, P.T., Decho, A.W., Stolz, J.F., Bebout, B.M., Dupraz, C., Macintyre, I.G., Paerl, H.W., Pinckney, J.L., Prufert-Bebout, L., Steppe, T.F., DesMarais, D.J., 2000. The role ofmicrobes in accretion, lamination and early lithication of modern marine stromatolites. Nature 406, 989–992.

Reyes, K., Gonzalez, N.I., Stewart, J., Ospino, F., Nguyen, D., Cho, D.T., Ghahremani, N., Spear, J.R., Johnson, H.A., 2013. Surface orientation affects the direction of cone growth by leptolyngbya sp. Strain C1, a likely architect of coniform structures octopus spring (Yellowstone National Park). Appl. Environ. Microbiol. 79, 1302–1308. doi:10.1128/AEM.03008-12

Sarkar, S., Banerjee, S., 2014. Microbial mat records in siliciclastic rocks: Examples from Four Indian Proterozoic basins and their modern equivalents in Gulf of Cambay. J. Asian Earth … 5.

Schidlowski, M., 2001. Carbon isotopes as biogeochemical recorders of life over 3.8 Ga of Earth history: evolution of a concept. Precambrian Res. 106, 117–134. doi:10.1016/S0301-9268(00)00128-5

Schieber, J., 1999. Microbial Mats in Terrigenous Clastics : The Challenge of Identification in the Rock Record. Palaios 14, 3–12.

Schieber, J., 2004. Microbial mats in the siliciclastic rock record: a summary of diagnostic features, in: Eriksson, P.G., Altermann, W., Nelson, D.R., Mueller, W.U., Catuneanu, O. (Eds.), The Precambrian Earth: Tempos and Events. Elsevier (Developments in Precambrian Geology), Amsterdam, pp. 663–673.

Schieber, J., Bose, P.K., Eriksson, P.G., 2007. Atlas of microbial mat features preserved within the siliciclastic rock record. Elsevier, Amsterdam.

Schirrmeister, B.E., de Vos, J.M., Antonelli, A., Bagheri, H.C., 2013. Evolution of multicellularity coincided with increased diversification of cyanobacteria and the Great Oxidation Event. Proc. Natl. Acad. Sci. U. S. A. 110, 1791–6. doi:10.1073/pnas.1209927110

Schopf, J.. W., 1993. Microfossils of the Early Archean Apex Chert: New Evidence of the Antiquity of Life. S 260, 640–646.

Schopf, J.W., 1977. Biostratigraphic usefulness of stromatolitic Precambrian microbiotas: A preliminary analysis. Precambrian Res. 5, 143–173.

Schopf, J.W., 2004. Geochemical and submicron-scale morphologic analyses of individual Precambrian microorganisms. Geochemical Soc. Spec. Publ. 365–375.

Schopf, J.W., 2006. Fossil evidence of Archaean life. Philos. Trans. R. Soc. Lond. B. Biol. Sci. 361, 869–85. doi:10.1098/rstb.2006.1834

Schopf, J.W., 2011. The paleobiological record of photosynthesis. Photosynth. Res. 107, 87–101. doi:10.1007/s11120-010-9577-1

Schopf, J.W., Kudryavtsev, A.B., 2005. Three-dimensional Raman imagery of precambrian microscopic organisms. Geobiology 1–12.

Schopf, J.W., Kudryavtsev, A.B., 2009. Confocal laser scanning microscopy and Raman imagery of ancient microscopic fossils. Precambrian Res. 173, 39–49. doi:10.1016/j.precamres.2009.02.007

Shepard, R.N., Sumner, D.Y., 2010. Undirected motility of filamentous cyanobacteria produces reticulate mats. Geobiology 8, 179–90. doi:10.1111/j.1472-4669.2010.00235.x

Sim, M.S., Liang, B., A.P., P., Evans, A., Klepac-Ceraj, V., Flannery, D.T., Walter, M.R., 2012. Oxygen-Dependent Morphogenesis of Modern Clumped Photosynthetic Mats and Implications for the Archean Stromatolite Record. Geosciences 2, 235–259. doi:10.3390/geosciences2040235

Simpson, E.L., Eriksson, K.A., Mueller, W.U., 2012. 3.2 Ga eolian deposits from the Moodies Group, Barberton Greenstone Belt, South Africa: Implications for the origin of first-cycle quartz sandstones. Precambrian Res. 214-215, 185–191. doi:10.1016/j.precamres.2012.01.019

Stubblefield, W.L., McGrail, D.W., Kersey, D.G., 1984. Recognition of transgressive and post-transgressive sand ridges on the New Jersey continental shelf, in: Tillman, R.W., Siemers, C.T. (Eds.), Siliciclastic Shelf Sediments. SEPM, Tulsa, pp. 1–23.

Sumner, D.Y., 1997. Late Archean calcite-microbe interactions; two morphologically distinct microbial communities that affected calcite nucleation differently. Palaios 12, 302–318.

Taj, R.J., Aref, M. a. M., Schreiber, B.C., 2014. The influence of microbial mats on the formation of sand volcanoes and mounds in the Red Sea coastal plain, south Jeddah, Saudi Arabia. Sediment. Geol. 311, 60–74. doi:10.1016/j.sedgeo.2014.06.006

Terwindt, J.H.J., 1988. Paleo-tidal reconstructions of inshore tidal depositional environments, in: De Boer, P.L., Van Gelder, A., Nio, S.D. (Eds.), Tide-Influenced Sedimentary Environments and Facies. D. Reidel Publishing Company, Dordrecht, pp. 233–263.

Tice, M.M., 2009. Environmental Controls on Photosynthetic Microbial Mat Distribution and Morphogenesis on a 3.42Ga Clastic-Starved Platform. Astrobiology 9, 989–1000.

Tice, M.M., B.C., B., Lowe, D.R., 2004. Thermal history of the 3.5–3.2 Ga Onverwacht and Fig Tree Groups, Barberton greenstone belt, South Africa, inferred by Raman microspectroscopy of carbonaceous material. Geology 32, 37. doi:10.1130/G19915.1

Tice, M.M., Lowe, D.R., 2006. Hydrogen-based carbon fixation in the earliest known photosynthetic organisms. Geology 34, 37. doi:10.1130/G22012.1

Tice, M.M., Thornton, D.C.O., Pope, M.C., Olszewski, T.D., Gong, J., 2011. Archean Microbial Mat Communities. Annu. Rev. Earth Planet. Sci. 39, 297–319. doi:10.1146/annurev-earth-040809-152356

Toulkeridis, T., Goldstein, S.L., Clauer, N., Kröner, A., Todt, W., Schidlowski, M., 1998. Sm-Nd, Rb-Sr and Pb-Pb dating of silicic carbonates from the early Archaean Barberton Greenstone Belt, South Africa: evidence for post-depositional isotopic resetting at low temperature. Precambrian Res. 92, 129–144.

Trainer, M.G., Pavlov, A.A., Langley DeWitt, H., Jimenez, J.L., McKay, C.P., Toon, O.B., Tolbert, M.A., 2006. Organic haze on Titan and the early Earth. Proc. Natl. Acad. Sci. U. S. A. 18035–42. doi:10.1073/pnas.0608561103

Van Kranendonk, M., Smithies, R.H., Bennett, V.C., 2007. Earth's oldest rocks. Dev. Precambrian Geol. 15.

Viljoen, M.J., Viljoen, R.P., 1969. An introduction to the geology of the Barberton granite-greenstone terrain. Spec. Publ. Geol. Soc. S. Afr 2, 9–28.

Visser, D., 1956. The geology of the Barberton area. Geol. Soc. S. Afr. Spec. Publ. 15, 253.

Wacey, D., 2009. Early Life on Earth. A Practical Guide, Topics in Geobiology , Vol. 31. Springer.

Wacey, D., Gleeson, D., Kilburn, M.R., 2010. Microbialite taphonomy and biogenicity: new insights from NanoSIMS. Geobiology 8, 403–16. doi:10.1111/j.1472-4669.2010.00251.x

Wacey, D., Menon, S., Green, L., Gerstmann, D., Kong, C., McLoughlin, N., Saunders, M., Brasier, M., 2012. Taphonomy of very ancient microfossils from the ~3400Ma Strelley Pool Formation and ~1900Ma Gunflint Formation: New insights using a focused ion beam. Precambrian Res. 220-221, 234–250. doi:10.1016/j.precamres.2012.08.005

Wacey, D., Saunders, M., Roberts, M., Menon, S., Green, L., Kong, C., Culwick, T., Strother, P., Brasier, M.D., 2014. Enhanced cellular preservation by clay minerals in 1 billion-year-old lakes. Sci. Rep. 4, 5841. doi:10.1038/srep05841

Walsh, M.M., 1992. Microfossils and possible microfossils from the Early Archean Onverwacht Group, Barberton Mountain Land, South Africa. Precambrian Res. 54, 271–293.

Walsh, M.M., Lowe, D.R., 1985. Filamentous microfossils from the 3,500-Myr-old Onverwacht Group, Barberton Mountain Land, South Africa. Nature 314, 530–531.

Walsh, M.M., Lowe, D.R., 1999. Modes of accumulation of carbonaceous matter in the Early Archean: a petrographic and geochemical study of the carbonaceous cherts of the Swaziland Supergroup, in: Lowe, D.R., Byerly, G.R. (Eds.), Geologic Evolution of the Barberton Greenstone Belt, South Africa. Geological Society of America Special Paper 329, pp. 115–132.

Walsh, M.M., Westall, F., 2003. Archean biofilms preserved in the Swaziland Supergroup, South Africa, in: Krumbein, W.E., Paterson, D.M., Zavarzin, G.A. (Eds.), Fossil and Recent Biofilms: A Natural History of Life on Earth. Kluwer, Dordrecht, pp. 307–316.

Walter, M.R., Bauld, J., Brock, T.D., 1976. Microbiology and morphogenesis of columnar stromatolites (Conophyton, Vacerrila) from hot springs in Yellowstone National Park, in: Walter, M.R. (Ed.), Stromatolites. Elsevier, New York, pp. 273–310.

Wells, M.L., 1998. Marine colloids: A neglected dimension. Nature 391, 530–531.

Westall, F., De Ronde, C.E.J., Southam, G., Grassineau, N., Colas, M., Cockell, C., Lammer, H., 2006. Implications of a 3.472-3.333 Gyr-old subaerial microbial mat from the Barberton greenstone belt, South Africa for the UV environmental conditions on the early Earth. Philos. Trans. R. Soc. Lond. B. Biol. Sci. 361, 1857–75. doi:10.1098/rstb.2006.1896

Williams, R.M.E., Grotzinger, J.P., Dietrich, W.E., Gupta, S., Sumner, D.Y., Wiens, R.C., Mangold, N., Malin, M.C., Edgett, K.S., Maurice, S., Forni, O., Gasnault, O., Ollila, A., Newsom, H.E., Dromart, G., Palucis, M.C., Yingst, R. a, Anderson, R.B., Herkenhoff, K.E., Le Mouélic, S., Goetz, W., Madsen, M.B., Koefoed, A., Jensen, J.K., Bridges, J.C., Schwenzer, S.P., Lewis, K.W., Stack, K.M., Rubin, D., Kah, L.C., Bell, J.F., Farmer, J.D., Sullivan, R., Van Beek, T., Blaney, D.L., Pariser, O., Deen, R.G., 2013. Martian fluvial conglomerates at Gale crater. Science (80-.). 340, 1068–72. doi:10.1126/science.1237317

III.

Evidence for cavity-dwelling microbial life in 3.22 Ga tidal deposits

Martin Homann[1], Christoph Heubeck[2], Tomaso R.R. Bontognali[3], Anne-Sophie Bouvier[4], Lukas P. Baumgartner[4], and Alessandro Airo[1]

Geology, 2016, v. 44, no. 1, p. 51–54, doi:10.1130/G37272.1

[1]Institute of Geological Sciences, Freie Universität Berlin, Malteserstr. 74-100, 12249 Berlin, Germany
[2]Department of Geosciences, Friedrich-Schiller-Universität Jena, Burgweg 11, 07749 Jena, Germany
[3]Geological Institute and Institute of Geochemistry and Petrology, ETH Zurich, Sonneggstr. 5, 8092 Zürich, Switzerland
[4]Institute of Earth Sciences, University of Lausanne, Geopolis, 1015 Lausanne, Switzerland

---

III.1 Abstract

Cavities are considered plausible and favorable habitats for life on early Earth. In such microenvironments, organisms may have found an adequate protection against the intense ultraviolet (UV) radiation that characterized the Archean ozone-free atmosphere. However, while there is clear evidence that benthic life existed in the Paleoarchean, the oldest traces of cavity-dwelling microbes (coelobionts) have been found in Neoarchean rocks. Here we present the results of a detailed investigation of early-silicified cavities occurring in the oldest well-preserved siliciclastic tidal deposits, the 3.22 Ga Moodies Group of the Barberton Greenstone Belt (South Africa). Downward-growing microstromatolitic columns, composed of kerogenous laminae, are commonly present in planar, bedding-parallel, now silica-filled cavities that formed in sediments of the peritidal zone. In situ $\delta^{13}C_{PDB}$ (PDB - Peedee belemnite) measurements of the kerogen range from -32.3‰ to -21.3‰ and are consistent with a biogenic origin. Scanning electron microscopy analysis of the silicified cavities shows well-preserved chains of cell-sized molds that are interpreted as fossil filamentous microorganisms. The geological context, the morphology of the microstromatolites, the $\delta^{13}C$ composition of the kerogen, and the presence of microfossils all suggest that a microbial community inhabited the cavities. These results extend the geological record of coelobionts by ~500 m.y., supporting the view that cavities were among the first ecological niches to have been occupied by early microorganisms.

IV.

The conquest of land: Terrestrial microbial mats at 3.22 Ga

Martin Homann[1], Christoph Heubeck[2], Martin J. Van Kranendonk[3], and Alessandro Airo[1]

In preparation

[1]Institute of Geological Sciences, Freie Universität Berlin, Malteserstr. 74-100, 12249 Berlin, Germany

[2]Department of Geosciences, Friedrich-Schiller-Universität Jena, Burgweg 11, 07749 Jena, Germany

[3]Australian Centre for Astrobiology, and School of Biological, Earth and Environmental Sciences, University of New South Wales, Sydney, NSW, 2052

IV.1 Abstract

More than forty years ago, most considered that Earth's earliest terrestrial ecosystems were plant-dominated and that the colonization of land occurred only in the early Phanerozoic. Today, however, it is generally accepted that earliest known life on land was microbial in nature and Precambrian in age. Their geochemical traces are found in paleosols or as fossil microbial mats. Currently, the oldest widely accepted terrestrial microbial signatures are found in ~2.8 Ga organic-matter-rich paleosols. Here, we report on the occurrence of widespread microbial mat remains in conglomerates and sandstones from the 3.22 Ga Moodies Group of the Barberton Greenstone Belt (BGB, South Africa), one of Earth's oldest well-preserved sedimentary sequences. The mats, preserved as up to 4-mm-thick kerogenous laminae, were thriving in near-coastal ponds on alluvial plains subject to flash flooding and subaerial exposure while being subsequently overlain by fluvial braidplain, shoreline sandy-evaporitic, and shallow-marine subtidal sandstones. The discovery of microbial communities in a Paleoarchean terrestrial habitat not only represents the oldest trace of life on land but also attests to a surprising adaptability and resilience of these microbial pioneers in the conquest of a new ecological niche.

IV.2 Introduction

Although microbial communities are ubiquitous in modern terrestrial settings, their Archean record is rather poor compared to coeval shallow-marine habitats; consequently, it remains unknown when land was colonized (Shear, 1991; Riding and Awramik, 2000; Beraldi-Campesi, 2013). This is surprising, as shallow-water marginal marine habitats (such as tidal flats, deltas, estuaries, and lagoons) are transitional to numerous terrestrial aquatic and non-aquatic environments (such as rivers, alluvial fans, ponds, lakes, dune fields, soils, subsurface cavities, and caves) and commonly interfinger and overlap in time with one another. Part of the problem lies in the difficulty of unambiguously identifying the terrestrial nature of a paleoenvironment since sedimentary structures (e.g., cross bedding, or mud cracks) are also common in many marine and shallow-marine settings. Unambiguous marine minerals (such as glauconite), fossils or sedimentary structures and textures (marine cementation, deep-water anoxia etc.) are almost exclusively a hallmark of the Phanerozoic.

Currently, the oldest convincing evidence for the presence of life on land comes from ~2.8 - 2.6 Ga organic-matter-rich paleosols (Rye and Holland, 2000; Watanabe et al., 2000), ~2.7 - 2.5 Ga old fluvial-lacustrine stromatolites (Buck, 1980; Buick, 1992; Awramik and Buchheim, 2009; Coffey et al., 2013) and 1.09 Ga fluvial-alluvial stromatolites with laterally-linked drapes over cobbles (Elmore, 1983; Fedorchuk, 2014). Remnants of cavity-dwelling microbial communities have also been identified in 2.75 Ga fluvial-lacustrine deposits (Rasmussen et al., 2009) and in a 1.2 Ga paleokarst cavity fill that contains preserved filamentous microfossils (Horodyski and Knauth, 1994). Additional evidence for the existence of terrestrial life is based on ~2 Ga microbial mats and putative biological soil crusts that developed within wet interdune and playa deposits (Simpson et al., 2012). Sheldon (2012) described 1.1 Ga terrestrial microbial mats preserved as organic-rich laminae overgrowing sand ripples in low-energy fluvial floodplain paleoenvironments. Despite this limited record, the notion that life on land may have evolved more-or-less in step with its marine counterpart since the Paleoarchean cannot be disregarded (Beraldi-Campesi, 2013), because estimates based on molecular clocks suggest that the colonization of land occurred at approximately 3.1 - 2.8 Ga (Battistuzzi et al., 2004). As well, Lalonde and Konhauser (2015) plausibly propose the antiquity of a terrestrial phototrophic biosphere with microbial-mat-covered riverbeds prior to the Great Oxidation Event (GOE).

Here, we describe the occurrence of well-preserved microbial mats and associated sedimentary structures that occur in gravelly sandstones interbedded with fluvial-alluvial conglomerates of the 3.22 Ga Moodies Group in the Barberton Greenstone Belt (BGB), South Africa. The mats are preserved as silicified kerogenous laminae and show striking similarities to fossil microbial mats of the adjacent Saddleback Syncline (~4 km south of the Dycedale Syncline), which have a reasonably well established biogenicity (see Heubeck, 2009; Gamper et al., 2012; and Homann et al., 2015 for a detailed discussion).

IV.3 Geological and stratigraphic context

The ca. 3.22 Ga Moodies Group is the uppermost and youngest of three stratigraphic units of the Barberton Greenstone Belt (BGB) of South Africa and Swaziland, located at the eastern margin of the Kaapvaal Craton (Fig. IV.1). The >3-km-thick Moodies strata are dominated by fine- to coarse-grained, mostly quartz-rich sandstones that are locally interbedded with conglomerates and were deposited in alluvial, fluvial, possibly eolian, deltaic, and tidal settings (Anhaeusser, 1976; Eriksson, 1977, 1978, 1979; Heubeck and Lowe, 1994a,b, 1999; Eriksson and Simpson, 2000; Eriksson et al., 2006; Simpson et al., 2012). The age of the Moodies Group is constrained by several stratiform dacitic air-fall tuffs and rare felsic dikes radiating from the Kaap Valley Tonalite (KVT) that crosscut Moodies deposits along the northern margin of the BGB (Layer et al., 1996; Heubeck et al., 2013; Fig. IV.1). Depositional ages of the volcanic beds throughout the Moodies Group indicate that deposition began ~3223 ± 1 Ma and had ended by ~3219 ± 9 Ma (De Ronde and Kamo, 2000; Heubeck et al., 2013). The deposits experienced only lower greenschist-facies metamorphic overprint and are preserved in several northward-overturned synclines that are tectonically separated by major faults (De Ronde et al., 1991; Toulkeridis et al., 1998; Javaux et al., 2010).

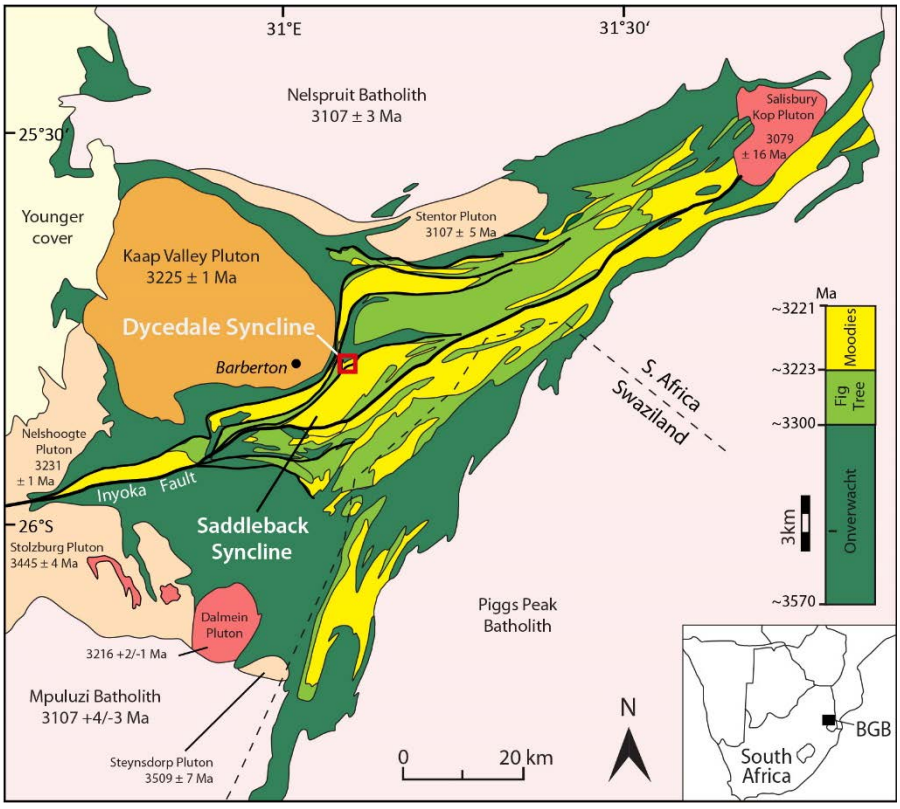

Figure IV. 1: *Simplified geological map of the Barberton Greenstone Belt (BGB) of South Africa and Swaziland and the surrounding plutons. The study region is located in the Dycedale Syncline, a small triangular-shaped synform in the central part of the BGB.*

Steeply dipping strata in a southwestward-plunging fold located 2 km east of the town of Barberton make up the Dycedale Syncline, which is bordered by the Barbrook Fault in the north and by the Saddleback Fault in the south (Fig. IV.1; Visser, 1956; Heubeck and Lowe, 1994a; Lowe et al., 2012). The stratigraphy and structure of the Dycedale Syncline has only been partially explored because most of it is located in the wide valley of Hislop's Creek and poorly exposed. In its western part, however, Moodies strata are well exposed along steep slopes between the converging Barbrook and Saddleback faults (Fig. IV.1). A prominent short ridge just north of the Saddleback Fault has received particular attention by geologists due to its ready accessibility (Heubeck and Lowe, 1994a; Eriksson et al., 2006; Noffke et al., 2006) although only a partial measured section, ~130 m-thick, has been recorded to-date (Eriksson et al., 2006). Lithologies in this section were assigned (base to top) to four units: (1) conglomerate, (2) conglomerate-sandstone, (3) cross-bedded tuffaceous sandstone, and (4) rhythmically interlaminated sandstone-siltstone and mudstone (Eriksson et al., 2006). The succession has previously been interpreted to record a transition from alluvial-fluvial to tide-influenced sedimentation (Heubeck and Lowe, 1994a; Eriksson et al., 2006). Overlying units towards the synclinal axis include thick cross-bedded sandstones, overlain by tuffaceous shales, thin BIFs and a prominent lava; they record the transition from tidal to shallow-marine or prodelta facies. Our study mainly focuses on the lower, conglomerate-dominated part of this succession (unit A in Fig. IV.2).

The conglomerates, interbedded with biolaminated sandstones (unit A) at the base of the section (Fig. IV.2), decrease in clast size, thickness and abundance upsection as they grade into locally gravelly but abundantly rippled and shale-draped, well-sorted sandstones with rip-up shale clasts (unit B). These, in turn, grade upsection to low-angle cross-bedded, gravel-free well-sorted sandstones with occasional rip-up clasts and mud-cracked shale laminae (unit C). Several putative paleosols and a thin bed of dacitic lava also occur within this unit. Unit C is overlain by a thick section of white, high-angle cross-bedded, tuffaceous sandstone with bidirectional cross bedding and rare erosive channels transporting tuffaceous and evaporitic clasts in a sandy-tuffaceous matrix (unit D). Mudcracks and biolaminae are absent; silicified vadose-zone concretions occur in units C and D. Higher up, the cross-bedded sandstones also include dewatering structures and thin tuffaceous shales (unit E), overlain by thick-bedded, tuffaceous, cross-bedded sandstones with large ball-and-pillow structures (unit F).

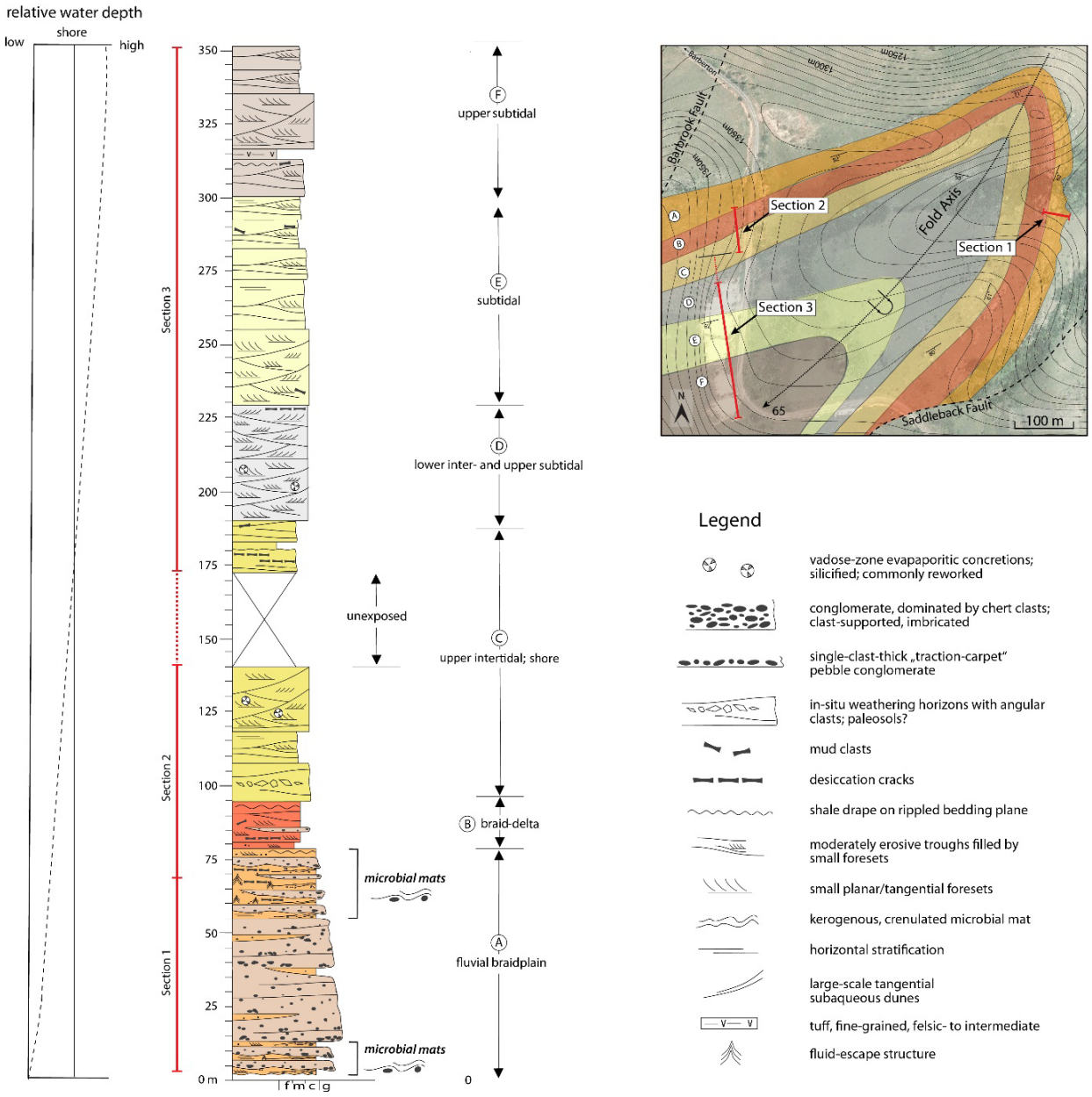

Figure IV. 2: *Composite stratigraphic column of the Dycedale Syncline, part of unit MdQ1 (Anhaeusser, 1976). The position of the measured section is shown in the geological map in the upper right. Note that microbial mats occur at the basal part of the section (unit A) and are confined to gravelly sandstones interbedded with alluvial-fluvial conglomerates.*

IV.3 Microbial mats in conglomerates

The mat-bearing unit A is up to 75-m-thick and consists a ~40-m-thick, mostly clast-supported conglomerate, which is under- and overlain by 10- and 25-m-thick microbial-mat-bearing sandstones with intercalated conglomerate beds (Fig. IV.2).

IV.3.1 Conglomerates

The conglomerates can be easily traced around the hinge of the Dycedale Syncline and on both of its limbs for a total of about 1.2 km prior to being truncated along the fault-bounded northern and southern margin of the syncline (Fig. IV.2). The thick-bedded conglomerate shows systematic thickening in the tight hinge zone of the syncline but no evidence of channeling or large-scale erosive downcutting. However, individual conglomerate beds (<2-m-thick) occurring within the sandstones are lens- or wedge-shaped, commonly vertically stacked, and show minor erosional downcutting (Figs. IV.3A - IV.3C). Clasts are angular to subrounded, poorly-sorted and pebble to boulder-size (max. ca. 40 x 40 cm), embedded in a quartz-rich coarse-sandy matrix. They are mainly composed of several varieties of black, grey, and black-and-white-banded chert derived from the Onverwacht Group and of white to yellow felsic porphyries of Fig Tree Group provenance. Clasts of altered, green ultramafic volcanic rocks and red jaspilites are rare. The clasts show rare imbrication and occasionally inverse gradation and the topmost clasts are commonly draped by thick kerogenous laminae (described below; Fig. IV.3C). The transitions to the overlying sandstones are generally sharp (Fig. IV.3D). Topmost clasts are commonly draped by thick microbial mats, which are described below.

IV.3.2 Sandstones

Sandstones over- and underlying the conglomerate as well as rare lenticular sandstone lenses <5 cm to >2 m thick within the conglomerate unit are mostly medium- to thin-bedded, subhorizontally stratified and locally show low-angle planar cross bedding. These sandstones consist of poorly sorted, in places gravelly, medium- to coarse-grained quartzofeldspatic sand grains and commonly contain discontinuous, single-clast-thick pebble-to-cobble stringers as well as clusters of pebbles lodged next to large cobbles. Importantly, cm-thick, discontinuous dark grey mudstones with abundant desiccation cracks on bedding planes are locally interbedded with the sandstones (Fig. IV.4D).

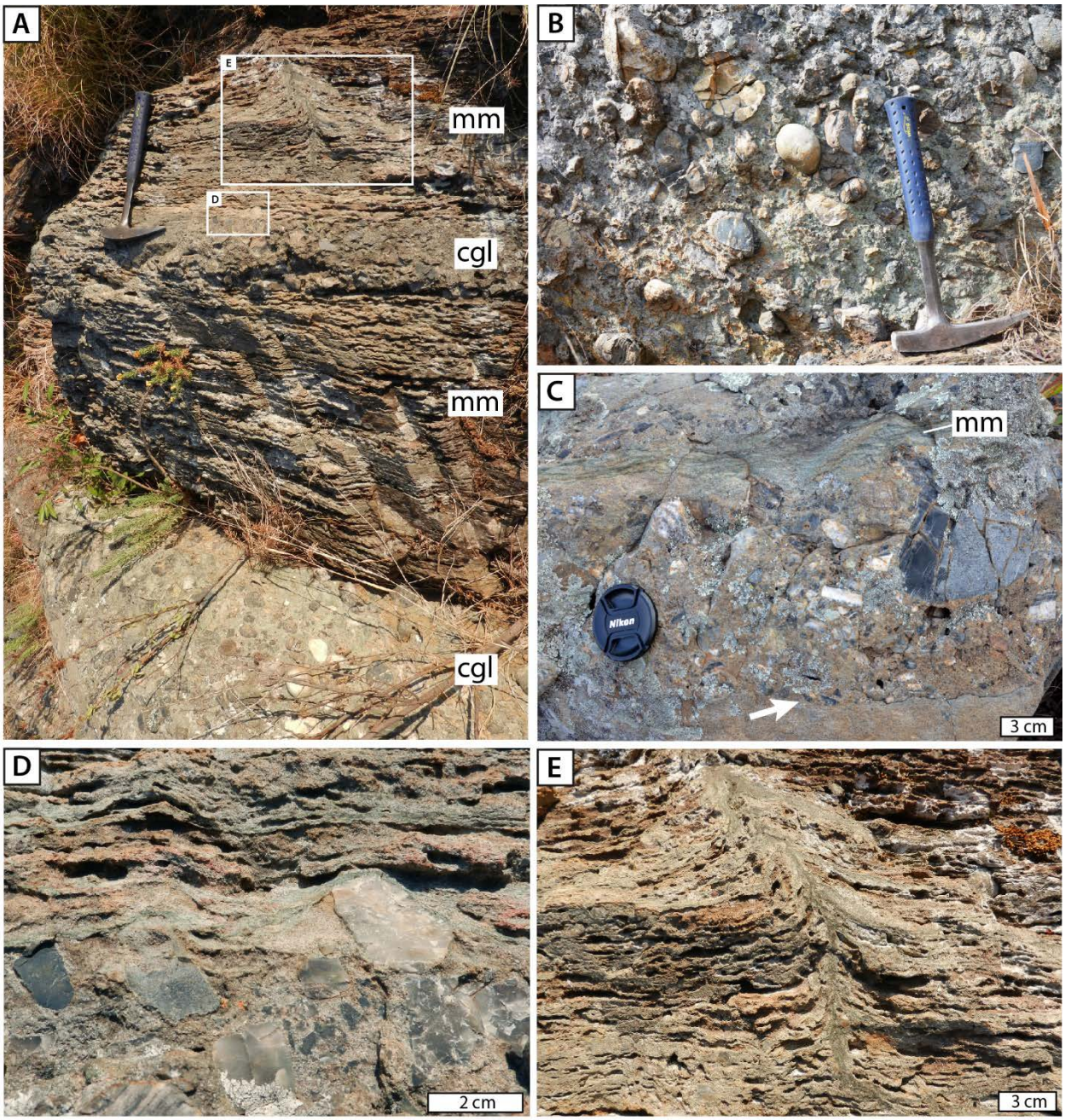

Figure IV. 3: *Field photographs of sandstones and conglomerates in the Dycedale Syncline. (A) Overview photograph showing interbedded microbial mats (mm) and conglomerates (cgl). (B) Close-up of clast-supported conglomerate, composed of rounded chert pebbles and cobbles. (C) Inversely-graded conglomerate with erosive base (arrow), overlain by microbial mats (mm). Lens cap is 5.6 cm in diameter. (D) Close-up view of the framed area in (A), highlighting the top of a conglomerate bed. Note that microbial mats drape "iceberg"-type clasts. (E) Close-up view of the framed area in (A), showing a subvertical fluid-escape structure with a well-defined central channel that disrupts the densely mat-laminated sandstone.*

IV.3.3 Kerogenous laminations

Within the sandstones and on top of conglomerate beds occur mm-spaced, crenulated ("crinkly"), interwoven kerogenous laminations that appear black in fresh samples and represent the fossil remains of microbial mats. These laminae are generally more weathering-resistant than interbedded sandstone devoid of kerogenous laminations, which results in characteristic banding and readily recognizable fenestral porosity patterns in outcrop (Figs. IV.4A, B). Laminae directly overlying conglomerate bed or clast stringers show commonly onlapping and draping geometries on the protruding clasts (Figs. IV.3D, IV.4A and B). Occasionally, planar kerogenous chips of up to several cm in length occur in plane-bedded and cross-laminated sandstones. Where these sandstones are interbedded within conglomerates, the fragments reach up to 50 cm in length and ~1 cm in thickness (Fig. IV.4C).

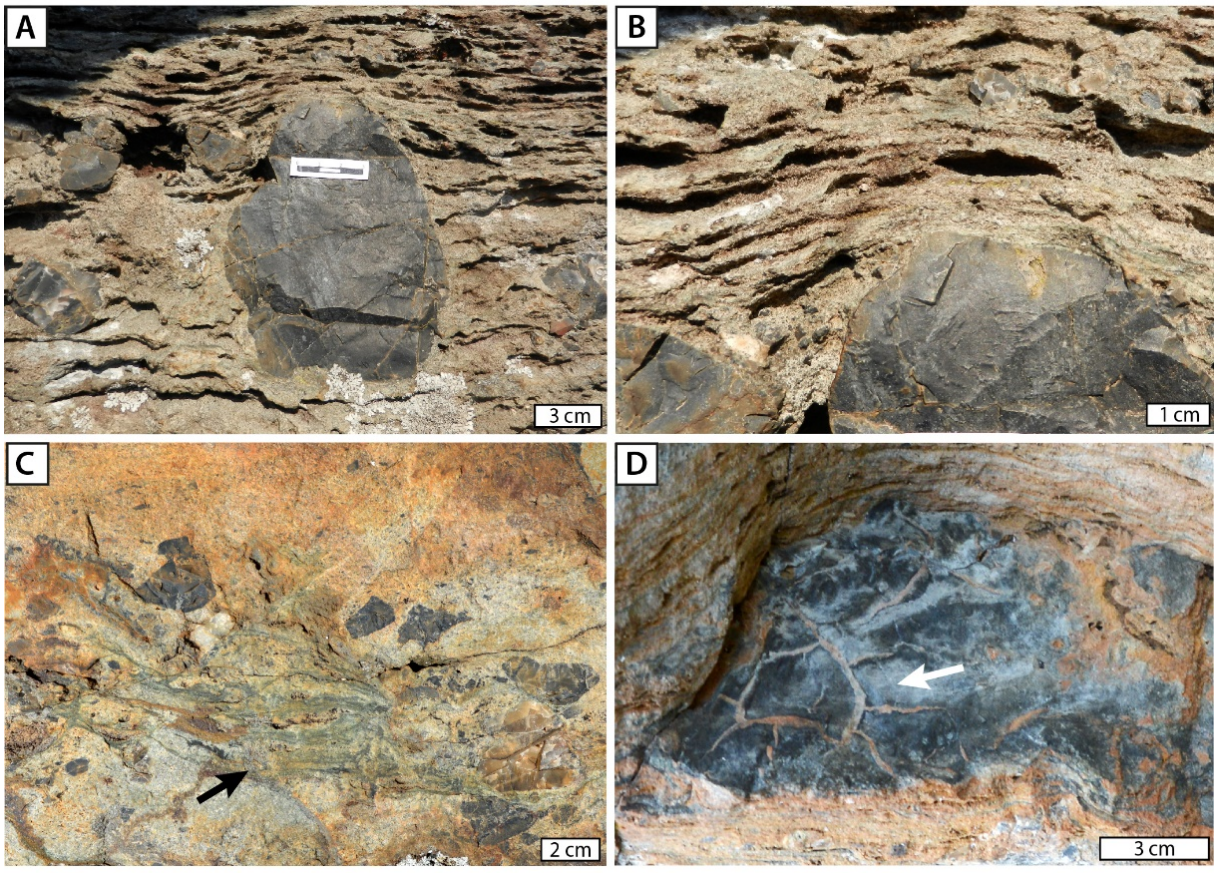

Figure IV. 4: *Field photographs of sedimentary structures associated with microbial mats. (A, B) Microbial mats onlapping and draping interbedded pebbles and cobbles. (C) Cross-section view of eroded microbial mat fragments (arrow) within pebbly sandstone. (D) Desiccation-cracked mudstone (arrow) interbedded with densely microbial-mat-laminated sandstones.*

Microbial mats in gravelly, poorly sorted coarse-grained sandstone are commonly disrupted and deformed by 10- to 50-cm-high, subvertical fluid-escape structures (Figs. IV.3A and IV.3E; Fig. IV.5A). The central dewatering channel is bordered by symmetrically upward-bent microbial mats and occasionally by clusters of pebbles (Fig. IV.5B and IV.5C).

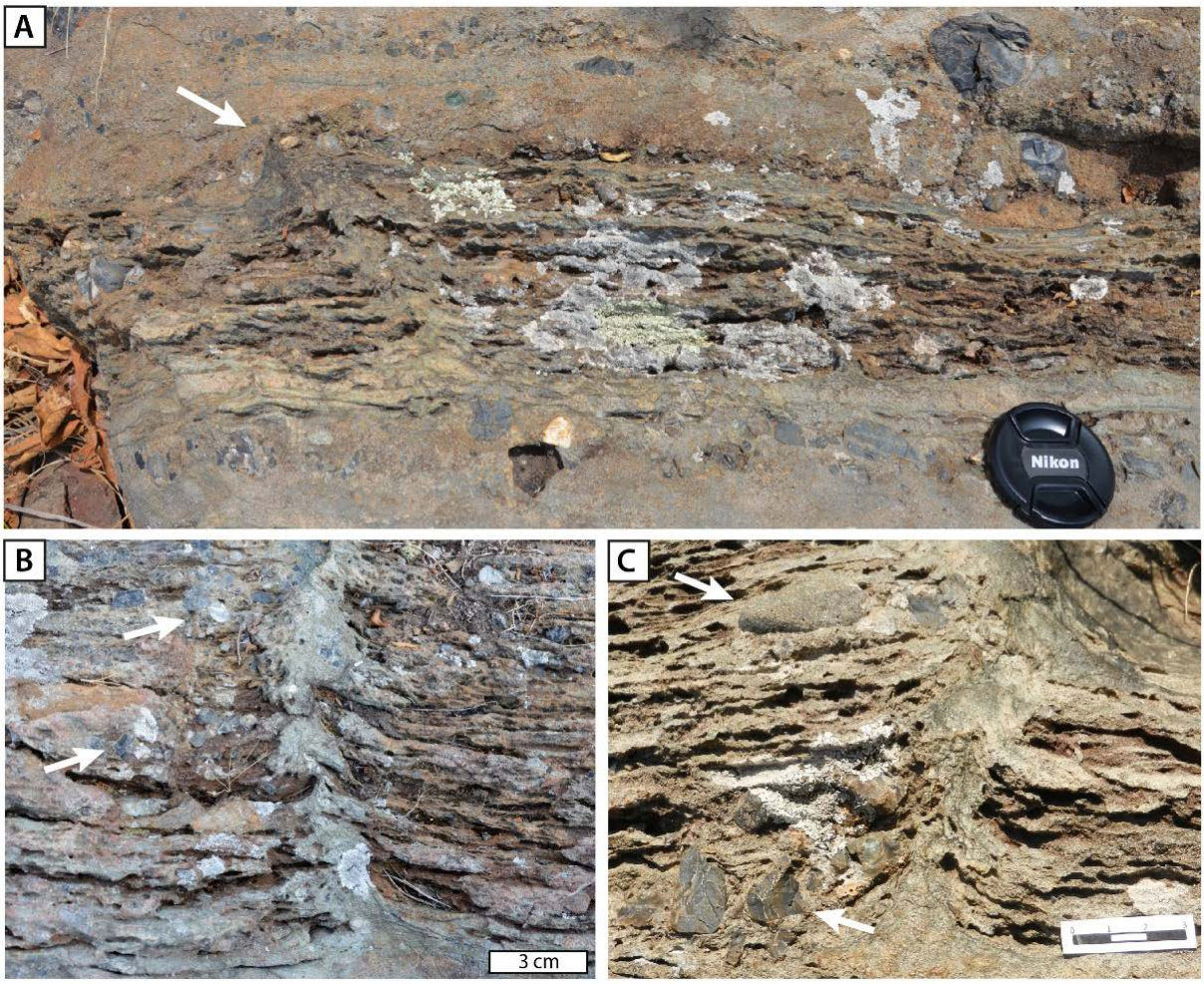

Figure IV. 5: *Field photographs of fluid-escape structures. (A) Subvertical fluid-escape structure (arrow) disrupting thin interval of microbial mats, which is buried by gravelly sandstone. (B and C) Upward-curved mats and pebbles bordering central dewatering channel (arrows).*

In the outcrop as well as in polished slabs, mats appear as densely spaced, 0.5 - 4 mm thick, crinkly laminae of silicified kerogenous material that drapes horizontally laminated and rippled sandstones, onlap individual clasts (Fig. IV.6A and IV.6B), and wrap around granules. Thick laminae include “floating” fine-grained detrital sand grains whose long axes are preferentially aligned with bedding (Figs. IV.6B and IV.6C).

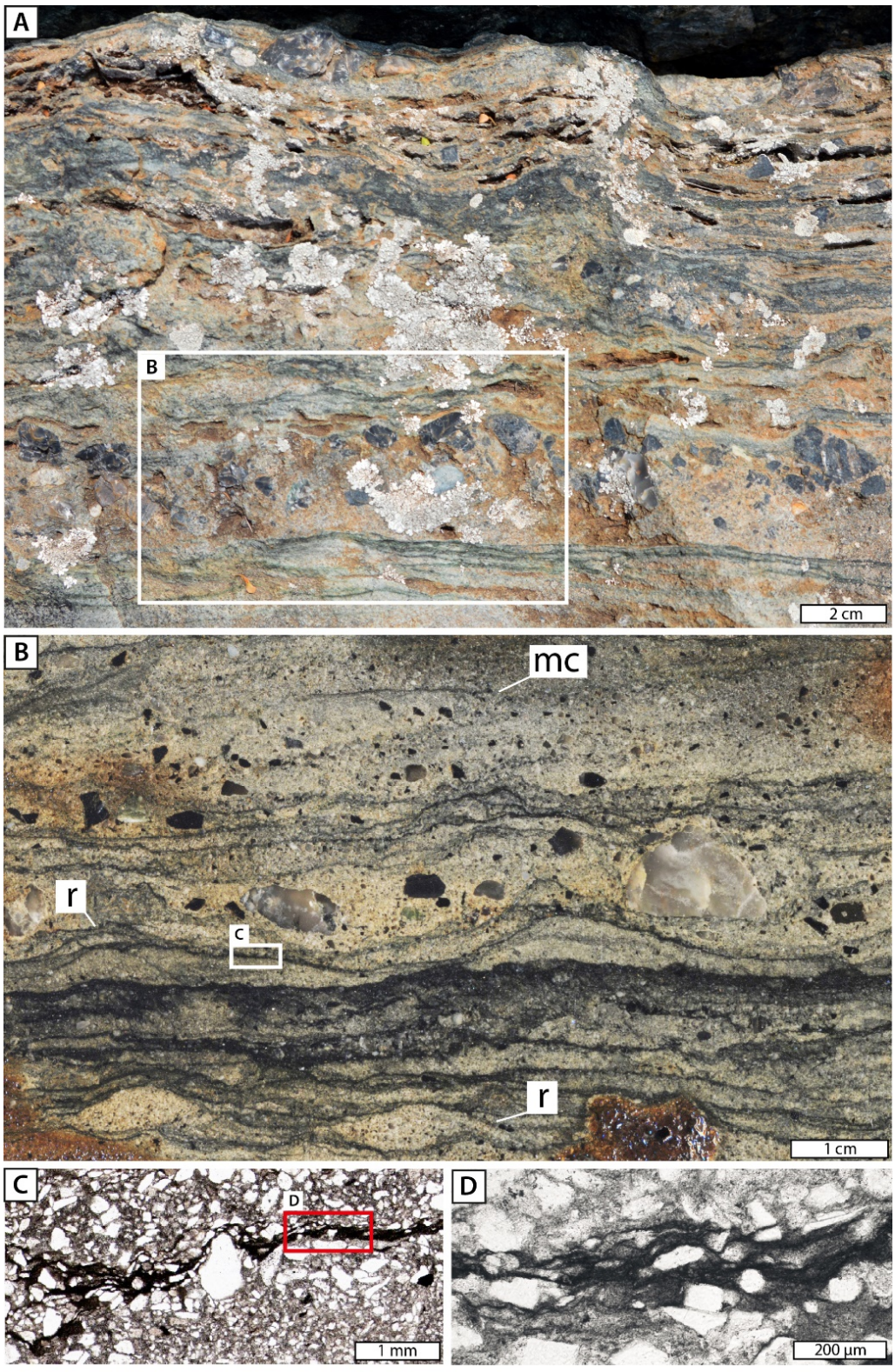

Figure IV. 6: *Outcrop, polished slab, and thin section photographs of crinkly microbial mats (dark laminae) interbedded with poorly sorted, pebbly sandstone, illustrating microbial-mat textures at different scales. (A and B) Mats onlap pebbles and drape horizontally laminated and rippled sand (r). Chips of fragmented microbial mats (mc) are transported in cross-laminated, granularly sandstone. (C and D) Thick kerogenous laminae coat protruding sand grains and contain fine-grained detrital sand. Note that the boxed areas in A-C only indicate representative areas.*

IV.4 Discussion

IV.4.1 Depositional environment

Overall, the stacked lithofacies of the studied stratigraphic succession (Fig. IV.2) suggests a progressively deepening-upward sequence, which begins in a mid- to lower alluvial fan setting, interfingering with a fluvial braidplain (unit A) and grading into a tidally-influenced braid-delta (unit B). The margins of the delta contain extensive beach, supratidal, and upper shoreface deposits (unit C) and are overlain by high-energy supra- and intertidal sandflats and tidal bars (unit D). The overlying units E and F appear to lack indicators of subaerial exposure and rather record high sedimentation rate and hindered dewatering in a subtidal setting.

Hence, the observed lithofacies trend indicates that the mat-bearing gravelly sandstones (unit A) are overlain in logical sequence by successively distal depositional environments and thus unit A represents the most proximal, landward facies. This interpretation is also supported by the fact that these thick-bedded conglomerates show poor sorting, poorly developed internal fabrics, and immature composition indicating a proximal sediment source associated with episodic, short-lived, high-energy transport. These fabrics are typical for sheet flow-dominated alluvial fans and/or proximal braided streams with highly fluctuating discharge (Miall, 2006; Nichols, 2009). The thin-bedded conglomerates intercalated with the mat-bearing sandstones show minor channel incision, rapid fill and frequent avulsion, characteristic of alluvial or fluvial discharge patterns. Furthermore, occasional inversely-graded conglomerate beds may have formed during high-energy episodic flash floods or in matrix-poor debris flows (Sohn et al., 1999; Rasmussen, 2000).

Based on this well-established stratigraphic context we conclude that the mats were thriving in one or several terrestrial aquatic paleoenvironments subject to occasional or frequent subaerial exposure, evidenced by the widespread presence of desiccation cracks. The microbial communities likely developed within gravel-filled braided fluvial channels during low current velocities and/or in shallow ephemeral ponds on the sandy-gravelly floodplain as similarly observed in 2.7 Ga fluvial-lacustrine stromatolites of the Ventersdorp Supergroup (South Africa; Buck, 1980), and 1.09 Ga fluvial-alluvial stromatolites within the Copper Harbor Conglomerates (Keweenaw Peninsula, Michigan, USA; Elmore, 1983; Fedorchuk, 2014). Although, we interpret this environment as being terrestrial, it cannot be fully excluded that the highest tides, which are thought of having been much higher in the Archean (Coughenour et al., 2009; Longhitano et al., 2012), could have occasionally flooded even the most landward, normally fluvially-dominated channels and braidplain ponds.

IV.4.2 Physical mat properties

The observation that thick beds of abrasive coarse-grained sands and gravel were repeatedly emplaced on top of the mats without severely damaging or eroding them indicates a high mat strength and cohesiveness. However, during gravel transport and therefore higher shear stresses, mats were partially eroded, transported, and deposited as fragments within the conglomerate. Subsequently, the microbial mats overgrew the gravelly conglomerate beds indicating a rapid and prolonged reestablishment of a suitable habitat for microbial growth.

The cohesive water-impermeable nature and lateral continuity of the mats is further indicated by the exclusive occurrence of numerous fluid-escape structures in mat-bearing deposits. The supposedly water-impermeable mats confined the escape of the pressurized pore water to a lateral flow through the permeable sand layers and escaping only vertically at locations were mats have been disrupted. The force of the escaping fluids was even strong enough to transport pebbles laterally within the fluidized sediment towards the dewatering channel and dragging multiple layers of cohesive mats upward into the central conduit. In modern mat-covered shallow-water deposits tidal pumping is known as main driver for fluidization (Taj et al., 2014), but since the here described microbial mats were not thriving in a tidal setting we assume that the pressurization was triggered by a rapid overburden of sediment consistent with high sedimentation rates in alluvial fans. The escaping water could have been sourced by the compaction of buried mats (typically containing between 80 and 90% water, Schieber, 2004) and loosely packed sediments.

IV.4.3 Implications of terrestrial life in the Archean

Overall, it is still enigmatic how the Archean world and the first continental landmasses looked like. Due to the scarcity of preserved terrestrial deposits, in contrast to marine sediments, there is particular little knowledge about the geomorphology of the Archean continents, the nature and extent of critical zone (Brantley et al., 2011), and finally to which degree microbial life affected these aspects as they strongly do on modern Earth. Today, microbial life takes great part in shaping the topography continental landscapes (Brantly et al., 2011). On the one hand, biologically-mediated weathering increases erosion rates, while on the other hand, the presence of a benthic cohesive mat can significantly reduce erosion rates, referred to as biostabilization (Cuadrado et al., 2011, 2014).

The colonization of the Archean land surface may also indicate an evolutionary leap of adaptation to harsh environments, since life in such a new environmental niche would have been subject to repeated desiccation, fluvial or aeolian abrasions, high temperature, and presumably intense UV radiation (Knauth and Lowe, 2003; Sleep and Hessler, 2006; Cockell and Raven, 2007). (1) High shear stresses require a cohesive and resistive mat, (2) short-term subaerial exposure can be overcome through the hygroscopic properties of the EPS matrix (Decho, 2013), whereas (3) prolonged periods of desiccation demand an ability

of the cells to survive in dormancy, and (4) high UV radiation requires either the synthesis of UV-screening pigments and/or enhanced ability of DNA-repair.

Concerning the metabolism of Archean microbial communities there is little certainty and only indirect evidence. In the present study there are multiple lines of evidence for photosynthesis:
(1) the mats thrived in a terrestrial shallow-water photic zone; (2) phototrophic microbial communities of very similar appearance have also been found in stratigraphically coeval intertidal deposits of the Moodies Group outcrops in the adjacent Saddleback Syncline (Heubeck, 2009; Homann et al., 2015); (3) moreover, evidence for photosynthetic communities have also been documented in up to 3.42 Ga shallow-marine deposits in the BGB (e.g. Tice and Lowe, 2004; Westall et al., 2006, 2011, 2015) and were possibly also involved in the formation of coniform stromatolites from both the 3.4 Ga Strelley Pool Formation and the 3.48 Ga Dresser Formation in the Pilbara Craton (Hofmann et al., 1999; Van Kranendonk, 2011); (4) the lack of indicators for sulfate- or iron-based metabolisms (e.g. iron oxides, biogenic pyrite etc.); and finally, (5) chemotrophic communities are not known to develop thick and cohesive microbial mats.

IV.5 Conclusions

Microbial mats preserved in the Dycedale Syncline of the 3.22 Ga Moodies Group thrived in episodically high-energy braided channels and ephemeral ponds on an Archean sandy floodplain adjacent to alluvial fans and tidally-dominated shorelines. The colonization of such a habitat in the photic zone required the microbial communities to adapt to harsh conditions, including desiccation, sediment abrasion, and high UV radiation. Our findings extend the record of Archean microbial ecosystems into near-coastal but clearly terrestrial aquatic settings by ~400 m.y.

IV.6 Acknowledgements

We thank Saskia Bläsing and Marc Grund for their detailed mapping of the Dycdale Syncline, logging of stratigraphy, and sample collection. Anna Giribaldi is thanked for thinsectioning.

IV.7 References

Anhaeusser, C.R., 1976, The geology of the Sheba Hills area of the Barberton Mountain Land, South Africa: with particular reference to the Eureka Syncline: Trans. Geol. Soc. S. Afr, v. 79, p. 253–280.

Awramik, S.M., and Buchheim, H.P., 2009, A giant, Late Archean lake system: The Meentheena Member (Tumbiana Formation; Fortescue Group), Western Australia: Precambrian Research, v. 174, no. 3-4, p. 215–240, doi: 10.1016/j.precamres.2009.07.005.

Battistuzzi, F.U., Feijao, A., and Hedges, S.B., 2004, A genomic timescale of prokaryote evolution: insights into the origin of methanogenesis, phototrophy, and the colonization of land.: BMC evolutionary biology, v. 4, p. 44, doi: 10.1186/1471-2148-4-44.

Beraldi-Campesi, H., 2013, Early life on land and the first terrestrial ecosystems: Ecological Processes, v. 2, no. 1, p. 1, doi: 10.1186/2192-1709-2-1.

Brantly, S.L., Megonigal, J.P., Scatena, F.N., Balogh-Brunstad, Z., Barnes, R.T., BRUNS, M.A., Van Cappellen, P., Dontsova, K., Hartnett, H.E., Hartshorn, A.S., Heimsath, A., Herndon, E., JIN, L., Keller, C.K., et al., 2011, Twelve testable hypotheses on the geobiology of weathering: Geobiology, v. 9, no. 2, p. 1–26, doi: 10.1111/j.1472-4669.2010.00264.x.

Buck, S.G., 1980, Stromatolite and ooid deposits within the fluvial and lacustrine sediments of the Precambrian Ventersdorp Supergroup of South Africa: Precambrian Research, v. 12, no. 1-4, p. 311–330, doi: 10.1016/0301-9268(80)90033-9.

Buick, R., 1992, The antiquity of oxygenic photosynthesis: evidence from stromatolites in sulphate-deficient Archaean lakes.: Science, v. 255, no. 5040, p. 74–77, doi: 10.1126/science.11536492.

Cockell, C.S., and Raven, J. a, 2007, Ozone and life on the Archaean Earth.: Philosophical transactions. Series A, Mathematical, physical, and engineering sciences, v. 365, no. 1856, p. 1889–1901, doi: 10.1098/rsta.2007.2049.

Coffey, J.M., Flannery, D.T., Walter, M.R., and George, S.C., 2013, Sedimentology, stratigraphy and geochemistry of a stromatolite biofacies in the 2.72Ga Tumbiana Formation, Fortescue Group, Western Australia: Precambrian Research, v. 236, p. 282–296, doi: 10.1016/j.precamres.2013.07.021.

Coughenour, C.L., Archer, A.W., and Lacovara, K.J., 2009, Tides, tidalites, and secular changes in the Earth–Moon system: Earth-Science Reviews, v. 97, no. 1-4, p. 59–79, doi: 10.1016/j.earscirev.2009.09.002.

Cuadrado, D.G., Carmona, N.B., and Bournod, C., 2011, Biostabilization of sediments by microbial mats in a temperate siliciclastic tidal flat, Bahia Blanca estuary (Argentina): Sedimentary Geology, v. 237, no. 1-2, p. 95–101, doi: 10.1016/j.sedgeo.2011.02.008.

Cuadrado, D.G., Perillo, G.M.E., and Vitale, A.J., 2014, Modern microbial mats in siliciclastic tidal flats: Evolution, structure and the role of hydrodynamics: Marine Geology, v. 352, p. 367–380, doi: 10.1016/j.margeo.2013.10.002.

Decho, A.W., 2013, The EPS matrix as an adaptive bastion for biofilms: Introduction to special issue: International Journal of Molecular Sciences, v. 14, no. 12, p. 23297–23300, doi: 10.3390/ijms141223297.

Elmore, R.D., 1983, Precambrian non-marine stromatolites in alluvial fan deposits, the Copper Harbor Conglomerate, upper Michigan: Sedimentology, v. 30, no. 6, p. 829–842, doi: 10.1111/j.1365-3091.1983.tb00713.x.

Eriksson, K.A., 1978, Alluvial and destructive beach facies from the Archaean Moodies Group, Barberton Mountain Land, South Africa and Swaziland, *in* Miall, A.D. ed., Fluvial Sedimentology, Can. Soc.

Petrol. Geol., Mem. 5, p. 287–311.

Eriksson, K.A., 1979, Marginal marine depositional processes from the Archaean Moodies Group, Barberton Mountain Land; South Africa: Evidence and significance: Precambrian research, v. 8, p. 153–182.

Eriksson, K.A., 1977, Tidal deposits from the Archaean Moodies Group, Barberton Mountain Land, South Africa: Sedimentary Geology, v. 18, p. 257–281.

Eriksson, K.A., and Simpson, E.L., 2000, Quantifying the oldest tidal record: The 3.2 Ga Moodies Group, Barberton Greenstone Belt, South Africa: Geology, v. 28, no. 9, p. 831, doi: 10.1130/0091-7613(2000)28<831:QTOTRT>2.0.CO;2.

Eriksson, K.A., Simpson, E.L., and Mueller, W.U., 2006, An unusual fluvial to tidal transition in the mesoarchean Moodies Group, South Africa: A response to high tidal range and active tectonics: Sedimentary Geology, v. 190, no. 1-4, p. 13–24, doi: 10.1016/j.sedgeo.2006.05.011.

Fedorchuk, N.D., 2014, Evaluating the Biogenicity of Fluvial-lacustrine Stromatolites from the Mesoproterozoic Copper Harbor Conglomerate , Upper Peninsula of Michigan , USA: University of Wisconsin-Milwaukee, 161 p.

Heubeck, C., Engelhardt, J., Byerly, G.R., Zeh, A., Sell, B., Luber, T., and Lowe, D.R., 2013, Timing of deposition and deformation of the Moodies Group (Barberton Greenstone Belt, South Africa): Very-high-resolution of Archaean surface processes: Precambrian Research, v. 231, p. 236–262, doi: 10.1016/j.precamres.2013.03.021.

Heubeck, C., and Lowe, D.R., 1994a, Depositional and tectonic setting of the Archean Moodies Group, Barberton greenstone belt, South Africa: Precambrian research, v. 68, p. 257–290.

Heubeck, C., and Lowe, D.R., 1994b, Late syndepositional deformation and detachment tectonics in the Barberton Greenstone Belt, South Africa: Tectonics, v. 13, no. 6, p. 1514–1536.

Heubeck, C., and Lowe, D.R., 1999, Sedimentary petrography and provenance of the Archean Moodies Grou, Barberton Greenstone Belt, *in* Lowe, D.R. and Byerly, G.R. eds., Geologic evolution of the Barberton Greenstone Belt, South Africa, Geological Society of America Special Paper 329, p. 259–286.

Hofmann, H.J., Grey, K., Hickman, A.H., and Thorpe, R.I., 1999, Origin of 3.45 Ga coniform stromatolites in Warrawoona Group, Western Australia: Geological Society of America Bulletin, v. 111, no. 8, p. 1256–1262, doi: 10.1130/0016-7606(1999)111<1256:OOGCSI>2.3.CO;2.

Homann, M., Heubeck, C., Airo, A., and Tice, M.M., 2015, Morphological adaptations of 3.22 Ga-old tufted microbial mats to Archean coastal habitats (Moodies Group, Barberton Greenstone Belt, South Africa): Precambrian Research, v. 266, p. 47–64, doi: 10.1016/j.precamres.2015.04.018.

Horodyski, R.J., and Knauth, L.P., 1994, Life on land in the precambrian.: Science (New York, N.Y.), v. 263, no. 5146, p. 494–498, doi: 10.1126/science.263.5146.494.

Javaux, E.J., Marshall, C.P., and Bekker, A., 2010, Organic-walled microfossils in 3.2-billion-year-old shallow-marine siliciclastic deposits.: Nature, v. 463, no. 7283, p. 934–8, doi: 10.1038/nature08793.

Knauth, L.P., and Lowe, D.R., 2003, High Archean climatic temperature inferred from oxygen isotope geochemistry of cherts in the 3.5 Ga Swaziland Supergroup, South Africa: Bulletin of the Geological Society of America, v. 115, no. 5, p. 566–580, doi: 10.1130/0016-7606(2003)115<0566:HACTIF>2.0.CO;2.

Van Kranendonk, M.J., 2011, Stromatolite morphology as an indicator of biogenicity for Earth's oldest fossils from the 3.5-3.4 Ga Pilbara Craton, Western Australia, *in* Reitner, J., Quéric, N.-V., and Arp, G. eds., Advances in Stromatolite Geobiology, Springer, Germany, p. 517–534.

Lalonde, S. V., and Konhauser, K.O., 2015, Benthic perspective on Earth's oldest evidence for oxygenic photosynthesis: Proceedings of the National Academy of Sciences, v. 112, p. 995–1000, doi: 10.1073/pnas.1415718112.

Layer, P.W., Kroner, A., and McWilliams, M., 1996, An Archean Geomagnetic Reversal in the Kaap Valley Pluton, South Africa: Science (New York, N.Y.), v. 273, p. 943–946.

Longhitano, S.G., Mellere, D., Steel, R.J., and Ainsworth, R.B., 2012, Tidal depositional systems in the rock record: A review and new insights: Sedimentary Geology, v. 279, p. 2–22, doi: 10.1016/j.sedgeo.2012.03.024.

Lowe, D.R., Byerly, G.R., and Heubeck, C., 2012, Geologic Map of the west-central Barberton Greenstone Belt, *in* South Africa, scale 1:25,000, Geological Society of America Map and Chart Series No. 103, Boulder.

Miall, A.D., 2006, The Geology of Fluvial Deposits: Springer Berlin Heidelberg, Berlin, Heidelberg.

Nichols, G., 2009, The Marine Realm: Morphology and Processes, *in* Sedimentology and Stratigraphy, Wiley-Blackwell, p. 163–178.

Noffke, N., Eriksson, K.A., Hazen, R.M., and Simpson, E.L., 2006, A new window into Early Archean life: Microbial mats in Earth's oldest siliciclastic tidal deposits (3.2 Ga Moodies Group, South Africa): Geology, v. 34, no. 4, p. 253, doi: 10.1130/G22246.1.

Rasmussen, H., 2000, Nearshore and alluvial facies in the Sant Llorenç del Munt depositional system: Recognition and development: Sedimentary Geology, v. 138, no. 1-4, p. 71–98, doi: 10.1016/S0037-0738(00)00144-5.

Rasmussen, B., Blake, T.S., Fletcher, I.R., and Kilburn, M.R., 2009, Evidence for microbial life in synsedimentary cavities from 2.75 Ga terrestrial environments: Geology, v. 37, no. 5, p. 423–426, doi: 10.1130/G25300A.1.

Riding, R.E., and Awramik, S.M. (Eds.), 2000, Microbial Sediments: Springer Berlin Heidelberg, Berlin, Heidelberg.

De Ronde, C.E.J., Hall, C.M., York, D., and Spooner, E.T.C., 1991, Laser step-heating 40Ar/39Ar age spectra from Early Archean (~3.5 Ga) Barberton greenstone belt sediments: A technique for detecting cryptic tectono-thermal events: Geochimica et Cosmochimica Acta, v. 55, p. 1933–1951.

De Ronde, C.E.J., and Kamo, S.L., 2000, An Archaean arc-arc collisional event: A short-lived (ca 3 Myr) episode, Weltevreden area, Barberton greenstone belt, South Africa: Journal of African Earth Sciences, v. 30, no. 2, p. 219–248, doi: 10.1016/S0899-5362(00)00017-8.

Rye, R., and Holland, H.D., 2000, Life associated with a 2.76 Ga ephemeral pond?: Evidence from Mount Roe #2 paleosol: Geology, v. 28, no. 6, p. 483–486, doi: 10.1130/0091-7613(2000)28<483:LAWAGE>2.0.CO;2.

Schieber, J., 2004, Microbial mats in the siliciclastic rock record: a summary of diagnostic features, *in* Eriksson, P.G., Altermann, W., Nelson, D.R., Mueller, W.U., and Catuneanu, O. eds., The Precambrian Earth: Tempos and Events, Elsevier (Developments in Precambrian Geology), Amsterdam, p. 663–673.

Shear, W.A., 1991, The early development of terrestrial ecosystems: Nature, v. 351, no. 6324, p. 283–289, doi: 10.1038/351283a0.

Sheldon, N.D., 2012, Microbially Induced Sedimentary Structures in the Ca . 1100 Ma Terrestrial Midcontinent Rift of North America, *in* Noffke, N. and Chafetz, H.S. eds., Microbial Mats in Silicilastic Depositional Systems Through Time, SEPM, Tulsa, p. 153–162.

Simpson, E.L., Eriksson, K.A., and Mueller, W.U., 2012, 3.2 Ga eolian deposits from the Moodies Group,

Barberton Greenstone Belt, South Africa: Implications for the origin of first-cycle quartz sandstones: Precambrian Research, v. 214-215, p. 185–191, doi: 10.1016/j.precamres.2012.01.019.

Sleep, N.H., and Hessler, A.M., 2006, Weathering of quartz as an Archean climatic indicator: Earth and Planetary Science Letters, v. 241, no. 3-4, p. 594–602, doi: 10.1016/j.epsl.2005.11.020.

Sohn, Y.K., Rhee, C.W., and Kim, B.C., 1999, Debris Flow and Hyperconcentrated Flood-Flow Deposits in an Alluvial Fan, Northwestern Part of the Cretaceous Yongdong Basin, Central Korea: The Journal of Geology, v. 107, no. 1, p. 111–132, doi: 10.1086/314334.

Taj, R.J., Aref, M. a. M., and Schreiber, B.C., 2014, The influence of microbial mats on the formation of sand volcanoes and mounds in the Red Sea coastal plain, south Jeddah, Saudi Arabia: Sedimentary Geology, v. 311, p. 60–74, doi: 10.1016/j.sedgeo.2014.06.006.

Tice, M.M., and Lowe, D.R., 2004, Photosynthetic microbial mats in the 3 , 416-Myr-old ocean fluorescence at the Geoanalytical Laboratory , Washington State University (Pullman ,: Nature, v. 431, no. September, p. 549–552, doi: 10.1038/nature02920.1.

Toulkeridis, T., Goldstein, S.L., Clauer, N., Kröner, A., Todt, W., and Schidlowski, M., 1998, Sm-Nd, Rb-Sr and Pb-Pb dating of silicic carbonates from the early Archaean Barberton Greenstone Belt, South Africa: evidence for post-depositional isotopic resetting at low temperature: Precambrian research, v. 92, p. 129–144.

Visser, D., 1956, The geology of the Barberton area.: Geol. Soc. S. Afr. Spec. Publ., v. 15, p. 253.

Watanabe, Y., Martini, J.E., and Ohmoto, H., 2000, Geochemical evidence for terrestrial ecosystems 2.6 billion years ago.: Nature, v. 408, no. 6812, p. 574–578, doi: 10.1038/35046052.

Westall, F., Campbell, K. a., Breheret, J.G., Foucher, F., Gautret, P., Hubert, a., Sorieul, S., Grassineau, N., and Guido, D.M., 2015, Archean (3.33 Ga) microbe-sediment systems were diverse and flourished in a hydrothermal context: Geology, v. 43, no. 7, p. 615–618, doi: 10.1130/G36646.1.

Westall, F., Cavalazzi, B., Lemelle, L., Marrocchi, Y., Rouzaud, J.N., Simionovici, A., Salomé, M., Mostefaoui, S., Andreazza, C., Foucher, F., Toporski, J., Jauss, A., Thiel, V., Southam, G., et al., 2011, Implications of in situ calcification for photosynthesis in a ~3.3Ga-old microbial biofilm from the Barberton greenstone belt, South Africa: Earth and Planetary Science Letters, v. 310, no. 3-4, p. 468–479, doi: 10.1016/j.epsl.2011.08.029.

Westall, F., De Ronde, C.E.J., Southam, G., Grassineau, N., Colas, M., Cockell, C., and Lammer, H., 2006, Implications of a 3.472-3.333 Gyr-old subaerial microbial mat from the Barberton greenstone belt, South Africa for the UV environmental conditions on the early Earth.: Philosophical transactions of the Royal Society of London. Series B, Biological sciences, v. 361, no. 1474, p. 1857–75, doi: 10.1098/rstb.2006.1896.

V.

Conclusions and outlook

Collectively, this work can be summarized in five major conclusions:

(1) The best-preserved microbial mats of the Moodies Group are located in the Saddleback and Dycedale Synclines in the central part of the BGB. They appear within a stratigraphically coherent interval of approx. 1000 m thickness, which extents laterally for approx. 15 km along strike. The microbial communities of the "Moodies ecosystem" were widespread and well-adapted to Paleoarchean shallow-water tidal and aquatic terrestrial settings.

(2) The mats, preserved as kerogen-rich laminae, show distinct morphological adaptations to different shallow-water settings, which formed as a response of the phototrophic microbial communities to changing physiochemical conditions. Tufted microbial mats, in particular, yield the most convincing indications that they were built by ancestral cyanobacteria.

(3) In situ $\delta^{13}C_{PDB}$ isotope measurements of kerogenous laminae yielded values (between -32.3‰ and -21.3‰) that are consistent with a biogenic origin. Raman spectra of the kerogen correlate with independently reconstructed regional peak metamorphic temperatures of the host rock and further support the biogenicity of the microbial mats.

(4) Microbial communities in elongated, former gas- and fluid-filled, bedding-parallel cavities beneath the mats extend the geological record of coelobionts by ~500 Ma and support the view that cavities were among the first ecological niches to have been occupied by early microorganisms.

(5) The local association of mats with alluvial-fluvial conglomerates and sandstones indicates the onset of colonialization of terrestrial habitats and extends the record of terrestrial life by ~400 Ma.

Future work will focus on unraveling the mats' metabolism. Several lines of evidence (e.g., tufted morphology) and comparison with modern analogs suggest that Moodies microbial communities were at least in part dominated by filamentous organisms. If cyanobacteria were indeed the only microorganisms capable of forming macroscopic tufts, their first appearance in the geological record could be potentially used as a valid morphological biosignature for the presence of cyanobacteria. However, unequivocal evidence for elevated oxygen concentration in the immediate vicinity of the mats remains to be demonstrated. If cyanobacteria were conceivably metabolizing oxygen at modern rates already at 3.2 Ga, the generated oxygen would have been quickly and locally consumed, leaving perhaps a distinct isotopic fingerprint in the adjacent sediments. Hence, combined investigations of Mo, Cr, Mn, U, and Se isotope values, as well a U could potentially constrain the mat metabolism(s).

Appendixes

A.1

Microbial mat, Moodies Group (BGB, South Africa)

Martin Homann

In: M. Gargaud, R. Amils, J.C. Quintanilla, H.J. Cleaves, W.M. Irvine, D. Pinti and M. Viso (Ed.)
Encyclopedia of Astrobiology, Springer-Verlag Berlin Heidelberg, 2015

doi: 10.1007/978-3-662-44185-5_5194

The Paleoarchean Moodies Group (~3.22 Ga, Barberton Greenstone Belt, South Africa), Earth's oldest known well-preserved shallow-water siliciclastic sequence, includes several units with common microbial mats which thrived in the photic zone of a tidally influenced shoreline. The fossil mats are preserved as kerogenous laminations up to 1 mm thick, are interbedded with medium- to coarse-grained sandstones and rare gravel beds (Fig. A1.1), and were early silicified. SEM observations of the laminae show interwoven and bundled microbial filaments (1-3 µm in diameter), confirming mat biogenicity. Microbial communities in the Moodies Group colonized at least three major depositional settings, each associated with a specific mat morphotype: (1) In the *coastal floodplain*, mats are typically flat and occasionally overgrew gravel beds; (2) tufted microbial mats, which reach 0.3 - 1 cm in height, are exclusively present in the supratidal zone and are commonly associated with gas and/or fluid escape structures; and (3) wavy-crinkly morphotypes with small microbial domes are characteristic of the intertidal zone. Modern tufted mats are dominantly built by filamentous cyanobacteria, suggesting that their ancient counterparts may have been constructed by filamentous organisms and required early mineralization for support. It is likely that Moodies microbial mats were (at least in part) photosynthetic communities because other potential metabolic strategies can be excluded, the morphology indicates phototactic behavior, and the mats consistently occur in shallow-water/photic-zone facies.

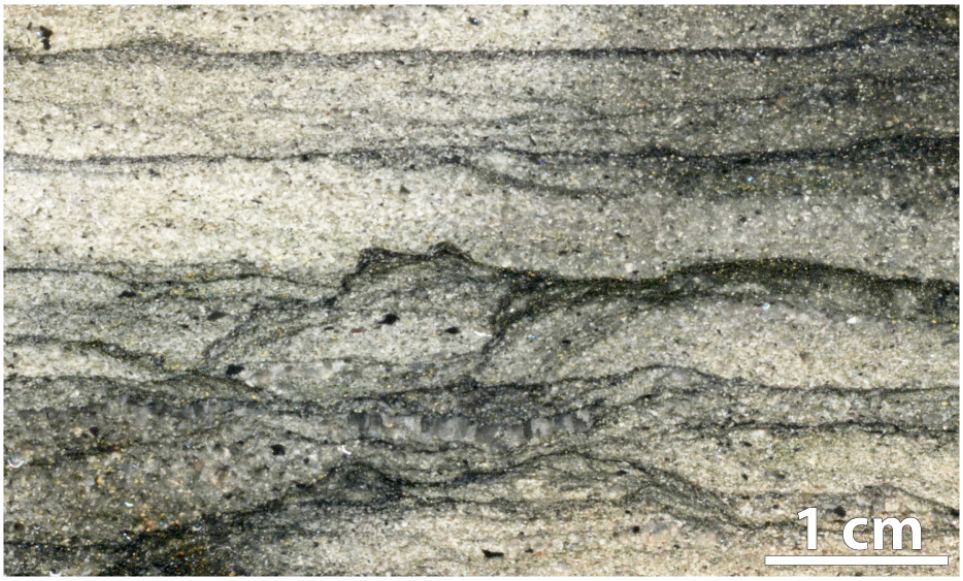

Figure A1. 1: *Photograph of a part of a polished slab of microbial mats (dark laminae) from the Moodies Group. Kerogenous laminae are interbedded with medium- to coarse-grained sandstone. They are of the wavy-crinkly morphotype and show small domes.*

A.2

Modern microbial mats and mat growth experiments

Studies of modern analogues and laboratory-grown mats are fundamental when working with fossil mats and can significantly improve the understanding of various morphological and geochemical biosignatures found in Archean sedimentary rocks.

Widespread microbial mats can be studied e.g. in several inter- to supratidal flats along the southeastern Mediterranean coast of Tunisia (Gerdes et al., 2000; Noffke et al., 2001b) and are particularly well-developed in the tidal channel of Bahar Alouane. The area is characterized by a sub-tropical semi-arid climate and a microtidal regime with tidal amplitudes ranging between 0.8 and 1.5 m (Davaud and Septfontain, 1995). The tidal flats are flooded and exposed daily at regular intervals. However, flooding can also occur at irregular intervals triggered by spring tides or strong land-directed winds that push water up to the supratidal zone (Bouougri and Porada, 2012). The low-gradient tidal flats are widely colonized by cohesive microbial mats, which are mainly formed by filamentous cyanobacteria of the species *Microcoleus chthonoplastes* and *Lyngbya aestuarii* (Gerdes et al., 2000). They form 1-10-mm-thick, carpet-like structures and produce patterns of reticulate ridges with tufts on the mat surface. Other mat-related structures are: gas domes, polygonal cracks (Noffke et al., 2001a; Gerdes, 2007), shrinkage cracks, roll-up structures, and mat chips. Low sediment input rates and the absence of predators facilitate the development and growth of microbial mats in these coastal environments. Solely burrowing beetles of the genus *Bledius* and Cerithid gastropods are found grazing in or below the mats and able withstand the high salinity ranging between 40‰ to 180‰ (Gerdes et al., 2000; Gerdes et al., 2008). Fieldwork and sample collection was carried out between 30.09. – 6.10.2013 with local support by Mohamed Soussi and Rached Lakhdar.

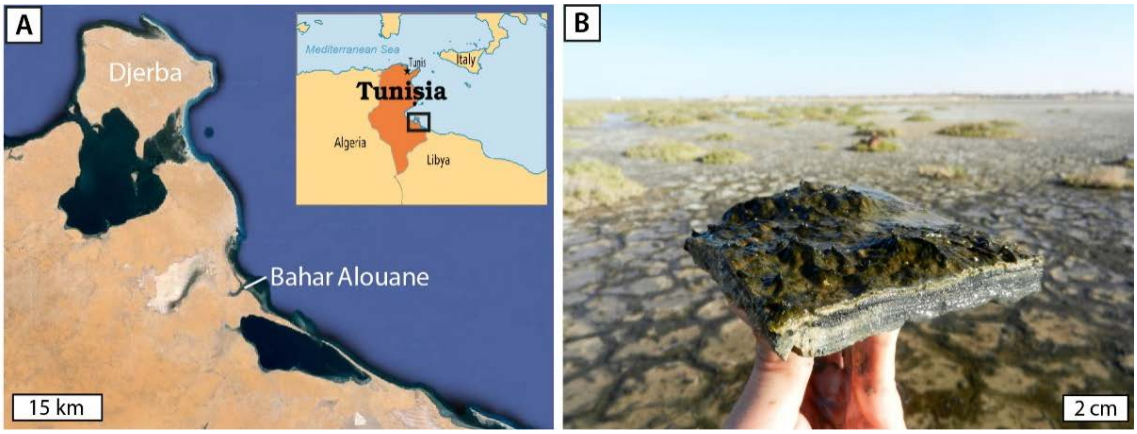

Figure A2. 1: *(A) Location of Bahar Alouane in southeastern Tunisia. (B) Field photograph of freshly-sampled microbial mat. Note the large spatial extent of mat-covered sedimentary surfaces in the background.*

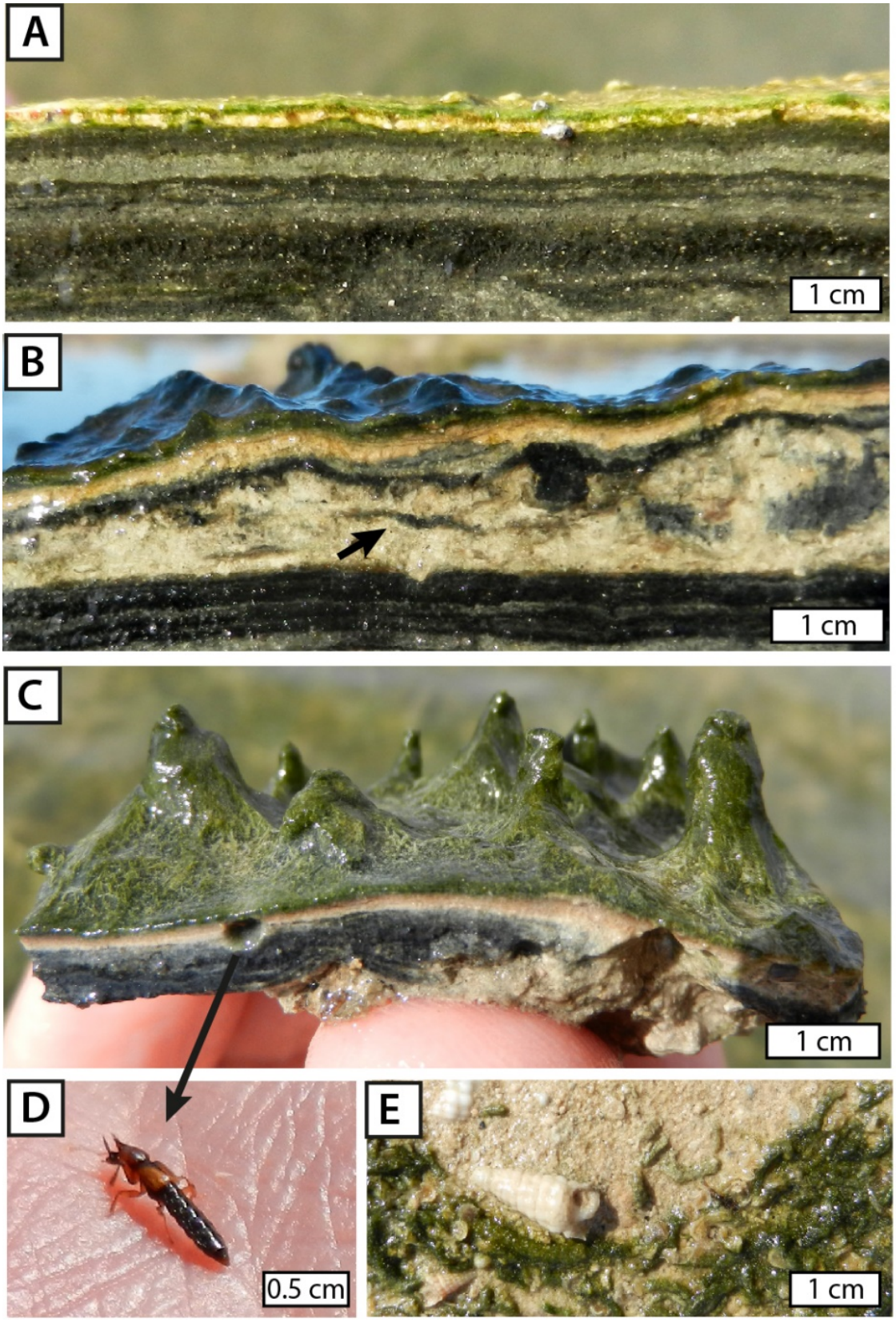

Figure A2. 2: *Cross-section view of planar (A) and tufted microbial mats (B, C). Note that the surficial live microbial mats appear in greenish colors whereas the underlying decaying mats appear as dark laminae. Mats are interbedded with fine-grained sediment, which occasionally contains eroded mat fragments (arrow in B). Burrowing Bledius beetles (D) and cerithid gastropods (E) represent the only grazing organisms associated with the microbial mats.*

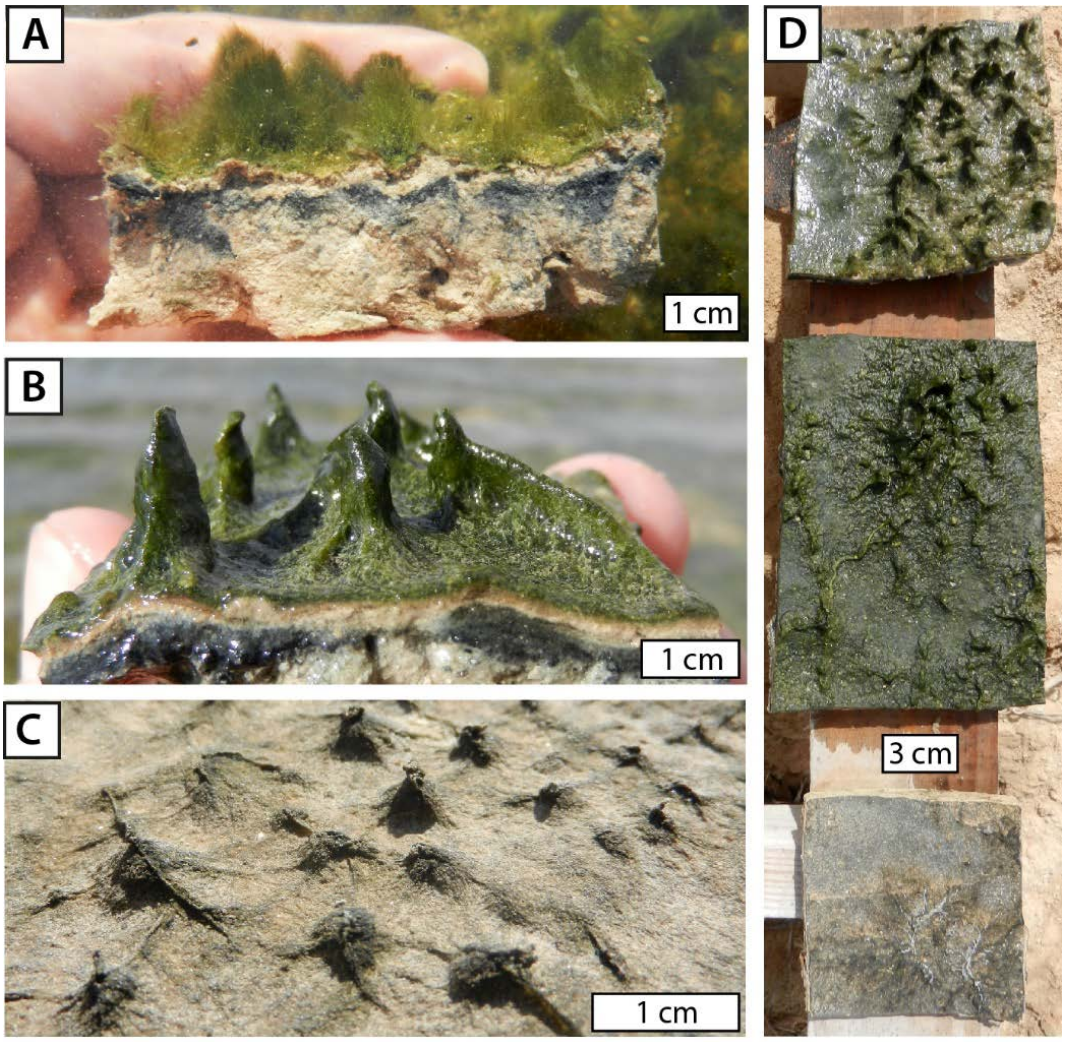

Figure A2. 3: *Comparison of submerged and exposed tufted microbial mats. (A) Underwater the tufts are actually a single mass of various, vertical-oriented "fluffy" filaments. (B) Outside of the water this mass is coalesced to dense nearly vertical tufts. (C) After several hours of exposure and desiccation the tufts are severely shrunk to small knobs. (D) Corresponding mat surface morphologies in plan view.*

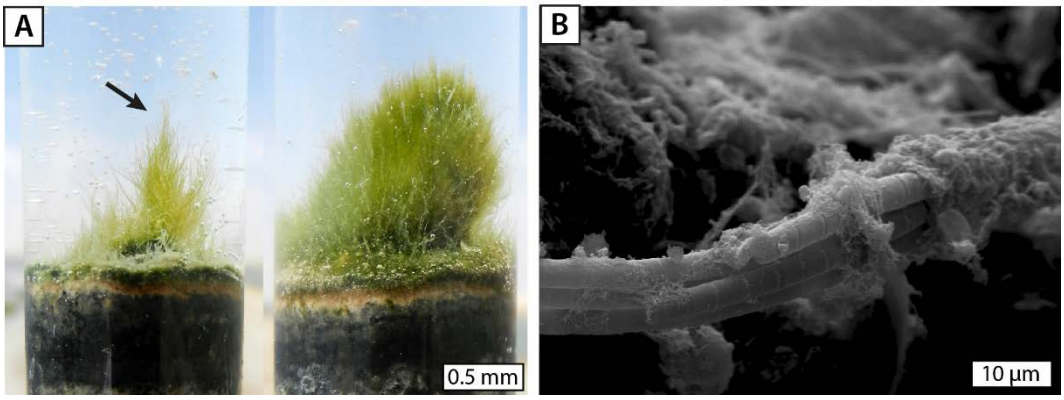

Figure A2. 4: *(A) Close-up view of freshly-sampled tufts in a water-filled vial. Note the vertical-erected cyanobacterial filaments (arrow). (B) SEM photomicrograph of bundled Microcoleus filaments extracted from tufted mat of Tunisia. Note also the well-developed segments within individual filaments. Photo credit: Stephanie Weigert.*

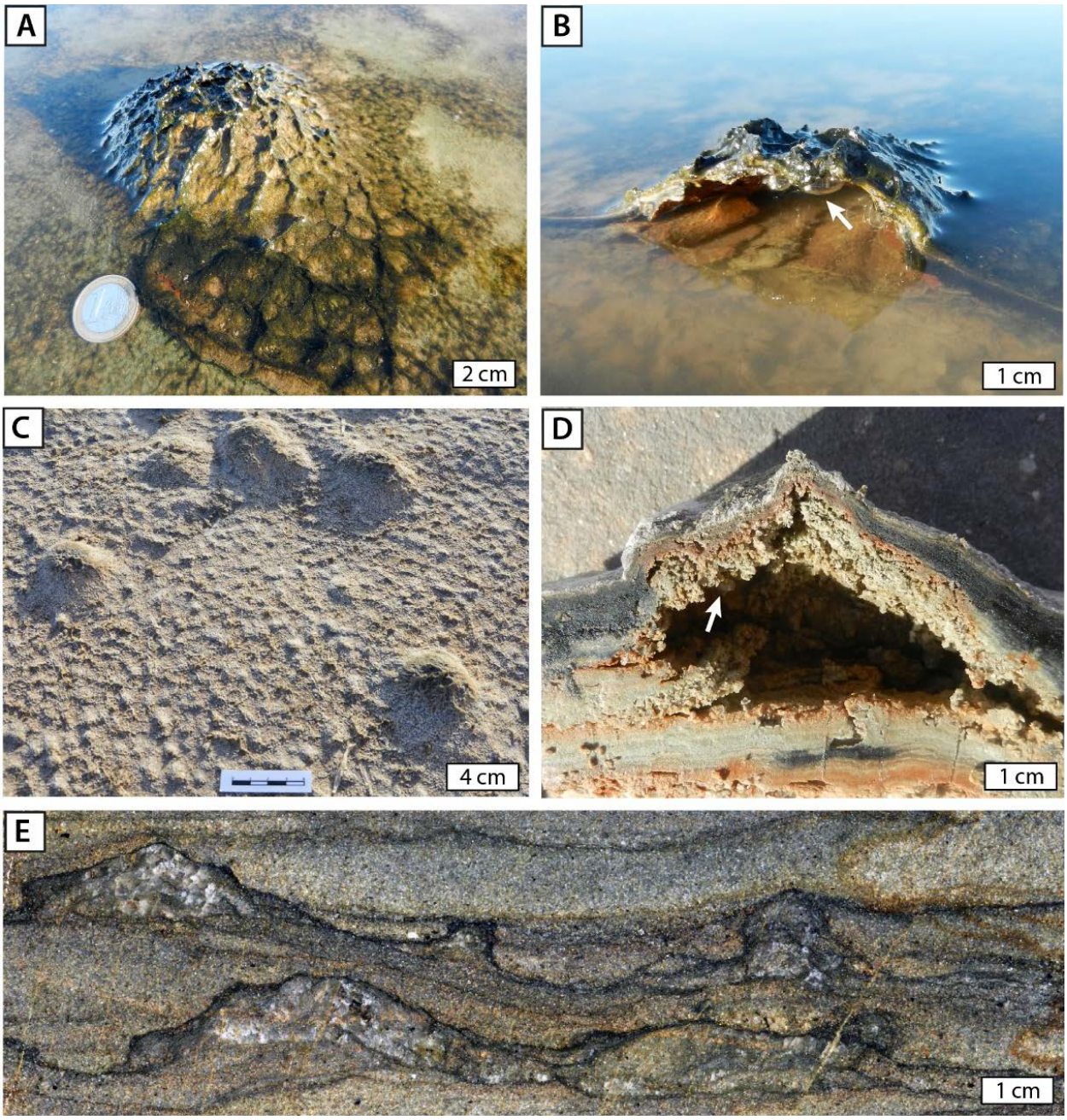

Figure A2. 5: *Field photographs of gas domes underneath cohesive and impermeable microbial mats (A-D) and comparison with fossil gas domes of the 3.22 Ga Moodies Group, BGB, South Africa (E). (A) Modern partly-exposed gas dome. Microbial growth seems to be induced on top of the elevated dome, which is covered by a dense network of reticulate ridges and tufts. (B) Cross-section through gas dome in A with preserved gas bubbles at the ceiling (arrow). (C) Desiccated microbial mat with several small gas domes in plan view. (D) Cross-section through dried out gas dome with small evaporite minerals precipitating at the ceiling of the cavity (arrow). (E) Cross-section view of polished slab showing fossil mat (dark laminae) underlain by chert-filled gas domes resembling in shape and size the Tunisian analogs. This implies that the Archean mats presumably had a similar thickness (Bose and Chafez, 2009).*

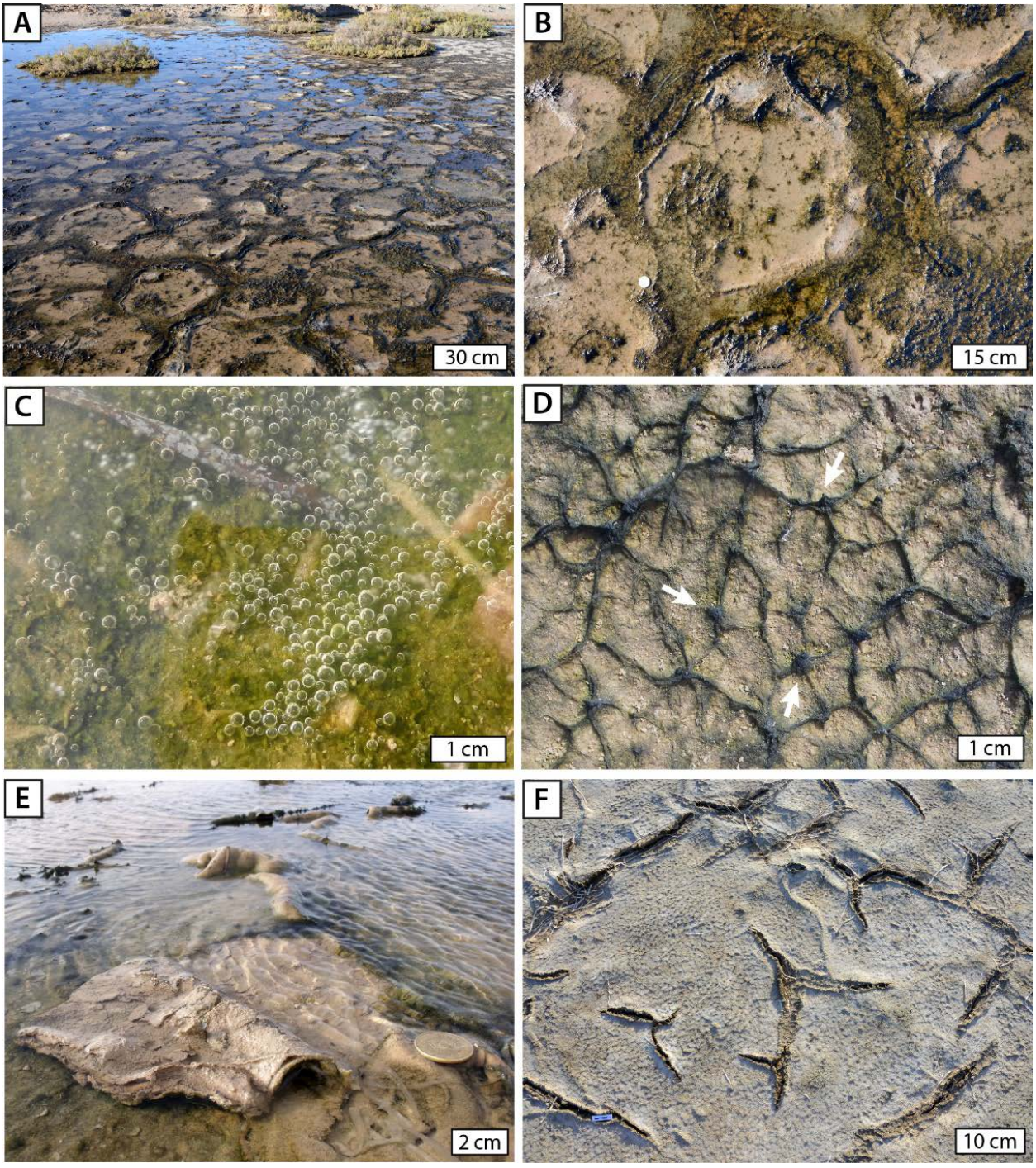

Figure A2. 6: *Field photographs of characteristic mat surface morphologies. (A) Mats with polygonal cracks resulting from periods of mat growth and expansion alternating with mat shrinkage and contraction during desiccation events. (B) Close-up view of mat polygon with upcurled margins. Note that mat growth is mainly concentrated in the water-filled cracks surrounding the polygon. (C) Mat surface covered by oxygen bubbles (produced by the mats through oxygenic photosynthesis). Note that the mat is covered by a thin layer of water, which is almost invisible in the photograph. (E) Roll-up structure formed due to increased current velocities during storms. Photo credit: Christoph Heubeck. (F) Completely desiccated mat with abundant shrinkage cracks.*

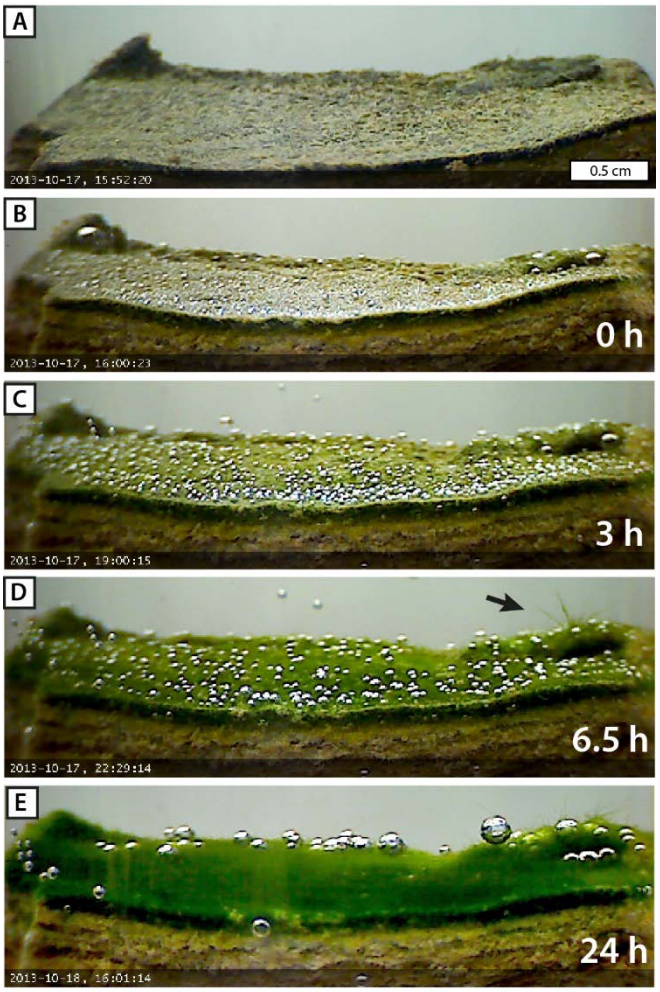

Figure A2. 7: *Laboratory growth experiment with piece of cyanobacterial mat of Tunisia, which was revitalized after 2 weeks of desiccation. (A) Desiccated mat surface. (B) Addition of water. (C) After 3 hours the mat has soaked up water and starts to revitalize. Note that the small surficial bubbles are derived from degassing of air trapped in pore space. (D) First motile filaments become visible at the surface (arrow) after 6.5 hours. Abundant oxygen bubbles, produced by the cyanobacterial community during photosynthesis, are trapped in the upper parts of the mat. (E) 24 hours after the addition of water the mat has entirely recovered from dormancy, significantly increased its biomass and is actively producing oxygen.*

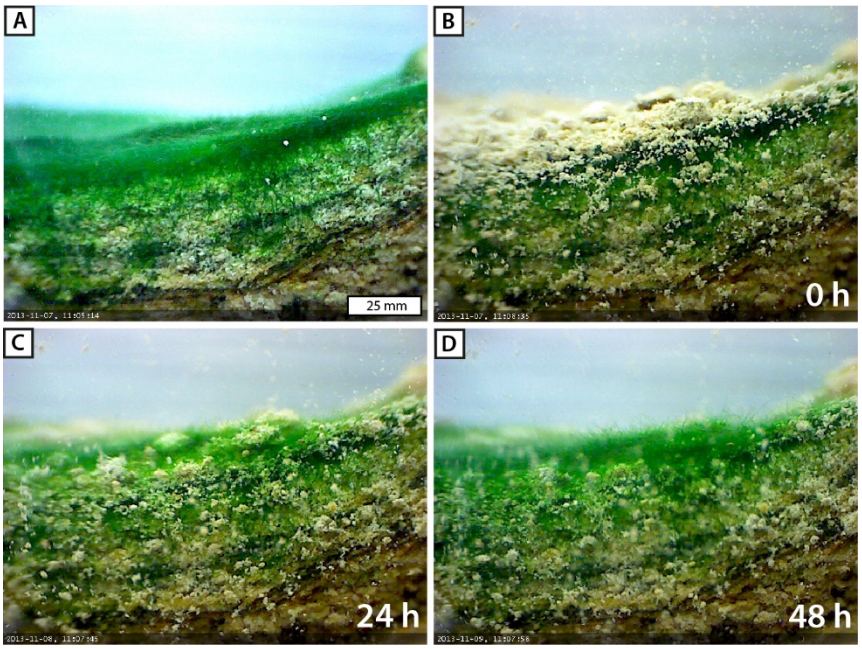

Figure A2. 8: *Laboratory experiment with cyanobacterial mat of Tunisia (A) invistigating the mats response to sediment input and burial (B-D). After approximatelly 24 hours the filamentous microorganisms had partly, and after 48 hours entirely recolonized the added fine-grained sediment.*

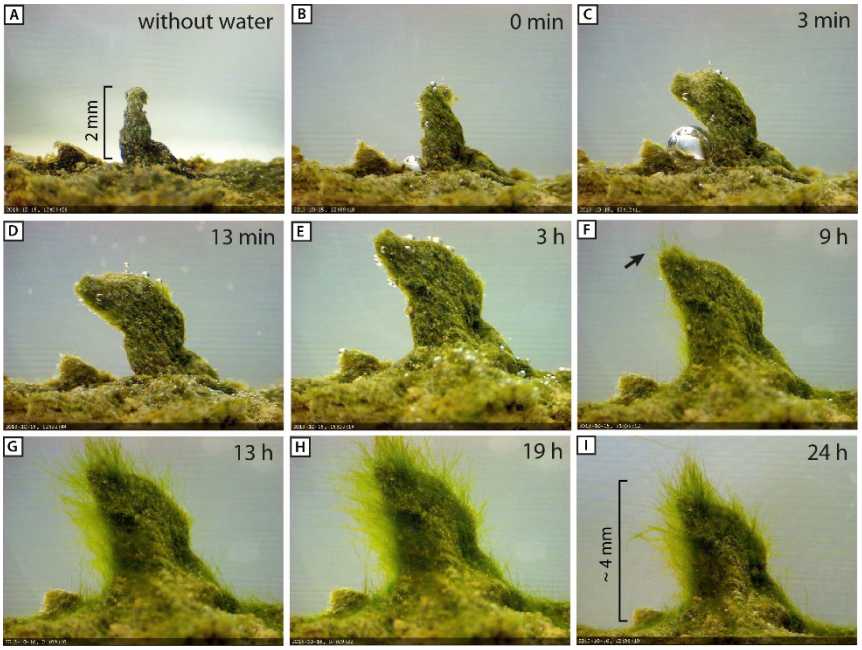

Figure A2. 9: *Laboratory growth experiment with desiccated microbial tuft (A) of Tunisia revitalized through the addition of water. First the tuft is soaking up the water (B-E) and increasing its volume. After 9 hours the first vertically-erected filaments become clearly visible (arrow in F) and successively cover the tuft (G-H). After 24 hours the tuft had almost doubled its size (I). Note that the camera had to be adjusted twice during the experiment (between E-F and H-I).*

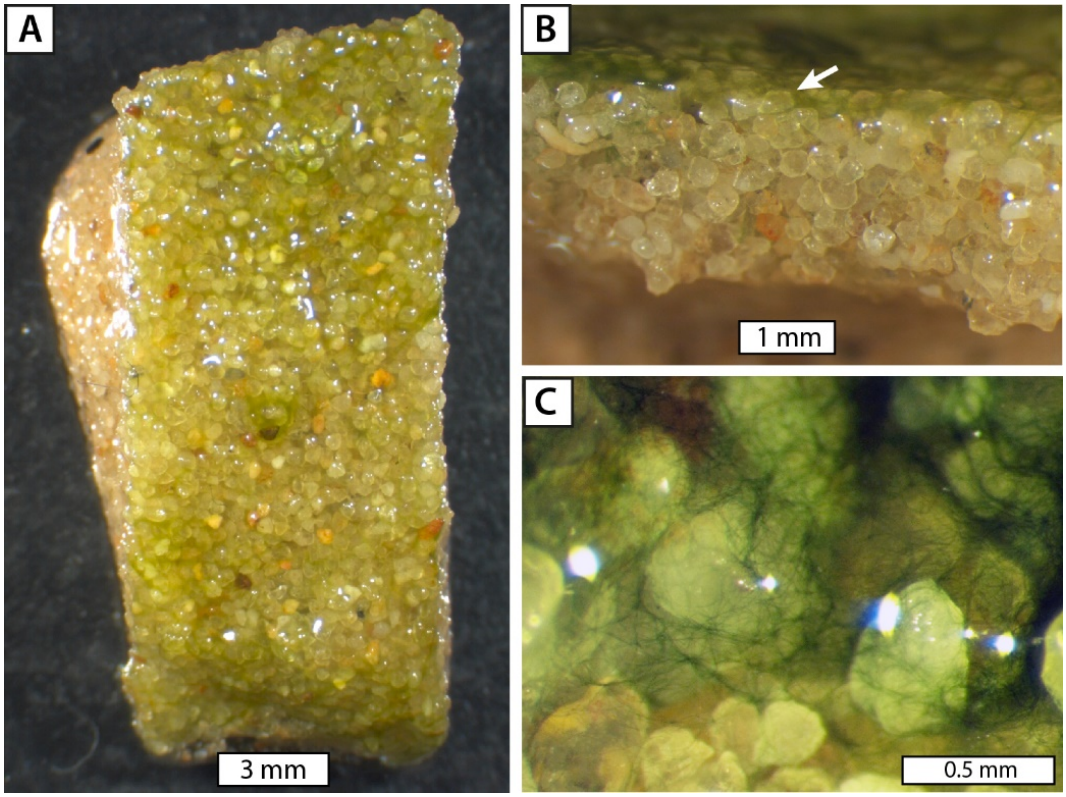

Figure A2. 10: *Laboratory-grown cyanobacterial mat of the species Microcoleus chthonoplastes. (A) Mat in plan view. (B) Side view of surficial microbial mat (arrow) underlain by ~3mm-thick layer of mat-bound sediment. This shows that even relatively thin but EPS-rich microbial mats have an enormous sediment binding and biostabilization capacity. (C) Close-up view of stabilized quartz grains coated by interwoven meshworks of filamentous cyanobacteria. Photo credit: Christof Sager.*

Methods

The cyanobacterial mats of Tunisia were cultivated in an incubator with BG11 growth media (Figs. A.2.7 – A.2.9). Microscopic photographs were captured at set intervals and then encoded into time-lapse movies using the software YAWCAM 0.4.2. High resolution 5 Megapixel USB microscopes (dnt DigiMicro Pro) with manually adjustable optical elements were used to take photos and document mat growth. The cultivation of *Microcoleus chthonoplastes* mats (Fig. A.2.10) was carried out in Erlenmeyer flasks containing BG11 growth media and at 25°C under a constant illumination (Weigert, 2014).

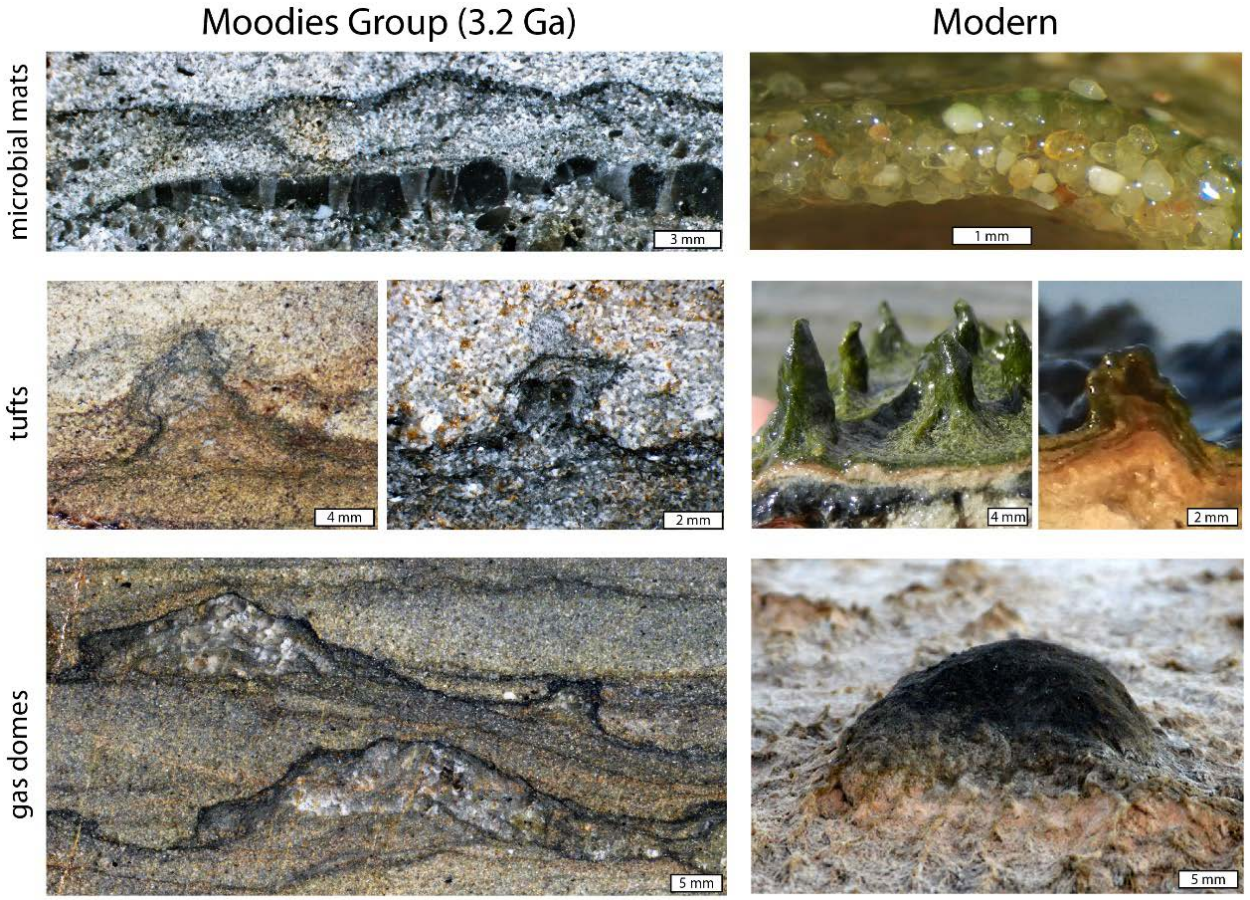

Figure A2. 11: *Comparison of 3.22-Ga old microbial mats, tufts, and gas domes (left) with modern microbial mats from Bahar Alouane, Tunisia (right), which are predominantly built by filamentous cyanobacteria. Note the striking similarities in shape and size of the microbial structures. The bedding-parallel chert layers beneath the Archean mats and the silicified voids within tufts and domes presumably represent former gas-filled cavities.*

References

Bouougri, E., and Porada, H., 2012, Wind-induced mat deformation structures in recent tidal flats and sabkhas of SE-Tunisia and their significance for environmental interpretation of fossil structures: Sedimentary Geology, v. 263-264, p. 56–66, doi: 10.1016/j.sedgeo.2011.12.011.

Davaud, E., and Septfontain, M., 1995, Post-Mortem Onshore Transportation of Epiphytic Foraminifera: Recent Example from the Tunisian Coastline: SEPM Journal of Sedimentary Research, v. Vol. 65A, doi: 10.1306/D426804F-2B26-11D7-8648000102C1865D.

Gerdes, G., 2007, Structures Left by Modern Microbial Mats in Their Host Sediments, *in* Schieber, J., Bose, P.K., Eriksson, P.., Banerjee, S., Sarkar, S., Altermann, W., and Catuneanu, O. eds., Atlas of Microbial Mat Features Preserved within the Siliciclastic Rock Record, Elsevier, Amsterdam, p. 5–38.

Gerdes, G., Klenke, T., and Noffke, N., 2000, Microbial signatures in peritidal siliciclastic sediments: a catalogue: Sedimentology, v. 47, p. 279–308.

Gerdes, G., Porada, H., and Bouougri, E.H., 2008, Bio-sedimentary structures evolving from the interaction of microbial mats, burrowing beetles and the physical environment of Tunisian coastal sabkhas: Senckenbergiana maritima, v. 38, no. 1, p. 45–58, doi: 10.1007/BF03043868.

Noffke, N., Gerdes, G., Klenke, T., and Krumbein, W., 2001a, Microbially induced sedimentary structures - A new category within the classification of primary sedimentary structures: Journal of Sedimentary Research, v. 71, no. 5, p. 649–656.

Noffke, N., Gerdes, G., Klenke, T., and Krumbein, W.E., 2001b, Microbially induced sedimentary structures indicating climatological, hydrological and depositional conditions within Recent and Pleistocene coastal facies zones (Southern Tunesia): Facies, v. 49, p. 23–30.

Weigert, S., 2014, Meso- and microscopic morphological development of Microcoleus chthonoplastes under different fluid flow conditions as an analogy study for Archean microbial mats (master thesis): Freie Universität Berlin, 1-86 p.

A.3

Rock-Eval pyrolysis of extracted kerogens of the Moodies microbial mats

Sample info	Sample ref.	APT ID	S1 (mg/g)	S2 (mg/g)	S3 (mg/g)	Tmax (°C)	PP (mg/g)	PI (wt ratio)	HI (mg HC/ g TOC)	OI (mg CO2/ g TOC)	TOC (%)*
G012421	11-034	106915	0.02	0.02	0.04	332	0.04	0.50	42	83	0.05
G012422	11-196-2	106916	0.02	0.02	0.07	340	0.04	0.50	41	145	0.05
G012423	11-262	106917	0.11	0.07	0.16	263	0.18	0.61	92	211	0.08
G012424	12-303	106918	0.02	0.04	0.05	416	0.06	0.33	161	202	0.02
G012425	12-323	106919	0.02	0.06	0.17	332	0.08	0.25	59	168	0.10
G012426	12-332	106920	0.02	0.04	0.10	338	0.06	0.33	128	321	0.03

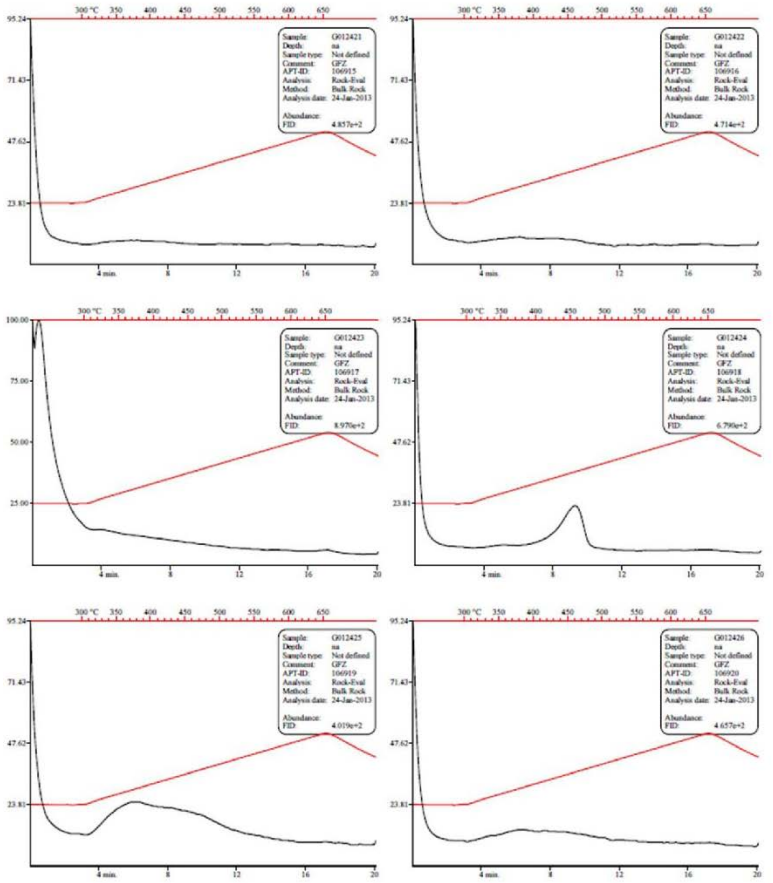

Figure A.3. 1: *The results show a maximum total organic carbon (TOC) content of 0.1‰ and a temperature range between 263 and 416°C, which is consistent with the peak metamorphic temperatures of the surrounding host rock. Credit to Hans-Martin Schulz (GFZ Potsdam, Germany).*


Barberton Greenstone Academy
est. 1975